Formulating a theory for analyzing acoustic instability of low Mach number reacting flow systems using method of multiple scales

A THESIS

submitted by

VINU VARGHESE P.

for the award of the degree

of

DOCTOR OF PHILOSOPHY

DEPARTMENT OF AEROSPACE ENGINEERING
INDIAN INSTITUTE OF TECHNOLOGY MADRAS.

SEPTEMBER 2015

THESIS CERTIFICATE

This is to certify that the thesis titled **Formulating a theory for analyzing acoustic instability of low Mach number reacting flow systems using method of multiple scales**, submitted by **Vinu Varghese P.**, to the Indian Institute of Technology, Madras, for the award of the degree of **Doctor of Philosophy**, is a bona fide record of the research work done by him under our supervision. The contents of this thesis, in full or in parts, have not been submitted to any other Institute or University for the award of any degree or diploma.

Prof. R. I. Sujith
Research Guide
Professor
Dept. of Aerospace Engineering
IIT-Madras, 600 036

Place: Chennai

Date: 28 October 2015

ACKNOWLEDGEMENTS

I would like to thank my Ph. D. advisor Prof. R. I. Sujith for giving me the opportunity to pursue this interesting research work. I thank my teachers Prof. V. Balakrishnan for teaching dynamical systems theory, Prof. Chakravarthy and Dr. Amit Kumar for teaching the course combustion explosion and detonation. I would like to thank Prof. K. Bhaskar, Prof. K. Srinivasan, Prof. T. Sundararajan, Dr. T. M. Muruganandam and Dr. Sunetra Sarkar for providing helpful feedback during my doctoral committee meetings. My friends Vishnu R., Priya S., Sathesh Mariappan, Gopalakrishnan E. A. and Vineeth Nair have given me valuable suggestions from time to time to improve my research work. I have learned from Priya S. the art of understanding the beauty of every small detail of the work we do. This has helped me in explaining my own work to others. Vishnu R. has taught me the value of patience and has offered his friendship over the course of time I have been in IIT. This endeavor would not have been successful if not for Shilpa's support. She has given me great strength while making critical decisions in my life. There has been many occasions when my daughter Eva's smile has cheered me to go on. I would like to thank my parents for their patience and their affection which has always made me happy.

ABSTRACT

KEYWORDS: Combustion instability; thermal-acoustic interaction; acoustic-hydrodynamic interaction; method of multiple scales; dynamical system theory; bifurcations; nonlinear instabilities.

Thermo-acoustic instability in combustion chambers has attracted the attention of researchers involved in the design and operation of rocket motors and gas turbine engines. Thermo-acoustic instability has its origin in confined combustion environment, where flow processes exchange energy with the heat sources and the acoustic field in the confinement. A positive feedback can exist between the heat sources and the acoustic field that results in the growth of acoustic pressure amplitude.

In this thesis, we attempt to study the origin of combustion instability in low Mach number reacting flows. Towards this purpose, we need to investigate various coupling mechanisms that establish the interaction between the acoustic and hydrodynamic fields. To account for multiple time and spatial scales associated with the acoustic and hydrodynamic fields, we use method of multiple scales (MMS) for the analysis of low Mach number reacting flows. Through a rigorous mathematical derivation, the governing equations - continuity, momentum and energy equations - for low Mach number reacting flows are decomposed into acoustic perturbation equations for the acoustic and hydrodynamic field variables. These perturbation equations describe the evolution of acoustic field variable on two time scales and two spatial scales. Using the perturbation equations, we can explain the influence of various acoustic sources from the reacting flow field, on the growth of acoustic pressure amplitude. Therefore, these equations can be used to compute the characteristics of combustion generated sound.

Further, we use the perturbation equations to explain the feedback mechanism that exists between the acoustic and hydrodynamic fields. We also develop a convection reaction diffusion (CRD) system to explain the transition to oscillatory state aided by

the hydrodynamic sources and the coexistence of oscillatory state and non-oscillatory state for the acoustic pressure. Solving for our system of equations, we obtain two stable solutions for the same control parameter - one an oscillatory state, and another a non-oscillatory state. Therefore, these equations give a better description of hysteresis observed during acoustic instability. Further, we also explain that the transition from non-oscillatory state to oscillatory state is a consequence of acoustic-hydrodynamic interaction.

TABLE OF CONTENTS

LIST OF TABLES

LIST OF FIGURES

ABBREVIATIONS

MMS	Method of multiple scales
NLC	Nonlinear convective instability
NLA	Nonlinear absolute instability
CRD	Convection reaction diffusion

NOTATION

α, θ, ϑ	Coefficients of the nonlinear terms
ρ, $\vec{u}$, p, T	Density, velocity vector, pressure and temperature field variables
ρ_0, $\vec{u}_0$, p_0, T_0	Leading order density, velocity, pressure and temperature variables
ρ_2, $\vec{u}_1$, p_{2a}, T_2	Perturbation variables corresponding to density, velocity, pressure and temperature
ϵ	A small number proportional to Mach number ($\sqrt{\gamma}M$)
Re, Pr	Reynolds number and Prandtl number respectively

CHAPTER 1

INTRODUCTION

1.1 Motivation

Thermo-acoustic instability, widely studied because of its significance in the development and operation of gas turbine engines and rocket motors, is believed to be the consequence of acoustic - heat release rate interaction. The unsteady reacting flow that prevails in a combustion chamber also contributes to thermo-acoustic instability. The positive feed back between the heat release rate, the acoustic field and the flow field results in a self sustained oscillation of acoustic pressure. The oscillation can prove detrimental to the smooth operation of any combustion system.

The contributing elements of instability, the fluid flow disturbances and resulting unsteady heat release rate, results in the addition of energy to the acoustic field in the combustion chamber. Earlier investigations (discussed in Sections 1.1.1 and 1.1.2) attempt to study the mechanism of energy transfer between the unsteady heat release rate and the acoustic field inside the combustor. We realize, from the shortcomings of these investigations, the need for incorporating simultaneously multiple time and space scales in developing a theory to explain thermo-acoustic instability. This theory, which we attempt to develop, describes a general mechanism that explains the energy transfer between unsteady heat release rate and acoustic field. A criterion to the test the validity of any theory, that explains thermo-acoustic instability, is to see if the linear and nonlinear processes in the system are considered (Zinn and Lieuwen, 2006). We attempt to introduce a new nonlinear mechanism, that arise from chemical - acoustic interaction, as significant in establishing self sustained acoustic oscillation.

1.1.1 Unsteady reacting flow

In a combustion system, the fluid flow governs the convection, diffusion, mixing and reaction of reactive mixtures. The contribution of fluid flow, in establishing the acoustic - heat release rate interaction, is thus significant in determining the stability of a thermo-acoustic system. To be precise, thermo-acoustic instability is a result of the interaction between the flow, flame and acoustics. In real gas turbine engines, the study of interaction between the flame and fluid flow fluctuations is an active area of research. These fluctuations can be introduced in a combustion chamber due to the vortices or coherent structures present in the flow. The generation, propagation and attenuation of vortices are an integral part of combustion system. The favorable environment for unsteady reacting flow includes mixing layers which are formed at the interface of fuel and oxidizer while they mix together before reacting. Another configuration where vortices can be naturally present is a recirculation bubble formed behind a backward facing step or flow behind a bluff body. The swirl stabilized combustors also feature unstable acoustic modes that arise due to the recirculation region (Steinberg *et al.*, 2012; Paschereit *et al.*, 2000). The shear layer instabilities also contribute to unsteady flow dynamics near a sudden expansion. A common geometry used in the combustion literature is a backward facing step (Ghoniem *et al.*, 2005). Ghoniem *et al.* (2005) considers a backward facing step featuring the separated shear layer with a recirculation bubble which is of importance as far as combustion is considered. The flow field in the combustor governs the mixing of fuel and oxidizer and thereby the chemical reaction. The recirculation bubble aids in stabilizing the flame by increasing the residence time of the reactants, allowing them to react. The flame formed as a result of chemical reaction is thus governed by the geometry of the combustor. Flow velocity profiles - one that is seen in the mixing layers, and the one associated with the recirculation bubble in a rearward facing step - are studied for their potential for instability by Keller *et al.* (1988). The underlying mechanisms that lead to these flow instabilities are widely studied.

The common instabilities that are present in the shear layer are due to 1) velocity difference in the shear layer causing Kelvin - Helmholtz instability, and, 2) density difference caused by the heat release rate from chemical reaction in the mixing layer. The effect of viscosity in the shear layer usually damps the instability. However, at high

Reynolds number, the viscous effects can be neglected and the instabilities are treated as inviscid instability. In a typical combustion system, a mixing layer is formed at the point where the fuel and oxidizer jets meet. The fuel and oxidizer are supplied into the combustion chamber at different velocity. The velocity shear in the mixing layer can then give rise to the above mentioned instabilities. The Reynolds number over a wide range starting from $O(10^2)$ can cause instabilities in the mixing layer (Lessen, 1948). The density difference in the mixing layer is caused by the temperature rise in the mixing layer owing to the chemical reaction. An explanation to such a phenomenon is given by Michalke (Michalke, 1984).

From the above discussion, we know that the flow field oscillation is inherent to all combustor configurations. Flow filed oscillation is sustained by a mutual interaction between the flow and the flame. The flow field oscillation leads to unsteady heat release rate. Unsteady heat release rate is one of the sources of acoustic energy. Thus a theoretical framework to study thermo-acoustic instability should identify the coupling mechanism between the flow fluctuations and the flame.

1.1.2 Thermo-acoustic instability

A positive feedback between the unsteady reacting flow and the acoustic field in a combustor often leads to thermo-acoustic instability. This instability, characterized by large amplitude pressure oscillations, is detrimental to the operation of propulsion systems including rocket motors and gas turbines used for propulsion and power generation. The oscillation in pressure result in the fatigue of turbine walls and eventually lead to the shutdown of power plants (Zinn and Lieuwen, 2006). The prevention of such instabilities is achieved by designing control systems that analyze the growth rate of instability and identifying the unstable modes in the combustor (Poinsot *et al.*, 1989; Zinn and Neumeier, 1997; Culick and Palm, 2009).

Originated as an academic problem, with the observation of ‘singing flames’ (Jones, 1945), the interest in the study of thermo-acoustic instability grew with the advent of huge power generation plants (Günther, 1972). The occurrence of pressure oscillations, with amplitude of 100 % of the mean pressure in F1 rocket motors emphasize that

thermo-acoustic instability is of serious concern in rocket motors (Blomshield, 2001). Such high amplitudes indicate the possibility that nonlinear mechanisms can be significant in the growth of instability (Zinn and Lieuwen, 2006). Dump combustor configurations, often seen in ramjets, are also prone to combustion instability owing to the unsteady flow field (Culick and Rogers, 1980). This unsteady flow field arises from the vortex shedding. Aerodynamic or flow instability at the injectors is also a cause of combustion instability in jet engines (Konrad *et al.*, 1998).

In combustors, the energy available from the unsteady combustion drives large amplitude pressure oscillations. As the combustion process responds to the changes in temperature, pressure and density fields, the fluctuations in these fields determine the amplitude of acoustic pressure fluctuations (Culick, 2006). Historically, the study of unsteady pressure oscillations in liquid rocket motors is performed by considering the contribution from the unsteady processes in subsystems such as injectors and mixing chambers. These subsystems can have geometries that cause unsteady base flow. Mixing process in a liquid fueled rocket motors is governed by the generation of vortices which creates an unsteady flow field. Combustion instability in rocket motors are subjected to large amplitude pressure fluctuations. Combustion instability in solid propellants are investigated using a response function. Response function (R_p) is a measure of the extent of modulation in burning rate from the pressure fluctuations.

$$R_p = \frac{m'/\bar{m}}{p'/\bar{p}} \tag{1.1}$$

Propellant response can also be measured with respect to the velocity fluctuations. Response function tells us how an initial disturbance in the pressure, velocity or temperature fields is related to the conversion of propellant from condensed state to gaseous state. This conversion may lead to increased reaction rate and in turn an increase in the heat release rate. The phase between the incoming disturbances and the heat release rate decides whether the disturbance is destabilizing. The formulation of a response function assumes the burning to be confined to an interface. Combustion instability in solid rocket motors is also influenced by the distributed combustion (Culick, 2006). Distributed combustion occur away from the propellant burning surface. In such cases, instead of a thin sheet where the burning is assumed to be concentrated, the combustion

is completed only inside the chamber away from the surface. Such a combustion has significant influence in the burning of aluminum and thereby influences the attenuation of acoustic wave due to particle damping (Beckstead *et al.*, 1984).

The stability of acoustic oscillations are investigated with classical acoustic theory as a starting point. The main reason for this assumption is the low Mach number flow that prevails in a combustion chamber (Culick, 2006; Lieuwen *et al.*, 2001). However, the convective effects are to be considered when nonlinear effects become predominant (Culick, 1997). In terms of perturbation theory, these nonlinear effects can be studied only using 'higher order' equations. The classical acoustic theory is formulated as 'lower order' or first order equations. The theoretical studies deal with expressing the growth of acoustic oscillations $p' \propto e^{\alpha}t$ as a solution to a linear second order equation, also called as an 'oscillator' model. The nonlinear effects can be incorporated by adding a nonlinear term as a source to the second order oscillator modeled by Eq. (1.2).

$$\frac{d^2\eta}{dt^2} + \omega^2\eta = F_L + F_N \tag{1.2}$$

where F_L and F_N represent the linear and nonlinear sources. Using a second order model, Balasubramanian and Sujith (2008) have studied the effect of non-normality on the transient growth of acoustic oscillations. Such a second order ordinary differential equation modeling the premixed flame - acoustic interaction, with a nonlinear heat release rate source term, is proposed by Subramanian *et al.* (2010). Subramanian and Sujith (2011) have used this model to study the bifurcations in a Rijke tube resulting from the acoustic-heat release rate interaction.

The acoustic-heat release rate interaction is theoretically expressed as:

$$\frac{d^2\eta}{dt^2} + \omega^2\eta = (\gamma - 1)\int \frac{\partial \dot{Q}'}{\partial t}\psi dV \tag{1.3}$$

where ψ is the spatial distribution of pressure. $\dot{Q}'$ is the fluctuation in the heat release rate. In Eq. (1.3) the acoustic pressure is expressed as $p' = \bar{p}\eta\psi$. The advantage of using this decomposition is that the spatial harmonic motion can be decoupled from the acoustic pressure amplitude η. Therefore, the governing equation can be expressed as an ordinary differential equation (ODE). The expression for heat release rate depend on

the type of heat source; i.e. electrically heated mesh or premixed flame. Heckl (1990) constructed a nonlinear model relating the heat release rate fluctuation with the acoustic velocity for a horizontal Rijke tube. She proposed that there could be nonlinear effects when acoustic velocity $u' > \bar{u}/3$, where $\bar{u}$ is the mean flow velocity. In experiments, the mean flow is established using a blower.

When the heat source is a premixed flame, the wrinkling effects can cause flame surface area change. The fluctuations in flame surface area lead to heat release rate fluctuation. The flame front need to be tracked to determine the heat release rate. The evolution of premixed flame in response to the acoustic field is computed using front tracking algorithm (Kerstein *et al.*, 1988; Dowling, 1999). Response of the flame front to acoustic velocity perturbations can then be studied (Boyer and Quinard, 1990). This response is studied and proposed in the form of a transfer function (TF) which can be expressed as:

$$TF = \frac{\dot{Q}'}{\bar{\dot{Q}}} / \frac{u'}{\bar{u}} \tag{1.4}$$

The linear and nonlinear processes governing $\dot{Q}'$ and u' are determined to understand the onset of instability. Once the instability criterion is determined, control algorithms are developed.

1.1.2.1 Mechanisms of combustion instability

Efficient implementation of control algorithms require the knowledge of the system under consideration. The coupling mechanism between significant processes, such as the unsteady flow and the acoustic wave propagation, that govern the dynamics of thermoacoustic system are studied by Byrne (1983). Studies were conducted in a dump combustor with rearward facing step. The formation and propagation of coherent structures, a flow feature associated with the dump combustor, is still a major area of investigation. The flow disturbances introduced by these coherent structures can influence the heat release rate fluctuations and also couple with the acoustic modes in the combustor (Schadow *et al.*, 1981). Experimentally, in dump combustors with bluff body flame holders, the unsteady combustor flow field is shown to be a major mechanism causing instability (Kaskan and Noreen, 1955; Smith and Zukoski, 1985). The energy addition

to the acoustic field by the unsteady heat release rate, through gas expansion, is dictated by the famous Rayliegh criterion (Rayleigh, 1878). Rayliegh criterion, though a commonly accepted guideline in the design of control algorithms, is not a sufficient criterion for the onset of instability. The energy transfer into the system should exceed the loss of energy from the system. This additional constraint motivates the search for a general mechanism governing the transfer of energy between the reacting flow field and the acoustic field.

The study of flow-flame-acoustic interaction deals with the influence of unsteadiness in the heat release rate on the acoustic wave propagation. Unsteady heat release rate can arise from the vortex-flame interaction. There can be nonuniform distribution of heat release rate inside the flame region. Apart from the unsteady flow, equivalence ratio fluctuations can also contribute to the nonuniform heat release rate. Equivalence ratio fluctuation can be a consequence of the interaction of acoustic wave with the inlet fuel flow rate (Lieuwen and Zinn, 1998). The pressure oscillations in the combustion zone reach the fuel and oxidizer inlets. These pressure oscillations causes the velocity oscillations. Velocity oscillations causes the fluctuations in the mass flow rates of fuel and oxidizer, thereby causing equivalence ratio fluctuation.

$$\frac{\phi'}{\bar{\phi}} = \frac{m'_f}{\bar{m}_f} - \frac{m'_o}{\bar{m}_o} \tag{1.5}$$

In solid propellant rockets, the fluctuation in the mass flow at the surface of the propellant ($\dot{m}'$) arise from the interaction with the pressure or velocity oscillations. These mechanisms are called as pressure coupling and velocity coupling respectively. The acoustic field can be generated because of the vortex shedding from obstacles. Conversion of vorticity mode to the acoustic mode is an active area of theoretical investigation (Noiray *et al.*, 2009). In liquid propellant rockets, mechanism of instability is associated with the droplet evaporation and burning. Contradictory evidence exist in this field of investigation as to whether droplets add energy to acoustic field or attenuate the acoustic oscillation. Tong and Sirignano (1986) suggest that droplets evaporation and burning add energy to the acoustic oscillations. Wooten (1967) shows that droplets attenuate acoustic oscillations. Experimental and theoretical investigations focus on the mode of energy transfer between the acoustic field and the reactive flow field.

1.1.2.2 Experimental

Experiments confirm the interactions between flame, flow and acoustics (Smith and Zukoski, 1985). An experimental study by Poinsot *et al.* (1987), in a confined combustion chamber, confirms the role of coherent structures causing the unsteady heat release rate. This unsteady heat release rate and the acoustic field interact with each other in a feedback loop. This process may eventually satisfy the Rayleigh criterion resulting the growth of acoustic pressure amplitude. The significance of fluid mechanical processes is evident from their experiment. The role of fluid mechanical processes is significant even in unconfined configurations. The heat release rate fluctuation as a source of instability is emphasized by Langhorne (1988). Durox *et al.* (2005) show that the flow velocity fluctuations result in formation of vortices in the jet shear layer. This, in turn, modulates the heat release rate. The acoustic pressure field created by this process may set up a feed back loop with the combustion processes (i. e. flame and fluid mechanical) resulting in thermo-acoustic instability.

1.1.2.3 Acoustic sources in the reacting flows

Experiments (Smith and Zukoski, 1985; Poinsot *et al.*, 1987; Durox *et al.*, 2005) show that flow field velocity fluctuations have effect on the acoustic pressure. It is also evident that heat release rate is another factor influencing the stability of a thermo-acoustic system. The fluctuating heat release rate, arising from the unsteady flow, may further contribute to hydrodynamic instabilities. The heat release rate will cause a dilatation in the flow. The dilatation modifies the flow field. The dilatation is a source for the production of sound (Balaji and Chakravarthy, 2010). The convection of heat release rate fluctuations along the length of the flame should also be accounted for while studying thermo-acoustic instability. Thus, entropy source becomes the third contributing factor for instability. The entropy mode along with convection mode is found to be a governing factor in the study of combustion instability. The instability can thus be thought of as a mixed mode type (Yu *et al.*, 1991).

1.1.2.4 Theoretical

The theoretical attempts aim at understanding the mechanisms underlying the flow - flame - acoustic interaction. The pioneering research done by Culick and his co-workers (Culick, 2006; Yang and Culick, 1986; Culick, 1968) aim at identifying the sources of acoustic field in reacting flows. These research employ perturbation methods to determine the acoustic sources (Culick, 1997). The perturbation methods and its variants such as averaging methods laid the foundation for theoretical analysis of a thermo-acoustic system. The 'modes' as reported by Culick (2006) constitutes the acoustic, fluid dynamical and entropy sources present in a reacting flow. In the combustion chamber, these modes undergo fluctuations due to the unsteady nature of combustion - acoustic interaction. To determine the role of these fluctuations in the stability of the thermo-acoustic system, they have to be separated from the mean values. This separation was the motivation behind the use of perturbation methods.

In such an analysis, the computation of the mean flow is separated from the computation of fluctuating variables. This is the shortcoming of such an approach; i.e. the source terms need to be explicitly modeled to express the relation with the base flow field. The significant coupling mechanisms, such as the coupling between acoustic field and 'DC shift' that would modify the base flow field are neglected. Later various researchers (Wu *et al.*, 2003; Wu, 2005; Mariappan and Sujith, 2011; Subramanian *et al.*, 2013) employed perturbation approach to identify the sources that couple the fluctuating quantities with the mean field variables.

1.1.2.5 Acoustic sources from theoretical analysis

The idea behind the perturbation approaches was to determine higher order equations which represent the flow - flame - acoustic interactions. Culick (2006) show that at higher order perturbation equations:

$$\frac{\partial \rho'}{\partial t} + \bar{\rho}\nabla.M' = S_1 \tag{1.6}$$

$$\bar{\rho}\frac{\partial M'}{\partial t} + \nabla p' = S_2 \tag{1.7}$$

$$\frac{\partial p'}{\partial t} + \gamma\bar{p}\nabla.M' = S_3 \tag{1.8}$$

Equations (1.6, 1.7, 1.8) are evolution equations for fluctuating quantities of density, momentum and energy respectively. They are derived from the law of conservation of mass, momentum and energy. S_1, S_2 and S_3 constitute entropy, convective and acoustic sources. These source terms represent 1) the interaction between linear acoustics with the mean flow, 2) nonlinear acoustics with the mean flow and 3) coupling between fluctuating variables. The mechanism by which the base flow is modified by the fluctuating field is still absent. Also, the expressions for these sources were absent in the analysis of Culick and his coworkers (Culick, 2006). However, they are assumed to contain all relevant processes in a reacting flow field. This type of analysis (i.e. finding the evolution for fluctuations, eg. acoustic field variables, governed by the source terms) can be extended to specific cases such as laminar premixed flames. Such an approach is possible when the source terms relevant to those cases are determined.

Wu and coworkers (Wu *et al.*, 2003; Wu, 2005) follow this approach where they solve the acoustic wave equation with the sources from fluid mechanical processes. Wu *et al.* (2003) try to determine the influence of a premixed flame, localized in a duct, on the acoustic field set up inside the duct. Here, fluctuating quantities represent the acoustic field variables. The source terms introduced by the premixed flame appear on the right hand side of the acoustic wave equation. The evolution of the flame is described by a variable F, which gives the location of the flame front. The influence of localized heat release rate is expressed by a function of F. The discontinuity in the acoustic velocity $[u_a] = q(\overline{(1 + (\nabla F)^2)^{1/2}} - 1)$ also modifies the flow velocity as $[U_0] = q((1 + (\nabla F)^2)^{-1/2} - \overline{(1 + (\nabla F)^2)^{1/2}})$. In this manner, the strong heat release rate can modify both the acoustic and base flow velocities establishing the feedback loop. In their theoretical analysis, Wu and coworkers (Wu *et al.*, 2003; Wu, 2005) found that the source relevant to the mean flow - acoustic field interaction is the heat release rate.

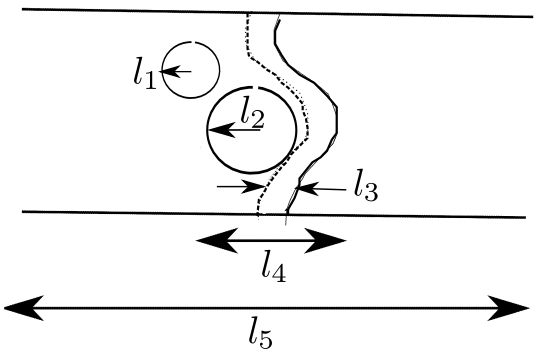

Figure 1.1: Typical length scales in a Rijke tube burner. l_5 represent the long wavelength of acoustic wave. l_4 represent the hydrodynamic zone and l_1 and l_2 represent sizes of eddies. l_3 is the length scale of reaction zone.

Sources for acoustic field are governed by different time scales. The entropy, convective and acoustic modes act at various time scales. There were many attempts to develop perturbation equations for computing the acoustic pressure from these sources. Giauque and Pitsch (2009) performed an acoustic - hydrodynamic splitting to understand how sources from hydrodynamics are responsible for the generation of acoustic pressure. However, there is only one time scale considered. Two time scales, one representing acoustics and one representing hydrodynamics are necessary to identify the different sources. Due to the existence of disparate time scales, the full compressible simulation for computing the acoustic perturbation such as the one performed by Birbaud and Pitsch (2008) require huge computational resources. LES, URANS and coupled CFD/CAA approaches require the same amount of resources. An interesting description of these methods can be found in the book by Schwarz (2009). An acoustic perturbation equation which will save computational time and at the same time identify the time scales associated with the flow - flame -acoustic interaction is necessary.

An attempt at incorporating multiple length scales by Mariappan and Sujith (2011) and Klein *et al.* (2001) revealed interesting information about the coupling due to source terms. Figure 1.1 shows a typical geometry used for theoretical studies. The length scales considered in their analysis consist of a length scale representing the hydrodynamic zone and a length scale for incorporating long wavelength acoustic wave. These length scales are related to each other as $l_4 = \epsilon l_5$, where ϵ is proportional to the Mach number. Klein *et al.* (2001) found that a term, which is the gradient of acoustic pressure, forces the fluid flow in the hydrodynamic zone. Mariappan and Sujith (2011) success-

fully applied this theory to explain thermo-acoustic instability in a Rijke tube. They found a source term $\partial u'/\partial t$, known as global acceleration, that causes flow - acoustic interaction.

The above discussed theoretical studies are limited to multiple length scales and single time scale. The thermo-acoustic instability being the consequence of flow - flame - acoustic interaction, it is worthwhile to investigate what we can achieve by incorporating various time scales associated with these processes in the theoretical anlayses.

1.2 Perturbation Methods

The flow in a combustor is responsible for sound production. The theory of determining the acoustic sources from the flow was introduced by (Lighthill, 1954) who pioneered the idea of sound generation from the flow. The theoretical framework involved computing acoustic sources from the flow and using it for the computation of acoustic field using a wave equation. The equation derived by Lighthill is as follows:

$$(\frac{\partial^2}{\partial t^2} - c_0^2\frac{\partial^2}{\partial x_i^2})\rho = \frac{\partial q}{\partial t} - \frac{\partial f_i}{\partial xi} + \frac{\partial T_{ij}}{\partial x_i \partial_{x_j}} \tag{1.9}$$

where T_{ij} is Lighthill's stress tensor. For low Mach number flow, $T_{ij} \approx \rho_0 v_i v_j$, where v is the velocity associated with the eddy motion and ρ_0 is the density of the fluid (Crow, 1970). There are various analytical solutions based on this formulation. The analytical solutions include an expression describing the role of vorticity on sound generation. The Lighthill's stress tensor here expresses vorticity as the contributing source to the wave equation (Howe, 2002). Differentiating T_{ij} twice lead to

$$\frac{\partial^2 v_i v_j}{\partial x_i \partial x_j} = \nabla.(\omega \times v) + \nabla^2(\frac{1}{2}v^2) \tag{1.10}$$

where $\omega = \nabla \times v$ is the vorticity. The term $\nabla.(\omega \times v)$ is often called Howe's source term. The famous Howe's analogy is based on the total enthalpy $H = \int dp/\rho + 1/2v^2$,

in terms of which a wave equation can be formulated as

$$(\frac{\partial^2}{\partial t^2} - c_0^2 \frac{\partial^2}{\partial x_i^2})H = \nabla.(\omega \times v) \tag{1.11}$$

The solution to this wave equation, in the farfield ($|x| \rightarrow \infty$), gives $\rho_0 H = p - p_0$. All the analytical expressions are valid only for the farfield.

The configuration studied by Mariappan and Sujith (2011) is such that the flow field is confined to a small length scale compared to the long length scale representing the acoustic field. This is the consequence of the low Mach number flow that prevail in a combustion chamber. The flow field with the heat source represents an inhomogeneity in an otherwise homogenous acoustic field. Following Lighthill's approach, we can compute the acoustic sources from the hydrodynamic zone to supply the source term for the wave equation. This type of problems are called singular perturbation problems. The Poincare-Lighthill-Kuo (PLK) method is one of those techniques which could solve the singular perturbation problems. Another approach is to consider the acoustic field as the compressible part of the incompressible flow field. Such a viewpoint has an advantage that acoustics can be taken into account as a perturbation to incompressible fluid flow. Klainerman and Majda (1982) did a pioneering work in splitting compressible fluid flow into incompressible part and compressible part. Most of the perturbation methods we use today has its foundation in the work of Klainerman and Majda. Geer and Pope (1993) and Munz *et al.* (2007) introduced multiple pressure variable as perturbations of $O(\epsilon)$ to find out a solution for acoustic pressure ($p = p_0 + \epsilon p_1 + \epsilon^2 p_2$). The leading order pressure variable p_0 represents the thermodynamic pressure and the higher order pressure variables p_1 and p_2 represent the hydrodynamic pressure driving the incompressible fluid flow and acoustic pressure respectively.

Apart from the use of multiple spatial scales, (Balaji and Chakravarthy, 2010) investigated the effects of such sources using multiple time/multiple spatial scales. The leading order equations resemble the incompressible fluid flow equations. The perturbation (or higher order) pressure and velocity variables satisfy acoustic wave equations. However, their formulation uses the acoustic sources such as dilatation as an averaged quantity over the short length scale fluctuations. However, the averaging performed

over short length scale fluctuations makes any information of the fluctuations due to localized perturbations of the flow unavailable. Also the evolution equations for acoustic field variables are on the acoustic time scale. The flow time scale phenomena due convection and diffusion appear as averaged quantities. These phenomena can have serious consequences on the stability of the system. For example, the heat release rate in a non-premixed combustion is governed by the diffusion and convection (Oran and Gardner, 1985).

An advantage of perturbation method, which we have employed in this thesis, is to decompose various sources responsible for instability. This can be performed using source filtering.

1.2.1 Source filtering

Extracting the acoustic sources from the compressible fluid flow equations requires a physical understanding of what constitutes the acoustic field and what represents the flow field. As we have discussed before, the identification of thermodynamic pressure, hydrodynamic pressure and acoustic pressure is a part of this physical understanding. Theoretically this understanding is obtained from the decomposition of field variables and to formulate the evolution equations for the decomposed variables. This decomposition is made possible by the perturbation method. Each evolution equation thus obtained represents a physical process (representing the modes) driven by their respective sources. These equations are called perturbation equations.

An interesting account of this procedure is given in the literature. For example, Noiray *et al.* (2009) experimentally identifies a mechanism by which acoustic and convective modes are generated by an orifice plate inside a duct. Durran (2008) used the filtering methods to filter sound waves from compressible flow to formulate a system of pseudo-incompressible fluid flow equations. Earlier this method was also used in determining the compressibility corrections for flows in the solar wind (Zank and Matthaeus, 1991). Once individual processes are identified, the types of sources can be identified by a method given by Ewert and Schröder (2003), originally designed for the study of aeroacoustic systems. Their method is outlined here.

1. Write the governing equations in the form $A\tilde{U} = \tilde{G}$. Where $\tilde{U}$ is the Fourier and Laplace transform of perturbed quantities, $\tilde{U} = (\tilde{\rho_2}, \tilde{u_1}, \tilde{p_{2a}})^T$. The Fourier trans form is done in space and Laplace transform in time as follows.

$$\tilde{f}(\alpha, \beta, \omega) = \frac{1}{(2\pi)^3} \int_0^\infty \int \int_{-\infty}^{\infty} f(x, y, t) e^{-i(\alpha x + \beta y - \omega t)} dx dy dt$$

The operator A comes from the use of following properties to the spatial - tem poral operators

$$\Im(\frac{\partial^n f}{\partial x^n}) = (i\alpha)^n \tilde{f}$$

$$\Im(\frac{\partial^n f}{\partial y^n}) = (i\beta)^n \tilde{f}$$

$$\Im(\frac{\partial f}{\partial t}) = -i\omega\tilde{f} - \frac{1}{2\pi} f^*_{initial}$$

$\tilde{G}$ consist of source terms.

2. Find the eigenvalues and eigenvectors of the matrix operator A. These eigenvec tors correspond to the entropy, convective and acoustic modes.
3. Determine the filtering matrix that would eventually determine the sources con tributing to acoustic and convective modes.

The perturbation method was originally proposed for phenomena described by a single time scale. However, the solutions to the equations governing the flow - flame -acoustic interaction are functions of multiple time scales and multiple spatial scales. Then the acoustic sources act on different time and space scales. In this context, time and space scales which describe their interaction are chosen. An earlier attempt using this approach is by Culick (2006). He applied the method of averaging to formulate a theory to study the interactions on various time scales.

1.2.2 Method of averaging

The method of averaging, as proposed by Culick (2006), is motivated by the fact that the amplitude of acoustic pressure evolves on a slow time scale compared to the time scale of acoustic wave propagation. Therefore, he used a two time scale approach, pioneered

by Kevorkian and Cole (1996), to determine the averaged equations. Culick employed this method to determine the solution for a second order ODE as follows:

$$\ddot{\eta}_N + \omega_N^2 \eta_N = \mu G_N \tag{1.12}$$

where G_N are the sources. μ is a small parameter. The solution to the above equation is proposed as a product of a solution varying on the slow time scale and a solution varying on the fast time scale.

$$\eta_N = A(t) sin\omega_N t + B(t) cos\omega_N t \tag{1.13}$$

Where A and B are the slowly varying parts and the trigonometric parts varies on the fast time scale. A and B are the amplitudes which vary because of the source terms. Sources act on a different time scale compared to that of the amplitude. Finally, the evolution equations for the slowly varying part is found out as:

$$\frac{dA_N}{dt} = \frac{\mu}{\omega_N \tau} \int_t^{t+\tau} G_N cos\omega_N t' dt' \tag{1.14}$$

τ can be assumed to be the time period of the fundamental acoustic mode. The essence of this method is given by Eq. (1.14), where the sources are averaged over the fast time scale to determine the the slow evolution of amplitude. The method of averaging is promising when multiple scales are involved. However, the physical interpretation of these time scales and space scales are necessary to relate them to the physical variables such as thermodynamic pressure, hydrodynamic pressure etc.

1.2.3 Method of multiple scales

Describing the physical processes that govern a thermo-acoustic system requires multiple length scales along with multiple time scales. In this context, method of multiple scales (MMS) can be used as a generalized method of averaging. MMS is an ideal tool to incorporate multiple length and time scales into the analysis of thermo-acoustic system. Another advantage, which we will explore in this thesis, is that MMS provides a physical interpretation of the scales included in the analysis. A detailed description of

MMS will be given in Chapter 2.

1.3 Stability of a thermo-acoustic system

Instability in a thermo-acoustic system is characterized by limit cycle oscillations. Understanding the mechanisms that lead to the emergence of limit cycle oscillations is the first step in predicting the instability. Limit cycle oscillations occur when the acoustic pressure amplitude saturates by a nonlinear mechanism (Zinn and Lieuwen, 2006). As discussed before, the flow - flame - acoustic interaction depends on the acoustic sources in the reacting flows. These source can be linear or nonlinear. Further, these sources can also be classified into driving and damping factors of thermo-acoustic oscillations. The processes of driving and damping are depicted in Fig. (1.2). The point A_{LC} represent the condition when driving becomes equal to damping. To the left of A_{LC}, driving is more than damping and the operating condition shift to the right, eventually reaching A_{LC}. To the right of A_{LC}, damping exceeds driving and then operating condition shifts to left, eventually reaching A_{LC}. Thus the point A_{LC} is an equilibrium point. A theoretical framework to study this phenomena should identify the linear and nonlinear processes as follows:

$$H(A) = \epsilon_h A + H_n(A) \tag{1.15}$$
$$D(A) = \epsilon_d A + D_n(A)$$

Figure (1.3) shows the feedback loop which acts as a driving mechanism for thermo-acoustic instability. The unsteady flow can lead to fluctuating heat release rate. Heat release modulation can also occur due to the fluctuations due to acoustic field. The heat release rate fluctuation, in turn, modifies the flow field. These three factors: 1) the unsteady flow field, 2) the fluctuating heat release rate and 3) the acoustic field, drives each other to cause the growth in the acoustic pressure amplitude. The damping mechanisms involves the mechanisms which causes the loss of acoustic energy. These mechanisms arise in a thermo-acoustic system as one that cause transfer of acoustic energy to other modes such as convective and entropy modes (Menon, 2005*a*). The

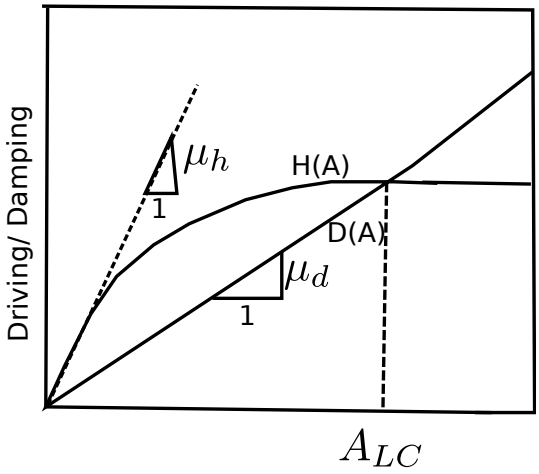

Figure 1.2: The representation of driving $H(A)$ and damping $D(A)$ process, adapted from Zinn and Lieuwen (2006), in a thermo-acoustic system leading to limit cycle oscillations.

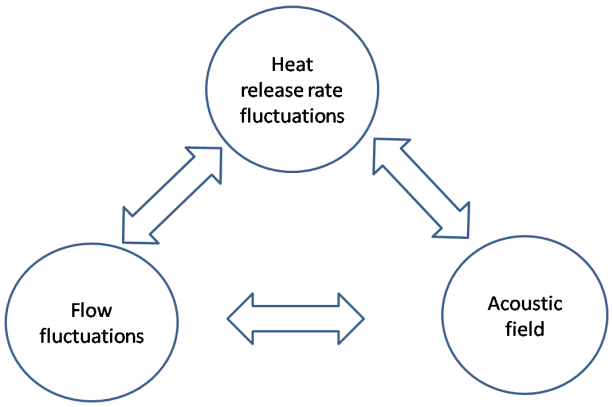

Figure 1.3: The driving mechanisms leading to thermo-acoustic instability

base flow may carry the acoustic energy out of the domain causing the acoustic pressure amplitude to decay to zero. In addition, there can be thermal dissipation that compete with the driving mechanisms.

1.3.1 Bifurcations

Bifurcation means a qualitative change in the behavior of a dynamical system in response to the change in control parameter. For example, Hopf bifurcation leads to limit cycle oscillations from a non-oscillatory state. Bifurcation is a nonlinear phenomenon. Bifurcation diagrams which show the response of a thermo-acoustic system to various system parameters help us to identify the stability criteria for instability. Significant advance in this direction is achieved due to the work of Burnley and Culick (1996), Mariappan and Sujith (2011), Ananthkrishnan *et al.* (2005) and Subramanian *et al.* (2013). At present the instability in a thermo-acoustic system is found to be arising from two types of bifurcations-supercritical and subcritical bifurcations.

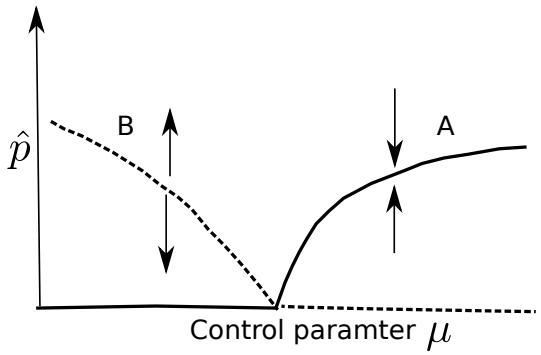

Figure 1.4: Subcritical and supercritical bifurcations. The branch A (supercritical branch) is a stable branch with any perturbation eventually converging to A as the final state. The branch B (subcritical) is an unstable branch with perturbations above this branch diverging and the perturbations below the branch converge to zero amplitude state.

Among the bifurcations, supercritical bifurcation is realized numerically for the instability in a Rijke tube (Mariappan and Sujith, 2011). The existence of subcritical bifurcation as shown in Fig. (1.4) is not realizable as there is no finite amplitude stable branch in such a bifurcation. In such bifurcation, the saturation to a finite amplitude limit cycle amplitude is possible through a fold point. This phenomena is theoretically

studied by Subramanian *et al.* (2013) in the context of a horizontal Rijke tube. Other oscillatory branches indicating quasiperiodicity and chaotic oscillations are found in experiments (Kabiraj and Sujith, 2012). An efficient numerical scheme, using matrix-free continuation, which computes these branches is proposed by (Waugh *et al.*, 2014). Researchers, studying the supercritical and subcritical bifurcations in thermo-acoustic system (Subramanian *et al.*, 2013; Clavin *et al.*, 1994), attempt to represent the bifurcations using a simple mathematical equation known as normal form.

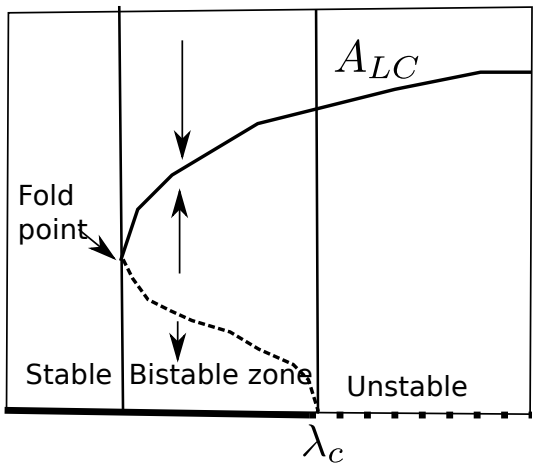

Figure 1.5: Subcritical bifurcation shown as dashed line followed by a fold point. After the fold point a stable solution branch (shown as solid line) is achieved indicating limit cycle amplitude A_{LC}. The bistable zone shows the coexistence of a stable zero amplitude branch and a stable finite amplitude branch. A small perturbation in the unstable regime results in the system approaching A_{LC}. However, in the bistable zone a large perturbation (above the threshold value shown by the dashed line) is needed for the system to reach A_{LC}. In the stable regime perturbation of any magnitude will eventually die down.

1.3.1.1 Normal form of bifurcations

Equations (1.16) and (1.17) represent the normal form of supercritical and subcritical bifurcations respectively. The control parameter λ is expressed as the coefficient of linear term. Variation in the control parameter will result in the bifurcations shown in Fig. (1.4).

$$\dot{x} = \lambda x - x^3 \tag{1.16}$$

$$\dot{x} = \lambda x + x^3 \tag{1.17}$$

Equations (1.16, 1.17) also show that the bifurcations are nonlinear in nature. The saturation of the linear growth ($\dot{x} = \lambda x$) is caused by the cubic nonlinear term. In experiments, bifurcation is accompanied by the hysteresis (Kabiraj and Sujith, 2012). The hysteresis is caused by the existence of a bistable regime in the control parameter space. Origin of this phenomenon is also due to the competition between driving and damping mechanisms in a thermo-acoustic system.

1.3.1.2 Bistability

Figure (1.5) shows the coexistence of a limit cycle solution in a control parameter space along with the stable zero amplitude solution. This stability characteristic of thermo-acoustic system is called bistability. While operating in a bistable zone, the system can approach a finite amplitude branch from zero amplitude branch for a sufficiently large perturbation. This phenomenon is known as 'triggering' (Wicker *et al.*, 1996). The system can also approach the finite amplitude branch for any small perturbation when the control parameter exceeds a critical value (λ_c). While the system is in the state of limit cycle oscillation, even by changing the control parameter below λ_c will not cause the decay of limit cycle amplitude. This phenomenon is known as hysteresis of a thermo-acoustic system.

As discussed earlier, when the driving exceeds damping, the oscillation will start to grow in amplitude until the finite amplitude A_{LC} is achieved. This happens when the value of control parameter exceeds λ_c. Therefore, determining the control parameter for a system helps us to identify the growth mechanism in that system. Also in the bistable zone, a large perturbation can overcome the damping in the system resulting in A_{LC}. An understanding of driving and damping sources is inevitable in the control of a thermo-acoustic system (Culick, 2006; Zinn and Lieuwen, 2006).

We believe that, determining a mechanism that causes the transition from the zero to finite amplitude branch is an outstanding issue in the study of stability. In the next section, we will describe the theoretical approach that we have adopted in developing a

theory to study the stability in thermo-acoustic systems.

1.4 Objective and overview of thesis

This thesis primarily aims at developing a theoretical framework for the study of flow - flame - acoustic interaction that leads to thermo-acoustic instability. Towards this purpose, we have employed method of multiple scales (MMS) to incorporate various time scales and length scales involved in a thermo-acoustic system. The governing equations for compressible reacting flows are decomposed into perturbation equations governing the individual (flow, flame and acoustic) physical processes. We show the dependence of these processes on the time scales and length scales chosen. Eventually, through a rigorous mathematical derivation from compressible fluid flow equation, we have developed a new theory to study the stability of a thermo-acoustic system. This theory formulated in the form of a set of convection - reaction - diffusion (CRD) equations explains the stability characteristics such as limit cycle oscillations and bistability of a thermo-acoustic system.

In Chapter 2, a detailed description and demonstration of the MMS is given. The methods discussed in Chapter 2 is the basis of the formulation of the theoretical framework. The detailed derivation of CRD equations, in the low Mach number limit, is given in Chapter 3. These equations are introduced for the first time in thermo-acoustics. Previously, reaction - diffusion equations were used to study in combustion research to track passive scalars such as temperature (Schvab - Zeldovich equation). However, the CRD equations developed in this thesis describe the evolution of acoustic pressure and thermal fluctuation. The advantage of CRD equations is that they have inherent stability characteristics such as bistability. The fact that these equations are derived from the governing equations for reacting flow makes it evident that the thermal - acoustic interaction and resultant instability are inherent to the reacting flows.

We have shown in this thesis how the physical processes such as unsteady fluid flow, heat release rate, DC shift compete with each other to drive and damp the instability. The study of this competing behavior, as we have discussed in the Section (1.3), starts with the identification of linear and nonlinear processes. As we have discussed in Sec-

tion (1.3.1.1), the bifurcation is a consequence of a linear and a nonlinear mechanism. The CRD equations model this mechanism. The CRD equations show the relation between the convection, heat release rate and thermal dissipation. In Chapter 4, the presence of various sources and their respective time scales are discussed. In Chapter 5, we show that the nonlinearity inherent to all low Mach number reacting flows arise from the chemical - acoustic interaction. The linear growth of acoustic pressure amplitude is shown to be the result of heat release rate, DC shift and thermal dissipation. In Chapter 6, we show that during the thermal-acoustic interaction, acoustic pressure amplitude grows in time due to the interaction between the acoustic and hydrodynamic fields, leading to high amplitude sustained oscillations. This transfer of energy is shown to be the cause of bistability in a thermo-acoustic system. Finally, in Chapter 7 we discuss the conclusions from the present work and the possible application of the present theory to other interesting phenomena in thermo-acoustic systems

CHAPTER 2

Method of multiple scales

The method of multiple scales (MMS) is a perturbation method. In the past, perturbation methods aided many advancements in fluid dynamics. For example, in boundary layer theory, the thin layer where viscous forces are dominant introduces a length scale that is small compared with the length scale of the domain where the inviscid flow prevails (Kevorkian and Cole, 1996). Determining a uniformly valid solution for the boundary layer and the domain of inviscid flow motivated the use of perturbation methods in boundary layer theory.

2.1 Boundary layer theory

If Navier Stokes equations governing the fluid flow is written as,

$$\begin{aligned} \frac{\partial u}{\partial t} + u\frac{\partial u}{\partial x} + v\frac{\partial u}{\partial y} + \frac{\partial p}{\partial x} &= \epsilon(u_{xx} + u_{yy}) \\ \frac{\partial v}{\partial t} + u\frac{\partial v}{\partial x} + v\frac{\partial v}{\partial y} + \frac{\partial p}{\partial y} &= \epsilon(v_{xx} + v_{yy}) \\ \frac{\partial u}{\partial x} + \frac{\partial v}{\partial y} &= 0 \end{aligned} \tag{2.1}$$

then the inviscid fluid flow is governed by Euler equations.

$$\begin{aligned} \frac{\partial u}{\partial t} + u\frac{\partial u}{\partial x} + v\frac{\partial u}{\partial y} + \frac{\partial p}{\partial x} &= 0 \\ \frac{\partial v}{\partial t} + u\frac{\partial v}{\partial x} + v\frac{\partial v}{\partial y} + \frac{\partial p}{\partial y} &= 0 \\ \frac{\partial u}{\partial x} + \frac{\partial v}{\partial y} &= 0 \end{aligned} \tag{2.2}$$

The equations governing the fluid flow inside the boundary layer are formulated by scaling $u = U(X, Y, T)$, $v = \eta V(X, Y, T)$, $p = P(X, Y, T)$, $X = x$, $Y = y/\delta$ and

$T = t$. Variables U, V, P, X, Y and T are used to describe the flow inside the boundary layer. Upon these scaling, we obtain the Navier Stokes equations as follows

$$\begin{aligned} \frac{\partial U}{\partial T} + U\frac{\partial U}{\partial X} + \frac{\eta}{\delta}V\frac{\partial U}{\partial Y} + \frac{\partial P}{\partial X} &= \epsilon U_{XX} + \frac{\epsilon}{\delta^2}U_{YY} \quad (2.3) \\ \frac{\partial V}{\partial T} + U\frac{\partial V}{\partial X} + \frac{\eta^2}{\delta}V\frac{\partial V}{\partial Y} + \frac{1}{\eta}\frac{\partial P}{\partial Y} &= \epsilon\eta V_{XX} + \frac{\epsilon\eta}{\delta^2}V_{YY} \quad (2.4) \\ \frac{\partial U}{\partial X} + \frac{\eta}{\delta}\frac{\partial V}{\partial Y} &= 0 \quad (2.5) \end{aligned}$$

The inner solution (solution inside the boundary layer) requires the dependent variables inside the boundary layer to match the inviscid solution (outer solution). The transverse gradient terms decide the variation of dependent variables inside the boundary layer. If we write $\eta = \delta$ and $\delta = \sqrt{\epsilon}$, then the transverse gradient terms in Eq. (2.3) ($\frac{\eta}{\delta}V\frac{\partial U}{\partial Y}$ and $\frac{\epsilon}{\delta^2}U_{YY}$) and in Eq. (2.4) ($\frac{\eta^2}{\delta}V\frac{\partial V}{\partial Y}$ and $\frac{\epsilon\eta}{\delta^2}V_{YY}$) will be of the same order. Upon using this scaling ($\eta = \delta$ and $\delta = \sqrt{\epsilon}$), we obtain at leading order (ϵ^0):

$$\begin{aligned} \frac{\partial U}{\partial T} + U\frac{\partial U}{\partial X} + V\frac{\partial U}{\partial Y} + \frac{\partial P}{\partial X} &= U_{YY} \quad (2.6) \\ \frac{\partial P}{\partial Y} &= 0 \\ \frac{\partial U}{\partial X} + \frac{\partial V}{\partial Y} &= 0 \end{aligned}$$

Equations (2.2) and (2.6) (Note that both these equations contains the leading order terms) give the outer and inner solution respectively. There exists a region of overlap where the inner and outer solutions match. For the flow over a flat plate ($y = 0$ representing the solid boundary), as $Y \to \infty$ the inner solution $U(X, Y, T)$ should match $u(x, y, t)$ as $y \to 0$.

2.2 Example problems for demonstrating secular and layer type problems

A review of model problems representing fluid flow phenomena is given by Lagerstrom and Casten (1972). These type of problems which involves disparate length scales are known as 'layer type' problems. There is another kind of problem where the disparity

is in the time scales. Such a problem is called 'secular type' problems. Solutions to secular type and layer type problems are carried out in three steps; 1) Determine the domains of interest, 2) construct solutions valid to each domain and 3) match these solutions at the region of overlap of domains. An example of a secular type problem is given below.

$$m\frac{d^2y_d}{dt_d^2} + 2\beta\frac{dy_d}{dt_d} + ky_d = 0 \tag{2.7}$$

Equation (2.7) is the governing equation for a spring - mass system. The nondimensionalization is carried out by choosing $y = y_d/L$ for the dependent variable (amplitude). L is the reference amplitude. There are two time scales. One is obtained as $T_1 = \sqrt{m/k}$ and the other $T_2 = \beta/k$. Therefore, time can be nondimensionalized with respect to any of these time scales. For example, when nondimensional $t = t_d/T_1$

$$\frac{d^2y}{dt^2} + 2\epsilon\frac{dy}{dt} + y = 0 \tag{2.8}$$

where $\epsilon = \beta/\sqrt{mk} = T_2/T_1$. For small damping, $\beta << \sqrt{mk}$. An approximate solution can be found for the following equation.

$$\frac{d^2y_0}{dt^2} + y_0 = 0 \tag{2.9}$$

with initial condition $y(0) = 0$ and $|dy_0/dt|_{t=0} = 0$. Solution to Eq. (2.9) can then be written as

$$y_0 = sint \tag{2.10}$$

where, y_0 is the leading order approximation to the full solution y. The full solution can be written as

$$y \sim \sum_{k=0}^{\infty} \epsilon^k y_k(t) \tag{2.11}$$

On the substitution of the solution (2.11) to the governing Eq. (2.8), we obtained for y_1

$$\frac{d^2y_1}{dt^2} + y_1 = -2cost \tag{2.12}$$

with $y_1(0) = 0$ and $|dy_1/dt|_{t=0} = 0$. The solution for y_1 can then be expressed as

$$y_1 = -tsint \tag{2.13}$$

The next step is to see how good is the approximate solution (2.11). The error in approximation can be expressed as

$$y - (y_0 + \epsilon y_1) = O(\epsilon^2) \tag{2.14}$$

Towards this purpose, we look for the validity of the solution in a time interval $[0\ \tau]$. When the time τ is of $O(1)$ the convergence criterion given by (2.14) is satisfied. However, if τ is of $O(1/\epsilon)$ the solution of y_1 diverges and the convergence criterion is violated. Then, we do not have a good approximation for the solution y. To ensure the convergence of the solution expansion, we should therefore eliminate the secular terms.

The layer type problems will violate the convergence criterion due to 'singularity condition'. This is explained in the following example. When the mass is smaller than the damping ($mk << \beta^2$) the spring - mass equation can be represented as

$$\eta \frac{d^2y}{ds^2} + 2\frac{dy}{ds} + y = 0 \tag{2.15}$$

with initial conditions $y(0) = A$ and $|dy/ds|_{s=0} = B$, where $s = t_d k/\beta$. $\eta = km/\beta^2 = 1/\epsilon^2 = T_1^2/T_2^2$ is the small parameter. A solution expansion of the form

$$y \sim \sum_{k=0}^{\infty} \eta^k y_k \tag{2.16}$$

can be constructed in terms of η. The leading order equation is obtained as

$$2\frac{dy_0}{ds} + y_0 = 0 \tag{2.17}$$

A solution to the leading order equation is of the form

$$y_0 = Ae^{-s/2} \tag{2.18}$$

However, in the spatial interval $[0\ s]$, when $s = 0$, the velocity dy/ds gives the wrong value; i.e. the initial condition is violated. Therefore, a singularity exists at $s = 0$. However, the exact solution to Eq. (2.15) (Lagerstrom and Casten, 1972) shows that

when a correction of $O(\eta)$ (see Eq. (2.19)) is added to the leading order term

$$y \approx Ae^{-s/2} - \frac{1}{4}(A + 2B)e^{-2s/\eta}\eta \tag{2.19}$$

the velocity boundary condition is satisfied at $s = 0$. Here, the factor s/η is another time scale t_d/T_3, where $T_3 = m/\beta$.

In the above discussion, we see that to determine a uniformly valid solution; i.e. solution valid near $s = 0$ (the singular region) and everywhere else, we need at least two time scales (in secular type problems) and two length scales (in layer type problems). In layer type problems each domain is analyzed separately with its own length scale. However, in secular type problems both time scales are used simultaneously. In the next section we will discuss the procedure underlying the solution of secular and layer type problems.

2.2.1 Method

The method of multiple scales requires an initial solution expansion. Often, this solution expansion is known as asymptotic expansion. Construction of the asymptotic expansion follows certain conditions. These conditions are elaborated in the books by Kevorkian and Cole (1996), Nayfeh (2008) and in a review by Lagerstrom and Casten (1972). A brief outline of these conditions are given in the following section.

2.2.1.1 Asymptotic expansion

Asymptotic expansion is an approximate solution constructed to satisfy the governing equations of a physical problem. This procedure is required when the problem is layer type or secular type, as an exact solution is unavailable. An asymptotic expansion is expressed as follows;

$$y = \sum_{i=0}^{n} \phi^i(\epsilon) y_i \tag{2.20}$$

where y is an approximation to the actual solution. Each term in the approximation ($\phi^1 y_1$, $\phi^2 y_2$..) should be smaller than the preceding term. This is ensured by choosing

suitable asymptotic sequence (ϕ^1, ϕ^2..). The behavior of a asymptotic sequence $\phi(\epsilon)$ and the asymptotic expansion y; i.e. the convergence and divergence, as the limit approaches ($\epsilon \to 0$) is expressed using Landau symbols (Big O and small o). Landau symbols indicate the relative order of magnitude of each term in the expansion. In the next section, using simple examples we will explain the use of Landau symbols.

2.2.1.2 Landau symbols

For a domain D (a physical domain where we try to find the solution in terms of independent variable x) and in the interval $I : 0 < \epsilon < \epsilon_1$,

$$y(x;\epsilon) = O(v(x;\epsilon)) \tag{2.21}$$

implies that

$$y(x;\epsilon) \leq K(x)(v(x;\epsilon)) \tag{2.22}$$

where v is a gauge function. Gauge functions are used to measure the growth rate of asymptotic sequence (Nayfeh, 2008). Big O implies that $|y/v|$ is bounded by $K(x)$. If the condition (2.22) is true, then the solution given by y is uniformly valid in the domain D throughout the interval I. As an example,

$$x + \epsilon = O(1) \tag{2.23}$$

is uniformly valid in the domain $D : 0 < x < 1$ in the interval $I : 0 < \epsilon < \epsilon_1 < 1$. However, the expression

$$\frac{1}{x+\epsilon} = O(1) \tag{2.24}$$

is not uniformly valid as we cannot determine a finite constant (note that here the constant does not vary as x; i.e. constant is 1) which satisfy the above expression when $x \to 0$.

The other Landau constant states that

$$y(x;\epsilon) = o(v(x;\epsilon)) \tag{2.25}$$

which implies that for any domain D and interval $I : 0 < \epsilon < \epsilon_1$ we have

$$y(x;\epsilon) = \delta o(v(x;\epsilon)) \tag{2.26}$$

Expression (2.26) implies that $y << v$ as $\epsilon \to 0$ or in other words y is bounded. Hence the expression (2.26) implies (2.22). An asymptotic expansion can be constructed if we choose suitable asymptotic sequence $\phi^i(\epsilon)$ such that

$$\phi^{i+1} = o(\phi^i) \tag{2.27}$$

Such an asymptotic sequence will result in an asymptotic expansion:

$$y = \sum_{m=0}^{m=n-1} \phi^m(\epsilon) y_m + O[\phi^n(\epsilon)] \tag{2.28}$$

An example for such an asymptotic sequence is $\phi^i(\epsilon) = \epsilon^{i-1}$, where $i = 1, 2, 3, ,$.

2.3 Example problem with MMS - two time scales

As the first example we will discuss a problem with two time scales governed by an ODE. The physical problem described here is that of an oscillator with small damping. The contribution of the small damping term is negligible to the oscillatory process. However, over long time, these negligible contributions have a cumulative effect on the physical system. These problems are often encountered in nature. The motion of satellite around the earth is influenced by the thin atmosphere, gravity of the moon etc. over a long time. Similarly, the small damping can lead to the decay in the amplitude of oscillations. This 'invisible' time scale over which slow changes occur to the system has to incorporated in the analysis. A description of such problems can be found in the book by Kevorkian and Cole (1996). The following example is adapted from the book on perturbation methods by Nayfeh (2008). A linear damped oscillator can be represented as

$$\ddot{x} + x = -2\epsilon\dot{x} \tag{2.29}$$

An asymptotic expansion is chosen with an asymptotic sequence in terms of ϵ.

$$x = x_0 + \epsilon x_1 + \epsilon^2 x_2 + .. \tag{2.30}$$

The asymptotic expansion is substituted into Eq. (2.29) to obtain at various orders of ϵ

$$O(\epsilon^0) \rightarrow \quad \ddot{x}_0 + x_0 = 0 \tag{2.31}$$

$$O(\epsilon^1) \rightarrow \quad \ddot{x}_1 + x_1 = -2\dot{x}_0 \tag{2.32}$$

$$O(\epsilon^2) \rightarrow \quad \ddot{x}_2 + x_2 = -2\dot{x}_1 \tag{2.33}$$

Substituting solution to Eq. (2.31), which is $x_0 = \cos(t + \phi)$, in Eq. (2.32) we obtain the solution to x_1 as $x_1 = -at\ \cos(t + \phi)$. Similarly, solution to x_2 is obtained as $x_2 = (1/2)at^2\cos(t + \phi) + (1/2)at\ \sin(t + \phi)$. A close look at these solution shows that when $t = O(\epsilon^{-1})$, x_1 and x_2 becomes secular terms; i.e. $x_1, x_2 \rightarrow \infty$ as $t \rightarrow \infty$. The higher order variables x_1 and x_2 should be smaller than the leading order term for a converged solution. An exact solution to Eq. (2.29) is

$$x = ae^{-\epsilon t}cos[\sqrt{1-\epsilon^2}t + \phi] \tag{2.34}$$

In the above expression there are two time scales involved. Similar to the example in Section 2.1, where we used multiple space scales to remove the singularity, we may need an additional time scale to remove the secular terms. The next step is to choose suitable time scales for this purpose.

2.3.1 Choosing the time scales

Upon Taylor series expansion, we obtain

$$e^{-\epsilon t} = 1 - \epsilon t + \frac{1}{2}\epsilon^2 t^2 + .. \tag{2.35}$$

and

$$cos[\sqrt{1-\epsilon^2}t + \phi] = cos(t - \frac{1}{2}\epsilon^2 t + \phi)\frac{1}{8}\epsilon^4 t sin(t - \frac{1}{2}\epsilon^2 t + \phi) + .. \tag{2.36}$$

In the expansion (2.35), the terms of $O(\epsilon)$ and $O(\epsilon^2)$ are secular terms when t is of $O(1/\epsilon)$. The error in approximation will only grow as we add more terms to the Taylor series expansion. The variables ϵ and t are grouped together and a new time scale $T_1 = \epsilon t$ is introduced to keep the error within the limit. Similarly, for the expansion in (2.36) to converge, time scales $T_2 = \epsilon^2 t = O(1)$ and $T_4 = \epsilon^4 t = O(1)$ are to be introduced.

2.3.2 Incorporating the time scales into the analysis

The time scales are incorporated into the analysis as follows.

$$\frac{d}{dt} = \sum_{n=0}^{M} \delta_n(\epsilon) \frac{\partial}{\partial T_n} \tag{2.37}$$

Substituting the asymptotic expansion and time scale expansion into Eq. (2.29), we obtain at various orders of ϵ:

$$\frac{\partial^2 x_0}{\partial T_0^2} + x_0 = 0 \tag{2.38}$$

$$\frac{\partial^2 x_1}{\partial T_1^2} + x_1 = -2\frac{\partial x_0}{\partial x_0} - 2\frac{\partial^2 x_0}{\partial T_0 T_1} \tag{2.39}$$

$$\frac{\partial^2 x_2}{\partial T_2^2} + x_2 = -2\frac{\partial x_1}{\partial x_1} - 2\frac{\partial^2 x_1}{\partial T_0 T_1} - \frac{\partial^2 x_0}{\partial T_1^2} - 2\frac{\partial^2 x_0}{\partial T_0 T_2} - 2\frac{\partial x_0}{\partial T_1} \tag{2.40}$$

The leading order solution is obtained as

$$x_0 = A_0(T_1, T_2)e^{iT_0} + \overline{A}_0(T_1, T_2)e^{-iT_0} \tag{2.41}$$

Substituting this solution into the second order equation, we obtain

$$x_1 = A_1(T_1, T_2)e^{iT_0} + \overline{A}_1(T_1, T_2)e^{-iT_0} - (A_0 + \frac{\partial A_0}{\partial T_1})T_0 e^{iT_0} - (\overline{A}_0 + \frac{\partial \overline{A}_0}{\partial T_1})T_0 e^{-iT_0} \tag{2.42}$$

T_0 is $O(1)$ as long as t is $O(1)$. However, when t is $O(\epsilon^{-1})$, the above solution contains secular terms (the third and fourth terms), implying that the solution is not uniformly valid for all t. In the next section, we will demonstrate the how to ensure a uniform valid solution, thereby also ensuring the convergence of the asymptotic expansion.

2.3.3 Ensuring convergence of the solution

To remove the secular condition, we impose the following.

$$A_0 + \frac{\partial A_0}{\partial T_1} = 0 \tag{2.43}$$

Then $A_0 = a_0 e^{-iT_1}$ and $x_1 = A_1(T_1, T_2)e^{iT_0} + \overline{A}_1(T_1, T_2)e^{-iT_0}$. Similar condition are revealed while solving for x_2. Finally a solution which is guaranteed to converge is obtained (see (Nayfeh, 2008) for detailed derivation).

$$x = ae^{-\epsilon t}cos(t - \frac{1}{2}\epsilon^2 t + \phi) \tag{2.44}$$

In the next section, we will discuss problem with multiple spatial scales. The purpose of the next section is to demonstrate, using a simple example, the role of spatial inhomogeneity. The spatial inhomogeneity can arise naturally in the boundary layers and the need for incorporating the spatial scales to resolve this inhomogeneity is already discussed in the beginning of this chapter. In the next section, we introduce 'fast' and 'slow' variation of spatial variable describing the variation of physical quantities such as velocity and pressure, when there is a spatial inhomogeneity.

2.4 Example problems with MMS - two spatial scales

The following example is adapted from the book by Kevorkian and Cole (1996). We show in this example how the variation in the fast scale is averaged to provide an asymptotic approximation to the original equation. Such an equation is called a homogenized equation (Kevorkian and Bosley, 1998). An application for homogenization, used in the context of combustion instability can be found in a monograph by Culick (2006). Culick derived equations for acoustic field variables on a slower time scale. However, here we illustrate the method of homogenization using a simple and easy to follow example of heat conduction. Homogenized equation governing one dimensional heat

conduction, on a slower space scale, can be derived from the equation:

$$\frac{dq_x}{dx} = 0 = \frac{\partial}{dx}(k(x, \frac{x}{\epsilon})\frac{dT}{dx}) \tag{2.45}$$

The variable x describes the space scale for slow variation and $x^* = x/\epsilon$ is the space scale for describing the fast variation in the region of inhomogeneity. The boundary conditions are $T(0) = T_L$ and $T(1) = 0$. An asymptotic expansion for T can be formulated as

$$T(x;\epsilon) = T_0(x, x^*) + \epsilon T_1(x, x^*) + \epsilon^2 T_2(x, x^*) + ... \tag{2.46}$$

The spatial operator can be expressed as

$$\frac{d}{dx} = \frac{1}{\epsilon}\frac{\partial}{\partial x^*} + \frac{\partial}{\partial x} \tag{2.47}$$

Substituting (2.47), (2.46) into Eq. (2.45) gives at various orders

$$\frac{\partial}{\partial x^*}(k(x, x^*)\frac{\partial T_0}{\partial x^*}) = 0 \tag{2.48}$$

$$\frac{\partial}{\partial x^*}(k(x, x^*)\frac{\partial T_1}{\partial x^*}) = -\frac{\partial}{\partial x^*}(k(x, x^*)\frac{\partial T_0}{\partial x}) - \frac{\partial}{\partial x}(k(x, x^*)\frac{\partial T_0}{\partial x^*}) \tag{2.49}$$

$$\frac{\partial}{\partial x^*}(k(x, x^*)\frac{\partial T_2}{\partial x^*}) = -\frac{\partial}{\partial x^*}(k(x, x^*)\frac{\partial T_1}{\partial x}) - \frac{\partial}{\partial x}(k(x, x^*)\frac{\partial T_1}{\partial x^*}) - \frac{\partial}{\partial x}(k(x, x^*)\frac{\partial T_0}{\partial x}) \tag{2.50}$$

From Eq. (2.48), we obtain

$$\frac{\partial T_0}{\partial x^*} = \frac{B_0(x)}{k(x, x^*)} \tag{2.51}$$

Now, since x^* is rapidly varying with respect to x, we need to impose $B_0 = 0$. Otherwise, due to the linear growth of T_0, the asymptotic expansion will not converge (see the discussion in Section (2.2.1.1)). Then $T_0 = \theta_0(x)$, where θ_0 is the integration constant. Eq. (2.50) is substituted with the above expression to obtain

$$k(x, x^*)\frac{\partial T_1}{\partial x^*} = -k(x, x^*)\frac{\partial \theta_0}{\partial x} + B_1(x) \tag{2.52}$$

On integration,

$$T_1(x, x^*) = -x^* \frac{\partial \theta_0}{\partial x} + B_1(x) \int_0^{x^*} \frac{d\xi}{k(x, \xi)} + \theta_1(x) \tag{2.53}$$

To avoid the linear growth of T_1 in x^* we impose:

$$B_1(x) = \frac{1}{< k^{-1}(x) >} \frac{d\theta_0}{dx} \tag{2.54}$$

where

$$< k^{-1}(x) >= lim_{x^* \to \infty} \frac{1}{x^*} \int_0^{x^*} \frac{d\xi}{k(x, \xi)} \tag{2.55}$$

Similarly, for Eq. (2.51), we have the condition

$$\frac{d}{dx}(\frac{1}{< k^{-1}(x) >} \frac{d\theta_0}{dx}) = 0 \tag{2.56}$$

where $1/ < k^{-1}(x) >$ is the effective thermal conductivity. The resultant equation is a homogenized equation and provides a good approximation to the exact solution.

$$q_x = -k_{eff}(x) \frac{d\theta_0}{dx} \tag{2.57}$$

The main idea demonstrated by the examples is that to ensure a good approximation to the exact solution, the linear growth in the fast scale is to be avoided. The conditions prescribed to ensure a good approximation are called solvability conditions. The methods described in the preceding sections form the basis of techniques used in the field of aerodynamics sound generation (Crow, 1970; Lighthill, 1954; Geer and Pope, 1993), which we will discuss in the next section.

2.5 Aerodynamic sound generation

Crow (1970), for a very small Mach number ($M << 1$), provides a theoretical framework to study the aerodynamic sound generation from eddies. He regards such a problem as a singular perturbation problem. The motivation behind using singular perturbation method in the study of aerodynamically generated sound is the presence of multiple

length scales. The length scale representing the eddies (l) and the length scale for acoustic wave (λ) form a ratio $l/\lambda << 1$. The existence of localized eddy embedded in an acoustic field motivates one to decompose the velocity field into a rotational field and an acoustic field.

$$u = \nabla \times v + \nabla\phi \tag{2.58}$$

The source term T_{ij} in the Lighthill's equation (1.9) can then be expressed as an asymptotic expansion

$$T_{ij} = T_{ij}^0 + M^2 T_{ij}^1 + .. \tag{2.59}$$

The leading order T_{ij} decays rapidly outside the eddy zone. However, the higher orders are made to consist of both rotational and acoustic components. The uniformly valid solution is obtained by matching the solution inside the eddy with the solution for acoustic field that exist outside the eddy zone. An adaptation of this method is also used in thermo-acoustics when multiple length scales are encountered (Mariappan and Sujith, 2011). A similar application of Crow's approach is used by Geer and Pope (1993) while studying the sound from vibrating bodies. They used multiple length scales $x_0 = x$ and $x_i = M^i x$, where $i = 1, 2, ...$ The variable are expanded as

$$\rho = \sum_{j=0}^{\infty} \rho^j M^j \tag{2.60}$$

and

$$u = \sum_{j=0}^{\infty} u^j M^j \tag{2.61}$$

and the spatial derivative is expressed as

$$\nabla = \nabla_0 + M\nabla_1 + M^2\nabla_2 + .. \tag{2.62}$$

Geer and Pope (1993) applied the technique of singular perturbation theory to determine higher order perturbation equations governing the sound production and propagation. They found out, in addition to the linear wave equations, higher order nonlinear equations that predict the nonlinear features such as wave steepening.

The method of multiple scales as described in this chapter, although useful in treat-

ing the singular and secular type problems, is “problem dependent“. The discussion in this chapter serves as a guideline in dealing with different physical problems. The asymptotic expansion, the procedure for ensuring the convergence and the choice of small parameter depends on the physical nature of the problem. The asymptotic sequence have to be carefully chosen if the higher order equations are to be meaningful. In the context of thermo-acoustics, the method employed in the field of aerodynamically generated sound is worth exploring. However, the method has to be extensively modified to incorporate multiple time and space scales simultaneously. We will introduce such a methodology in Chapter 3.

CHAPTER 3

A theoretical framework to study flow - flame - acoustic interaction

3.1 Acoustic - flow interaction viewed as wave - mean flow interaction

The development of a theoretical framework to study flow - flame - acoustic interaction that leads to thermo-acoustic instability, involves choosing physically meaningful length scales and time scales. These scales include the time scales associated with physical processes such as convection, acoustic wave propagation and the length scales describing the flow, acoustic wave and the flame. These time scales and length scales are disparate and often arise from the inhomogeneity associated with the physical problem. Such an inhomogeneity, for a low Mach number flow, is the weak compressibility due to an acoustic field imposed over the incompressible fluid flow. Such a flow fits the description of a 'nearly incompressible flow' (Zank and Matthaeus, 1990). Similar phenomenon that occur in magnetohydrodynamic (MHD) flows was studied by Zank and Matthaeus (1990). They found the influence of weak compressibility on modifying the fluid flow using the method of multiple scales (MMS).

Apart from MHD flows, in atmospheric flows, where density varies with altitude, also feature such inhomogeneity (Bühler, 2009). In the context of atmospheric flows, Bühler (2009) formulated a theory to describe wave - mean flow interaction. In his theory, compressibility is represented as a 'wave' on the incompressible 'mean flow'. Such a system is similar to the nearly incompressible fluid flow. Buhler has successfully employed perturbation method, with the inclusion of multiple scales, to formulate his theory. As an extension to the theory by Zank and Matthaeus (1990), Hunana *et al.* (2006) attempted including large scale density inhomogeneity. This density variation

introduces volume expansion in the fluid flow. Therefore, with the large scale density variation, the nearly incompressible flows resemble reacting low Mach number flows.

Classifying the reacting low Mach number flow as a nearly incompressible flow or MHD flow has advantages. Now, we only have to find the mechanisms responsible for the wave - mean flow interaction in a reacting low Mach number flow. The existing tools, originally introduced by (Zank and Matthaeus, 1990), can be modified to study these mechanisms. The mutual coupling between the magnetohydrodynamic turbulence and the acoustic field is responsible for wave - mean flow interaction in nearly incompressible flows (Dastgeer and Zank, 2006). The volume expansion, due to the density inhomogeneity is the factor influencing atmospheric flows (Bühler, 2009). In a reacting flow, the volume expansion due to the heat release rate from chemical reaction influences the wave - mean flow interaction. The heat release rate can be fluctuating in a thermo-acoustic system due to unsteady flow. In this chapter, we will show that this volume expansion can be a significant coupling mechanism that lead to wave - mean flow interaction. This interaction is shown to be a suitable representation of acoustic - hydrodynamic interaction in a thermo-acoustic system. In such systems, a positive feedback loop between the acoustic sources in a reacting flow and acoustic pressure can lead to self sustained acoustic oscillations (Poinsot *et al.*, 1987; Culick, 1968, 1976*a*, *b*, 1997, 2006; Zinn, 1968; Yang and Culick, 1986; Poinsot *et al.*, 1987; Candel *et al.*, 2009; Keller *et al.*, 1982; Durox *et al.*, 2005; McIntosh, 2007; Duchaine *et al.*, 2009; Wu *et al.*, 2003; Wu, 2005; Subramanian *et al.*, 2013; Mariappan and Sujith, 2011).

Fluctuations in the heat release rate also result from this acoustic oscillation. Vortex shedding (Poinsot *et al.*, 1987) characterizing the unsteady reacting flow or intrinsic instabilities of flame (Searby, 1992) also cause localized heat release rate fluctuations. One of the reasons for the spatial inhomogeneity is due the disparity in the spatial scales corresponding to these fluctuations and the length scale describing the long wavelength acoustic wave. In this chapter, we will attempt to incorporate the influence of heat release rate fluctuations on the interaction between flame, flow and the acoustic field.

3.1.1 Coupling mechanisms

The mechanisms responsible for the coupling of the acoustic field with the heat release rate are to be investigated. Such a mechanism, proposed by (Dunlap, 1950), shows that the thermal fluctuations or acoustic pressure fluctuations in a reacting flow can influence the reaction rate. Earlier theoretical studies (Clavin *et al.*, 1990, 1994; Pelce and Rochwerger, 1992), also point towards this type of coupling. They used the terms 'temperature coupling' and 'pressure coupling' to describe this mechanism.

Velocity coupling mechanism introduced by (Markstein, 1970), describing the heat release rate fluctuation due to the gas flow velocity around the flame, is also a possible coupling mechanism. The modified flow field near the flame further causes the heat release rate fluctuation. We show that the aforementioned coupling mechanisms result in the nonlinear evolution of acoustic pressure amplitude.

The nonlinear evolution of acoustic field variables has been theoretically studied by various researchers (Wu *et al.*, 2003; Clavin *et al.*, 1990, 1994; Pelce and Rochwerger, 1992). From their investigations, the need for determining the characteristic time scale for the evolution of the acoustic field is evident. The two time scales - one for describing the acoustic wave propagation and another for describing the evolution of acoustic pressure amplitude - were included in the theoretical analysis of thermo-acoustic instability (Wu, 2005; Clavin *et al.*, 1990, 1994; Pelce and Rochwerger, 1992).

The coupling mechanisms between the acoustic field and the hydrodynamic field are studied analytically when the reaction zone is compact; i.e. length scale of the reaction zone is much less than the acoustic wavelength (Wu *et al.*, 2003; Wu, 2005; Matalon and Matkowsky, 1982). Then the reaction zone presents a discontinuity. The acoustic velocity across this discontinuity can be related by Rankine-Hugoniot relation (Wu *et al.*, 2003; Wu, 2005). The heat release rate and the acoustic field influence each other through velocity coupling (Matalon and Matkowsky, 1982; Wu *et al.*, 2003; Wu, 2005). However, when the heat release rate is distributed (for example, in a well stirred reactor), the flame is not a discontinuity. The acoustic pressure varies across the flame. Pressure coupling and temperature coupling dominate such cases (Clavin *et al.*, 1990, 1994). We believe that the contribution from the fluctuations (order of magni-

tudes of the acoustic velocity, acoustic pressure and thermal fluctuations) determines the coupling mechanism. (Clavin *et al.*, 1990) studied these contributions. We will show in this chapter that the orders of magnitudes of the field variables also determines the higher order nonlinear equations.

3.1.2 Nonlinear mechanisms

A study by Clavin *et al.* (1994), showed that the heat release rate fluctuation due to turbulence determined the nonlinear evolution of the acoustic pressure amplitude. This nonlinear behavior caused the transition of thermo-acoustic system to instability or self sustained oscillations. The nonlinear effects can also arise from the 'gas dynamic nonlinearity' (Culick, 1976*a*, *b*) for compressible flows. Such nonlinearities arise from sources such as $u'.\nabla u'$ and $p'\nabla p'$, where u' and p' are the acoustic velocity and pressure respectively. For weak compressibility; i. e., for low Mach number flows, these terms are negligible.

From the aforementioned discussions, we know that weak compressibility can influence the nonlinear behavior of a thermo-acoustic system. The nonlinear behavior causing the transition to instability arises from the coupling mechanisms between the acoustic field and the hydrodynamic field. In this chapter, we will show that such a coupling mechanism arises from the dilatation term due to chemical reaction. The volume dilatation is one of the acoustic sources in the reacting flows. First we will derive, from the governing equations for compressible fluid flow, a set of acoustic perturbation equations describing the acoustic sources in reacting flows. Then the coupling mechanisms will be determined from the sources. We show that this coupling mechanism is described by coupled convection reaction diffusion (CRD) equations. The influence of physical parameters, such as heat release rate, on the stability of a thermo-acoustic system is described by these equations. CRD equations are nonlinear and hence predict the nonlinear evolution of acoustic pressure amplitude.

3.2 Derivation of nonlinear equations from compressible fluid flow equations

3.2.1 Governing equations

The governing equations are given as follows.

$$\frac{\partial \rho}{\partial t} + \nabla.(\rho \vec{u}) = 0 \tag{3.1}$$

$$\frac{\partial \rho u}{\partial t} + \nabla.(\rho \vec{u}\vec{u}) + \frac{1}{\gamma M^2}\nabla p = \frac{1}{Re}\nabla.\tau \tag{3.2}$$

$$\frac{1}{(\gamma-1)}\frac{Dp}{Dt} = -\frac{\gamma}{(\gamma-1)}p\nabla.\vec{u} + H\,Da\,\dot{Q} + \frac{1}{RePr}\nabla^2 T \tag{3.3}$$

$$\frac{\partial \rho Y_i}{\partial t} + \nabla.\rho Y_i \vec{u} = \frac{1}{ReSc}\nabla.\rho D \nabla Y_i + Da\dot{\omega_k} \tag{3.4}$$

These equations are nondimensionalized by their reference values (Klein *et al.*, 2001). For a compressible fluid flow, Eqs. (3.1-3.4) represent the continuity, momentum, energy and species conservation equations respectively. ρ, p and T are density, pressure and temperature respectively. $\vec{u}$ is the velocity vector. Arrhenius law governs the reaction rate $\dot{\omega_k}$. In Eq. (3.3), Da, H and $\dot{Q}$ are the Damkohler number, heat release parameter and heat release rate respectively.

3.2.2 Method of multiple scales

An asymptotic expansion is constructed following the procedure outlined in Chapter 2. For a physically meaningful expansion, we use earlier theoretical studies (Clavin *et al.*, 1990, 1994; Pelce and Rochwerger, 1992) as guidelines. These studies by Clavin *et al.* (1990), and Pelce and Rochwerger (1992) suggest the orders of magnitude for the field variables in the context of combustion instability. With the acoustic pressure and thermal fluctuations of the same order (Clavin *et al.*, 1990) and the acoustic ve-

locity perturbation $O(1/M)$ times the acoustic pressure perturbation, the perturbation variables are incorporated into the asymptotic expansion as follows:

$$\rho = \rho_0 + \epsilon^2 \rho_2 \tag{3.5}$$

$$\vec{u} = \vec{u}_0 + \epsilon \vec{u}_1 \tag{3.6}$$

$$p = p_0 + \epsilon^2 (p_{2h} + p_{2a}) \tag{3.7}$$

$$T = T_0 + \epsilon^2 T_2 \tag{3.8}$$

In Eqs. (3.5-3.8), ϵ is the small number used for preparing the asymptotic sequence. Here, ϵ is proportional to the Mach number ($\epsilon = \sqrt{\gamma} M$). The singularity is seen directly from Eq. (3.2). The coefficient $1/(\gamma M^2)$ of the pressure gradient term in Eq. (3.2) causes the solution to diverge as $M \to 0$. To eliminate the singularity, the hydrodynamic pressure variable p_{2h} is chosen to be of second order (ϵ^2) in the solution expansion (3.7) (Klein *et al.*, 2001). For the construction of solution for heat release rate, we follow the suggestion by (Clavin *et al.*, 1990). The mean heat release rate $\dot{Q}_0$ and the heat release rate fluctuation (due to the acoustic wave) $\dot{Q}'$ are expressed to be of the same order.

$$\dot{Q} = \dot{Q}_0 + \dot{Q}' \tag{3.9}$$

All the mean flow field variables (here, the hydrodynamic field variables) are written with subscript 0. The only exception is for the hydrodynamic pressure p_{2h}, which is expressed as a second order term. Acoustic pressure is denoted by the higher order field variable p_{2a}. Acoustic velocity is $\vec{u}_1$. The second order density ρ_2 represents the density fluctuation and T_2 represents the second order thermal fluctuation. The heat release rate $\dot{Q}_0$ arises from the influence of hydrodynamics alone (due to the steady and unsteady part of the flow). The influence of the acoustic wave on the heat release rate ($\dot{Q}'$) is represented at the same order of the mean heat release rate. The next step is to incorporate multiple scales into the governing equations.

3.2.3 Incorporating multiple time and space scales

The low Mach number flow is characterized by two time scales and two length scales as $\tau = \tau'/\epsilon$ and $\eta = \xi/\epsilon$, where τ and τ' are the acoustic and the convective time scales respectively. η and ξ are the spatial scales representing the flow and the long wavelength acoustic wave respectively. The temporal operator can be then expressed as $\partial/\partial t = (1/\epsilon)\partial/\partial\tau + \partial/\partial\tau'$. The spatial operator is expressed as $\partial/\partial x = \epsilon\partial/\partial\xi + \partial/\partial\eta$ (Zank and Matthaeus, 1990).

3.2.4 Obtaining equations at various orders

The asymptotic expansion and operators are substituted into the governing equations (3.1-3.4). At leading order; i.e. $O(\epsilon^0)$, we obtain:

$$\frac{\partial \rho_0}{\partial \tau'} + \nabla_\eta \cdot \rho_0 \vec{u_0} = 0 \tag{3.10}$$

$$\frac{\partial \rho_0 \vec{u_0}}{\partial \tau'} + \nabla_\eta \cdot (\rho_0 \vec{u_0} \vec{u_0}) + \nabla_\eta p_{2h} - \frac{1}{Re} \nabla_\eta \cdot \tau_0 = 0 \tag{3.11}$$

$$\frac{1}{(\gamma - 1)} \frac{\partial p_0}{\partial \tau'} = \frac{-\gamma}{(\gamma - 1)} [p_0 \nabla_\eta \cdot \vec{u_0}] + HDa(\dot{Q}_0 + \dot{Q}') + \frac{1}{RePr} \nabla_\eta^2 T_0 \tag{3.12}$$

$$\frac{\partial \rho_0 Y_{i0}}{\partial \tau'} + \nabla_\eta . \rho_0 Y_{i0} \vec{u_0} = \frac{1}{ReSc} \nabla . \rho_0 D \nabla Y_{i0} + Da\dot{\omega}_k \tag{3.13}$$

$$p_0 = \rho_0 T_0 \tag{3.14}$$

Eqs. (3.10-3.13) imply that the unsteady hydrodynamics and its influence on heat release rate are described by the short length scale η and the convective time scale τ'.

Following (Zank and Matthaeus, 1990), the evolution of $\vec{u}_1$ on the fast time scale is obtained by collecting terms of $O(\epsilon)$ from Eq. (3.2) after the substitution of solution expansion.

$$\frac{\partial \rho_0 \vec{u}_1}{\partial \tau} + \nabla_\eta p_{2a} = 0 \tag{3.15}$$

The evolution equation for second order density is obtained at $O(\epsilon)$ as follows:

$$\frac{\partial \rho_2}{\partial \tau} + \nabla_\eta.(\rho_0 \vec{u_1}) + \nabla_\xi.(\rho_0 \vec{u_0}) = 0 \tag{3.16}$$

Equation (3.16) involves two spatial operators - one derivative with respect to the short length scale and another derivative with respect to the long length scale. This may lead to an unbounded solution ($\nabla_\xi = 1/\epsilon \nabla_\eta$) as $\epsilon \to 0$. This is the consequence of the dilatation term $\nabla.\vec{u_0}$. The dilatation term is the consequence of the volume expansion from heat release rate. Zank and Matthaeus, in their approach, has neglected this term to ensure convergence. In combustion, dilatation cannot be ignored as it is one of the acoustic sources. To ensure convergence, we follow a different approach with averaging. Averaging over the short length scale, the evolution equation for ρ_2 in the acoustic time scale is obtained.

$$\frac{\partial \overline{\rho_2}}{\partial \tau} = -\nabla_\xi.\overline{\rho_0 \vec{u_0}} \tag{3.17}$$

Integration in τ yields,

$$\rho_2 = \tau[-\nabla_\xi.\overline{\rho_0 \vec{u_0}}] \tag{3.18}$$

ρ_0, u_0 and T_0 (the hydrodynamic field variables) are independent of the acoustic time scale. Then $\rho_2 \to \infty$ as $\epsilon \to 0$ which is the case since $\tau = \tau'/\epsilon$. To guarantee the validity of asymptotic expansion, we impose the solvability condition as $\nabla_\xi.\rho_0 \vec{u_0} = 0$. In other words, we have shown that the hydrodynamic field variables are independent of the long length scale. The fast time scale evolution equation for the density perturbation ρ_2 is obtained as:

$$\frac{\partial \rho_2}{\partial \tau} + \nabla_\eta.(\rho_0 \vec{u_1}) = 0 \tag{3.19}$$

At $O(\epsilon)$, the evolution equation for acoustic pressure on the acoustic time scale is obtained.

$$\frac{\partial p_{2a}}{\partial \tau} + \gamma p_0 \nabla_\eta \vec{u_1} = -\gamma p_0 \nabla_\xi u_0 + \frac{\gamma}{RePr}[\nabla_\eta \nabla_\xi T_0 + \nabla_\xi \nabla_\eta T_0] \tag{3.20}$$

Integration with respect to τ leads to

$$p_{2a} = \tau[-\gamma p_0 \nabla_\xi u_0 + \frac{\gamma}{RePr}[\nabla_\eta \nabla_\xi T_0 + \nabla_\xi \nabla_\eta T_0]] - \gamma p_0 \int \nabla_\eta \vec{u}_1 + C \quad (3.21)$$

where C is $C(t, \eta, \xi)$. We know that the acoustic velocity $\vec{u}_1$ is a function of τ. The above expression shows that the terms with coefficient τ will grow linearly as $\epsilon \to 0$. Therefore, another solvability condition imposed to ensure the validity of asymptotic expansion is as follows:

$$-\gamma p_0 \nabla_\xi u_0 + \frac{\gamma}{RePr}[\nabla_\eta \nabla_\xi T_0 + \nabla_\xi \nabla_\eta T_0] = 0 \quad (3.22)$$

Then, from Eq. (3.21), the evolution equation for acoustic pressure p_{2a} on the acoustic time scale is obtained as

$$\frac{\partial p_{2a}}{\partial \tau} + \gamma p_0 \nabla_\eta \vec{u}_1 = 0 \quad (3.23)$$

From Eqs. (3.15) and (3.23), the linear wave equations for $\vec{u}_1$ and p_{2a} are obtained as

$$\frac{\partial^2 p_{2a}}{\partial \tau^2} - \nabla_\eta . c_0^2 \nabla_\eta p_{2a} = 0 \quad (3.24)$$

$$\frac{\partial^2 \vec{u}_1}{\partial \tau^2} - c_0^2 \nabla_\eta^2 \vec{u}_1 = 0 \quad (3.25)$$

where c_0 is the speed of sound. Then, we will assume a solution $A_i(\eta, \xi, \tau')e^{i\omega\tau}$ for the perturbation field variables, where $A_i = (\hat{\rho}_2, \hat{\vec{u}}_1, \hat{p}_{2a}, \hat{T}_2)$ and $e^{i\omega\tau}$ is the part of the solution which satisfies Eqs. (3.24) and (3.25). These equations imply that whenever there is a non-zero amplitude A_i, the acoustic pressure and velocity field variables admit an oscillatory solution.

The momentum equation at $O(\epsilon)$, the continuity equation at $O(\epsilon^2)$ and the energy equation at $O(\epsilon^2)$ yield the evolution equations for $\vec{u}_1$, ρ_2 and p_{2a} on the convective time scale. The solution form $A_i(\eta, \xi, \tau')e^{i\omega\tau}$ is substituted in the equations for $\vec{u}_1$, ρ_2 and p_{2a}. Applying the solvability conditions and collecting terms with coefficient $e^{i\omega\tau}$, a set

of weakly nonlinear equations are obtained for the convective time scale.

$$\begin{aligned}\frac{\partial \hat{\vec{u}}_1}{\partial \tau'} + \frac{1}{\rho_0}\nabla_\xi \hat{p}_{2a} = &- \vec{u_0}.\nabla_\eta \hat{\vec{u}}_1 - \hat{\vec{u}}_1.\nabla_\eta \vec{u_0} \\ &+ \frac{1}{\rho_0 Re}\nabla_\eta^2 \hat{\vec{u}}_1\end{aligned} \tag{3.26}$$

$$\frac{\partial \hat{\rho}_2}{\partial \tau'} + \rho_0 \nabla_\xi \hat{\vec{u}}_1 = -\nabla_\eta.(\hat{\rho}_2 \vec{u_0}) \tag{3.27}$$

$$\begin{aligned}\frac{\partial \hat{p}_{2a}}{\partial \tau'} + \gamma p_0 \nabla_\xi \hat{\vec{u}}_1 = &- \vec{u_0}.\nabla_\eta \hat{p}_{2a} - \gamma \hat{p}_{2a}\nabla_\eta.\vec{u_0} \\ &+ \frac{\gamma}{RePr}\nabla_\eta^2 \hat{T}_2\end{aligned} \tag{3.28}$$

The equation of state at $O(\epsilon^2)$ is obtained as follows:

$$p_{2h} + p_{2a} = \rho_0 T_2 + \rho_2 T_0 \tag{3.29}$$

Eqs. (3.26-3.28) have two spatial derivatives with respect to two length scales (η and ξ). Assuming $u_0 \to 0$ as $\xi \to \infty$ (far away from the heat source), the evolution equations for long wavelength acoustic wave can be obtained as:

$$\frac{\partial \hat{\vec{u}}_1}{\partial \tau'} + \frac{1}{\rho_0}\nabla_\xi \hat{p}_{2a} = \frac{1}{Re}\nabla_\eta^2 \vec{u}_1 \tag{3.30}$$

$$\frac{\partial \hat{\rho}_2}{\partial \tau'} + \rho_0 \nabla_\xi \hat{\vec{u}}_1 = 0 \tag{3.31}$$

$$\frac{\partial \hat{p}_{2a}}{\partial \tau'} + \gamma p_0 \nabla_\xi \hat{\vec{u}}_1 = \frac{\gamma}{RePr}\nabla_\eta^2 T_2 \tag{3.32}$$

From Eqs. (3.30-3.32), we see that the evolution of long wavelength acoustic waves is also governed by the dissipative forces. These dissipative forces are not found in previous analyses (Wu *et al.*, 2003; Wu, 2005). In flows such as low to moderate Reynolds number flows, the dissipative forces cannot be neglected. In such flows our analysis gives a better picture of flow - acoustic interaction. The damping of the long wavelength acoustic wave can result from the dissipative forces.

The evolution of acoustic field quantities on a short length scale, by assuming a solution of the form $A(\eta,\tau')e^{i\omega\tau}$, is obtained as follows:

$$\frac{\partial\hat{\vec{u}}_1}{\partial\tau'} + \vec{u_0}.\nabla_\eta\hat{\vec{u}}_1 + \hat{\vec{u}}_1.\nabla_\eta\vec{u_0} = -\frac{1}{\rho_0 Re}\nabla_\eta^2\hat{\vec{u}}_1 \tag{3.33}$$

$$\frac{\partial\hat{\rho}_2}{\partial\tau'} + \nabla_\eta.(\hat{\rho}_2\vec{u}_0) = 0 \tag{3.34}$$

$$\frac{\partial\hat{p}_{2a}}{\partial\tau'} + \vec{u}_0.\nabla_\eta\hat{p}_{2a} + \gamma\hat{p}_{2a}\nabla_\eta.\vec{u}_0 = \frac{\gamma}{RePr}\nabla_\eta^2\hat{T}_2 \tag{3.35}$$

Equations (3.33-3.35) describe the acoustic - hydrodynamic coupling. As discussed earlier, we have now obtained the coupling equations that describe the wave - mean flow interaction. For the physical phenomenon we study, we obtained the wave and mean flow variables as pressure and velocity corresponding to the acoustic and hydrodynamic fields respectively. The terms $\hat{\vec{u}}_1.\nabla_\eta\vec{u}_0$ and $\vec{u}_0.\nabla_\eta\hat{\vec{u}}_1$ in Eq. (3.33) and the terms $\hat{p}_{2a}\nabla_\eta.\vec{u}_0$ and $\vec{u}_0.\nabla_\eta\hat{p}_{2a}$ in Eq. (3.35) represent the mutual interaction of wave and mean flow.

The modification of the field around the flame arises from the dilatation $\nabla_\eta.\vec{u_0}$. The modified flow velocity is coupled with the acoustic velocity through $\hat{\vec{u}}_1.\nabla_\eta\vec{u_0}$ and $\vec{u_0}.\nabla_\eta\hat{u_1}$ terms in Eq. (3.33). These are Reynolds forces, which describe the mutual interaction between the acoustic field and the hydrodynamic field (Dastgeer and Zank, 2006). These terms are also known as convective ($\vec{u_0}.\nabla_\eta\hat{u_1}$) and lift-up terms ($\hat{\vec{u}}_1.\nabla_\eta\vec{u_0}$) in the study of destabilization of parallel flows which may eventually lead to turbulence (Marquet *et al.*, 2009). Here, we show that similar mechanism dominates the coupling of flow field near the flame with the acoustic field. The Reynolds force form a significant source term for acoustic field.

3.3 Concluding remarks

Perturbation equations are derived in this chapter, describing the flow - flame - acoustic interaction, using the method of multiple scales. We recover the linear wave equa-

tions for the acoustic field on the acoustic time scale. On the convective time scale, we derived perturbation equations describing wave - mean flow interaction. Through these perturbation equations, we show that the volume dilatation which arise from combustion can influence the acoustic velocity and pressure perturbations. A new mechanism, representing the velocity coupling, is represented by convective and lift up mechanisms. The sources of sound generation, obtained from acoustic perturbation equations, include dilatation due to heat release, convective effects of hydrodynamic field and thermal dissipation. The influence of unsteady flow field is captured using the terms $\hat{p}_{2a}\nabla_{\eta}.\vec{u_0}$ and $\vec{u_0}.\nabla_{\eta}\hat{p}_{2a}$ in Eq. (3.35). These terms are the sources to be computed from the incompressible flow field. The perturbation Eqs. (3.33-3.35) show that the interaction between the hydrodynamic and acoustic fields is weakly nonlinear; i.e. the coupling terms are the product of a mean flow term (leading order) and a perturbation quantity (small compared to the leading order term). The interaction is revealed on the hydrodynamic length scale where the convective and entropy sources are present. As discussed in chapter 1, we now can identify various sources from the perturbation equations derived.

CHAPTER 4

Identifying sources from acoustic perturbation equations

The combustion generated sound derives its energy from various types of sources. For example, heat release acts as an acoustic pressure source (Ducruix *et al.*, 2005). Since flow field affects the heat release rate during combustion, flow dynamics also influence the enhancement of acoustic pressure. Among these flow phenomena, widely seen in combustor geometries is the presence of vortex generation and the shedding of vortices. These vortices trap and carries with them the unburned gases, creating a non-uniform distribution of fuel in the combustor. The combustion, therefore happens non-uniformly, resulting in the non-uniform heat release rate. These hot spots of gas transported by the vortices travel at convective speed (Ducruix *et al.*, 2005; Poinsot *et al.*, 1987). Therefore, the source of sound is a convective - acoustic type (Zinn and Lieuwen, 2006; Shanbhogue *et al.*, 2009).

The convective - acoustic nature of the sources becomes significant in a low Mach number combustion. In low Mach number reacting flows, the convective processes and the acoustic processes act on different time scales. Sources, therefore act on multiple time scales. The behavior of acoustic field can be compared to that of a wave (see Chapter 11 Zinn and Lieuwen, 2006), that propagates on the acoustic time scale. However, the entropy and convective 'waves' are transported at the convective velocity on the convective time scale (see Chapter 11 Zinn and Lieuwen, 2006). Therefore, for each field variable; i.e. the density, velocity, pressure and temperature, there is a component that is transported on the acoustic time scale and a component transported at the convective time scale. In this chapter, we attempt to understand the relevance of each of these components (acoustic, entropy and convective sources) in exciting the acoustic field.

4.1 How sources are modeled in theoretical analysis?

The entropy, acoustic and convective sources in a combustion system are related to heat release rate arising from chemical reaction. The effect of heat release rate on the fluid flow field is through volumetric expansion ($\nabla.u$).

$$\nabla.u = \frac{-a}{\gamma p}\frac{Dp}{Dt} - \frac{1}{\rho}\sum_{k=1}^{n}\sigma_k\dot{\omega}_k \tag{4.1}$$

where $k = 1, 2, ..n$ represents the reactants. The volumetric expansion is one of the sources influencing the acoustic pressure. Volumetric expansion also forms one of the sources for the vorticity in a combustor.

$$\frac{D\Omega}{Dt} = (\Omega.\nabla)u - \Omega(\nabla.u) + \frac{\nabla\rho \times \nabla p}{\rho^2} \tag{4.2}$$

Therefore, investigations that focus on acoustic-vortex-flame interaction incorporate the influence of volumetric expansion to study the coupling mechanism between the acoustic field, flame and the flow field. However, the length scales of the flow, flame and the acoustic wave are different.

4.1.1 Time scales and length scales

The length scale of acoustic wave may range from 10^{-2} to 10^{0} (Lieuwen, 2003). The length scale for the vortices range from 10^{-5} to 10^{-1}. For acoustic - flame - vortex interaction to take place, their length scales should have an overlap (Zinn and Lieuwen, 2006, Chapter 11). Whenever there is an overlap in the length scale the transfer of energy between the acoustic and hydrodynamic fields is possible.

The coupling between the hydrodynamic field and the heat release rate is due to the presence of a thin reaction zone, with length scale comparable to the small scale eddies in the turbulent flows (Kim and Menon, 2000). However, in a laminar flow, this overlap is absent. When the flow is laminar, the overlap in time scales causes the acoustic - hydrodynamic interaction (Clanet *et al.*, 1999). Use of the method of multiple scales (MMS) to derive the perturbation equations is advantageous in this context.

Using MMS, perturbation equations can be obtained for different time and space scales. In this chapter, from the perturbation equations derived in Chapter 3, we show that the overlapping time and space scales can be represented by the convective time scale and the short length scale (representing incompressible fluid flow processes) respectively. The perturbation equations, obtained in Chapter 3, can now be examined for the presence of the acoustic, entropy and convective sources.

Equations (3.15, 3.19, 3.23) are the evolution equations for acoustic fluctuations on the acoustic time scale and Eq. (3.33, 3.34, 3.35) are evolution equations for acoustic amplitude on the convective time scale. The asymptotic expansions (3.5, 3.6, 3.7,3.8) contains the mean flow and fluctuating quantities. The final acoustic perturbation equations are the acoustic time scale Eqs. (3.15, 3.19, 3.23) and the convective time scale Eqs. (3.33, 3.34, 3.35). These equations describe the evolution of both acoustic modes and convective modes due to the convective (due to flow), acoustic, and entropy (due to the propagation of heat release rate fluctuations) sources. The identification of these modes and their corresponding sources is done using a method proposed by Ewert and Schröder (2003). Towards this purpose, the equations for fluctuations are written in the form $A\tilde{U} = \tilde{G}$. Each element in $\tilde{U}$ is expressed as:

$$\tilde{U} = (\tilde{\rho_2}(t,\tau,\eta), \tilde{u_1}(t,\tau,\eta), \tilde{v_1}(t,\tau,\eta), \tilde{p_{2a}}(t,\tau,\eta)) \tag{4.3}$$

$\tilde{U}$ is a combined Fourier and Laplace transform of the dependent variables. The combined Fourier - Laplace transform is expressed as:

$$\tilde{\phi}(\alpha,\beta,\omega) = \frac{1}{(2\pi)^3}\int_0^\infty \int_{-\infty}^\infty \int_{-\infty}^\infty \phi(x,y,t)e^{-i(\alpha x+\beta y-\omega t)}dxdydt \tag{4.4}$$

$\tilde{G} = (\tilde{S_1}, \tilde{S_2}, \tilde{S_3}, \tilde{S_4})^T$ represents the source vector. Applying the transformations to the evolution equations for density fluctuation (Eq. (3.19)), acoustic velocity and pressure field variables (Eq. (3.15) and Eq. (3.23) respectively), we find the first element of the source vector $\tilde{S_1} = -i\Im(u_1\nabla_\eta\rho_0)$ (arising from the source term for Eq. (3.19)).

The first element $\tilde{S_1}$ representing the density gradient due to heat release rate, is an entropy source. Also, we now know that the entropy source acts on the acoustic time scale. However, we still have to examine the contribution of entropy source on exciting

the acoustic modes. For the entropy source to have an effect on the acoustic time scale, we need to have a heat source that have modulation on the acoustic time scale. However, in this thesis we have assumed the mean heat release rate and the modulated heat release rate of the same order. We made that assumption based on a previous study of the pressure coupling mechanism (Clavin *et al.*, 1990). As a consequence, we may not expect the entropy source to have an influence on the acoustic modes. We will prove so using an acoustic filtering approach.

The second, third and fourth element corresponds to the initial conditions of u_1, v_1 and p_{2a} respectively, obtained as a result of Laplace transform. These correspond to the acoustic field that is established without the contribution from any sources in the reacting fluid flow. When there is no driving mechanism that sustains the initially established acoustic field, the amplitude of the field variables p_{2a} and $\vec{u}_1$ dies down. Therefore, our intention is to extract the sources that drive the acoustic field from the fluid flow field. We now know the sources. The next step is to determine the modes that are being driven by the above sources. Towards this purpose, we construct a matrix *A* that yields the eigenvalues for acoustic time scale equations. The eigenvalues are as follows:

$$\lambda_1 = \omega - c_s(\alpha^2+\beta^2)^{1/2}, \lambda_2 = \omega, \lambda_3 = \omega, \lambda_4 = \omega + c_s(\alpha^2+\beta^2)^{1/2} \tag{4.5}$$

The eigenvectors are

$$x_1 = \begin{pmatrix} c_s^{-2} & \alpha/\rho_0 c_s(\alpha^2+\beta^2)^{1/2} & \beta/\rho_0 c_s(\alpha^2+\beta^2)^{1/2} & 1 \end{pmatrix}^T \tag{4.6}$$

$$x_2 = \begin{pmatrix} 1 & 0 & 0 & 0 \end{pmatrix}^T \tag{4.7}$$

$$x_3 = \begin{pmatrix} 0 & \beta & -\alpha & 0 \end{pmatrix}^T \tag{4.8}$$

$$x_4 = \begin{pmatrix} c_s^{-2} & -\alpha/\rho_0 c_s(\alpha^2+\beta^2)^{1/2} & -\beta/\rho_0 c_s(\alpha^2+\beta^2)^{1/2} & 1 \end{pmatrix}^T \tag{4.9}$$

where c_s is the speed of sound.

The first and the fourth eigenvectors correspond to the acoustic modes. These modes correspond to the waves traveling at the speed of sound. Their presence is expected as we are analyzing the equations on the acoustic time scale. The second eigenvector has

only the first element non-zero and corresponds to the convection of density. Therefore, the second eigenvector is an entropy mode. The entropy mode arises from the density gradient source or the entropy source S_1. The second eigenvector does not correspond to the mode propagation at sound speed c_s. Therefore, second mode is not excited by the acoustic time scale sources.

The third one corresponds to the vortical mode that arises due to the presence of acoustic velocity components (i.e. u_1 and v_1). Such a mode will be present only if two dimensional or higher dimensional acoustic fields are considered (because of α and β appearing together). In a one dimensional or longitudinal acoustic field, the third eigenvector will represent a convective mode. Now, to determine the sources that excite specific modes, a filtering matrix is constructed. For an acoustic mode, the filtering matrix is $T^a = x_1(x_1^{-1}) + x_4(x_4^{-1})$. Similarly, the filtering matrix for the entropy mode $T^e = x_2 x_2^{-1}$ and the filtering matrix for the vortical mode $T^v = x_3 x_3^{-1}$ are constructed from the eigenvectors obtained. The sum of these matrices should be an identity matrix (i.e. $T^a + T^e + T^v = I$), confirming that the filtering matrices for all modes are accounted. Acoustic sources are obtained as

$$\tilde{G}^a = T^a \tilde{G} = \begin{pmatrix} S_1^a & S_2^a & S_3^a & S_4^a \end{pmatrix}^T \tag{4.10}$$

where,

$$\begin{aligned} S_1^a &= p^*_{2a(initial)} c_s^{-2}/2\pi \\ S_2^a &= u^*_{1(initial)} \alpha^2/2\pi(\alpha^2+\beta^2) + v^*_{1(initial)} \alpha\beta/2\pi(\alpha^2+\beta^2) \\ S_3^a &= u^*_{1(initial)} \alpha\beta/2\pi(\alpha^2+\beta^2) + v^*_{1(initial)} \beta^2/2\pi(\alpha^2+\beta^2) \\ S_4^a &= p^*_{2a(initial)}/2\pi \end{aligned} \tag{4.11}$$

The source vectors S_i^a, where $i = 1, 2, 3, 4$, consist of contribution from the initial conditions of acoustic field variables (i.e. $p^*_{2a(initial)}$, $u^*_{1(initial)}$ and $v^*_{1(initial)}$). The Fourier components α and β are constants. Our approach has helped to decompose acoustic, vortical and entropy modes from the governing equations. Note that we have not assumed the nature (acoustic, vortical or entropy) of the field variables at the beginning of our derivation. The nature of field variables are obtained in a straightforward man-

ner through our derivation. In the previous studies on combustion generated sound, the acoustic, vortical and entropy modes are accounted for using a Helmholtz decomposition of field variables (Noiray *et al.*, 2009). In such an approach, the decomposition of acoustic, vortical and entropy modes are made in the beginning of the analysis. Therefore, each field variable represents only one mode. However, when there are two time scales present, the field variables evolve on different time scales. Then, each of the field variables is excited by different type of sources. Use of MMS is advantageous in this context. The decomposition of field variables into various modes is helpful in describing the acoustic-flame-vortex interaction (Menon, 2005*b*). In this manner, the contribution from each mode - acoustic, vortical and the entropy fluctuations due to unsteady combustion - in driving the combustion instability can be analyzed. For example, in the case of evolution equations on the acoustic time scale, we now know that there are three modes - acoustic, vortical and entropy. Any field variable can be now decomposed as $\phi = \phi^a + \phi^v + \phi^e$, where $\phi = [\rho, \vec{u}_1, p_{2a}]$. We can also analyze the equations on different time scales and length scales. For example, on the acoustic time scale, we can now say that for a vanishing initial condition, there are no sources that drive the acoustic field. As discussed previously, from the source vector $\tilde{G^a}$, we now know that the entropy source ($\nabla_\eta \rho_0$) arising from heat release rate has no contribution to the acoustic mode in the acoustic time scale. Now, what are the sources that drives the entropy modes?. For the flame-acoustic-vortical interaction to occur, there should be a feedback from various sources to the entropy mode. Therefore, we extract the entropy source vector $\tilde{G^e}$ from the general source vector $\tilde{G}$, by applying the transformation:

$$\tilde{G^e} = T^e \tilde{G} \tag{4.12}$$

where S_i are obtained as:

$$\begin{aligned} S_1^e &= -\vec{u}_1 . \nabla_\eta \rho_0 + \rho^*_{2(initial)}/2\pi \\ S_2^e &= 0 \\ S_3^e &= 0 \\ S_4^e &= -p^*_{2a(initial)}/2\pi * c_s^{-2} \end{aligned} \tag{4.13}$$

Here we note that for vanishing acoustic initial conditions, the entropy source arises only from the density gradient. The density gradient arises from non-uniform combustion. In unsteady combustion, the local fluctuation in the burning rate created by the propagating coherent structures causes a local change in the density. This local change in propagated by the convection due to acoustic velocity $\vec{u}_1$. This process drives the entropy mode as indicated by the source S_1^e. There are no entropy sources that drive the acoustic field as the sources S_2^e and S_3^e are zeros. Also, the entropy sources are not driven the acoustic pressure field as $S_4^e \to 0$.

For vortical sources, the transformation

$$\tilde{G^e} = T^v \tilde{G} \tag{4.14}$$

is applied to obtained S_i as

$$\begin{aligned} S_1^v &= 0 \\ S_2^e &= (\beta^2/(\alpha^2+\beta^2))u^*_{1(initial)}/2\pi - (\alpha\beta/(\alpha^2+\beta^2))v^*_{1(initial)}/2\pi \\ S_3^v &= (-\alpha\beta/(\alpha^2+\beta^2))u^*_{1(initial)}/2\pi + (\alpha^2/(\alpha^2+\beta^2))v^*_{1(initial)}/2\pi \\ S_4^e &= -p^*_{2a(initial)}/2\pi * c_s^{-2} \end{aligned} \tag{4.15}$$

The sources indicate the contribution of vortical sources in driving the acoustic velocity field. $S_1^v = 0$ indicate that the vortical sources do not causes density fluctuations. However, for vanishing initial conditions S_2^v, S_3^v and S_4^v also vanishes and driving of the acoustic velocity and pressure fields is absent.

From the above discussion of sources on the acoustic time scale, in the absence of any initial acoustic field, the only possible driving mechanism is through the entropy source. However, when the entropy source causes the second order density fluctuations, the second order density is related to the acoustic pressure perturbation through the equation of state obtained at $O(\epsilon^2)$ i.e. Eq. (3.29). Therefore, the relation between the acoustic pressure and velocity fields is not evident from the acoustic time scale equations. However, the relation between the heat source that creates the density fluctuation and the acoustic velocity components is revealed through the higher order equations;

i.e. equations describing the evolution of acoustic field on the convective time scale.

Applying the transformations (4.4) to the convective time scale Eqs. (3.33, 3.34, 3.35), we obtain the sources that act on convective time scale. Equations (3.33), (3.34) and (3.35) are examined for sources that drives the fluctuation amplitudes. The eigenvalues are obtained as $\lambda_1 = \lambda_2 = \lambda_3 = \omega$. The corresponding eigenvectors are $x_1 = \begin{pmatrix} 1 & 0 & 0 & 0 \end{pmatrix}^T, x_2 = \begin{pmatrix} 0 & 1 & 0 & 0 \end{pmatrix}^T, x_3 = \begin{pmatrix} 0 & 0 & 1 & 0 \end{pmatrix}^T x_3 = \begin{pmatrix} 0 & 0 & 0 & 1 \end{pmatrix}^T$. We see from the eigenvectors that the convective time scale equations govern the evolution of convection modes. The sources that drives the amplitudes are found to be

$$S_1^c = \rho^*_{2_{initial}}/2\pi - i\Im(\rho_2 \nabla_\eta . \vec{u_0}) \tag{4.16}$$

$$S_2^c = u^*_{1_{initial}}/2\pi - i\Im(u_1 \nabla_\eta . \vec{u_0}) + i\Im(\frac{1}{\rho_0 Re}\nabla^2_\eta u_1) - \Im(\vec{u_0}.\nabla_\eta u_1)$$

$$S_3^c = v^*_{1_{initial}}/2\pi - i\Im(v_1 \nabla_\eta . \vec{u_0}) + i\Im(\frac{1}{\rho_0 Re}\nabla^2_\eta v_1) - \Im(\vec{u_0}.\nabla_\eta v_1)$$

$$S_4^c = p^*_{2a_{initial}}/2\pi - i\Im(p_{2a} \nabla_\eta . \vec{u_0}) + i\Im(\frac{1}{RePr}\nabla^2_\eta T_2) - \Im(\vec{u_0}.\nabla_\eta p_{2a})$$

The common factor in each of these source terms is the dilatation term that arise from the heat release rate ($\nabla_\eta . \vec{u}_0$) and the diffusion terms. The dilatation term couples the amplitudes of acoustic pressure, velocity and the density fluctuations. Therefore, the dilatation term serves to couple the heat release rate from the chemical reaction to the acoustic velocity field. The nature of this coupling is through the mutual transportation of the acoustic and hydrodynamic velocity fields. This mutual transportation is through a weak nonlinear coupling of the acoustic and hydrodynamic fields.

The weak nonlinear interaction between the acoustic and hydrodynamic fields act as a driving mechanism for the acoustic pressure amplitude. This nonlinear interaction is a major driving mechanism considered in the study of hydrodynamic instability (Marquet *et al.*, 2009) and magnetohydrodynamic instability (Dastgeer and Zank, 2004). In Eq. (3.33), $\vec{u_0}.\nabla_\eta \hat{u}_1$ and $\hat{u}_1.\nabla_\eta \vec{u_0}$ represent the nonlinear interaction. These terms are also known as Reynolds forces (Dastgeer and Zank, 2004). Reynolds forces, $\vec{u_0}.\nabla_\eta \hat{u}_1$ and $\hat{u}_1.\nabla_\eta \vec{u_0}$, govern the mutual transportation for acoustic and hydrodynamic field quantities. In the context of instabilities that causes transition to turbulence, $\vec{u_0}.\nabla_\eta \hat{u}_1$ and $\hat{u}_1.\nabla_\eta \vec{u_0}$ are also called convective and lift-up terms respectively (Marquet *et al.*,

2009). These mechanisms have not been discussed before in the study of combustion-acoustic coupling. The gas expansion around the flame causes the modification of the flow field around the flame. The modified flow field causes change in the acoustic velocity amplitude through convection (i.e. $\vec{u_0}.\nabla_\eta \hat{u}_1$). Then, from S_2^c and S_4^c we know that the nonlinear sources such as Reynolds forces are significant in the evolution of amplitudes of acoustic field variables.

4.2 Concluding remarks

Acoustic perturbation equations, derived using the method of multiple scales, reveals sources at various time and space scales. The significance of entropy, vortical and acoustic modes in the evolution of acoustic field is studied. The convective-acoustic nature of the sources is investigated. However, we see that the acoustic sources are present only on the acoustic time scale. The convective sources are present on the convective time scale. Therefore, a mechanism that couples the processes on two time scales is needed for the combustion-acoustic interaction. We observe that the dilatation arising from heat release rate is a possible candidate for this mechanism. The dilatation can cause changes in density at leading order, which in turn becomes the entropy source $\nabla_\eta \rho_0$ on the acoustic time scale.

The separation of sources according to the time scale in which they act is an outcome of applying the method of multiple scales (MMS). We also propose that the assumed order of heat release rate fluctuation is significant in determining the significance of each of the sources. We consider that an investigation in this direction will prove to be an improvement to the Helmholtz decomposition. In the analysis of a thermo-acoustic system, we have assumed the magnitude of heat release rate fluctuation to be of $O(1)$. Therefore, the sources that drive the acoustic pressure amplitude appear on convective time scale. As a consequence, we show that the volume dilatation which arises from combustion can influence the acoustic velocity and pressure perturbations. This interaction is represented by convective and lift up mechanisms. The sources of sound generation, obtained from acoustic perturbation equations, include dilatation due to heat release, convective effects of hydrodynamic field and thermal dissipation.

The convection of hot spots and the influence of unsteady flow field is captured using the terms $\hat{p}_{2a}\nabla_{\eta}.\vec{u_0}$ and $\vec{u_0}.\nabla_{\eta}\hat{p}_{2a}$ in Eq. (3.35). These terms are the sources to be computed from the incompressible flow field. The types of sources - acoustic, entropy and convective - are obtained from the perturbation equations. The perturbation Eqs.(3.33-3.35) show that the interaction between the hydrodynamic and acoustic fields is weakly nonlinear. The interaction is revealed on the hydrodynamic length scale where the convective and entropy sources are present.

CHAPTER 5

Nonlinear convection reaction diffusion equations

In this chapter, we describe the stability of a thermo-acoustic system by deriving a set of nonlinear equations. Our nonlinear equations belong to the class of reaction diffusion (RD) systems. RD system are well known to describe the bistable nature of many chemical reacting systems, Turing's work on morphogenesis being one among them (Turing, 1952). RD systems are widely studied in the context of pattern forming instabilities (Hoyle, 2006). Bistable solutions are an important characteristic of RD systems (Ebeling and Malchow, 1979).

The reaction diffusion equations are classified according the nonlinear terms present in these equations. Fisher's equation has a quadratic nonlinearity, whereas Newell-Whitehead-Segel equation used in the field of Rayleigh-Benard convection has a cubic nonlinearity (Gilding and Kersner, 2004). Zeldovich equation, with cubic nonlinearity, exhibiting a traveling wave solution is popular in combustion literature (Buckmaster, 1985). The traveling wave connects (form an interface between) the region of burnt and unburnt gases in a combustion process. The important characteristic of RD system is that, due to the presence of a diffusion term, a local disturbance can spread throughout the entire domain. Therefore, as proposed by Turing, a locally stable solution may become unstable.

RD system have a nonlinear reaction term and diffusion term. The diffusion coefficient is specific to the physical situation; i.e. the diffusion coefficient in the RD system corresponding to the chemically reacting system is a measure of the diffusion of mass concentration. In a system without the effects of fluid flow, the diffusion governs the transport of small but finite amplitude disturbances (perturbation in the concentration). However, in a thermo-acoustic system, the influence of fluid flow cannot be neglected. Therefore, a simple RD system will not suffice to describe the unstable phenomena caused by localized small pressure disturbances. Based on our perturbation equations Eqs. (3.33-3.35) governing the wave-mean flow interaction, we are going to

derive nonlinear convection reaction diffusion equations to describe the instabilities in a thermo-acoustic system. Here, we also include the influence of fluid flow through a convection term.

The combustion resulting from the chemical reaction influences the flow field in a thermo-acoustic system. In this chapter, we derive a class of nonlinear convection reaction diffusion (CRD) equations which incorporate the influence of convection. In the CRD system, the chemical reaction source that causes flow field modification is represented by a nonlinear reaction term. This nonlinear reaction term is obtained from the dilatation term. Therefore, we show that the dilatation that arise from combustion causes the flow field modification. From Eq. (3.12),

$$\nabla_\eta \cdot \vec{u_0} = \frac{\gamma-1}{\gamma p_0} HDa(\dot{Q}_0 + \dot{Q}') + \frac{\gamma-1}{\gamma p_0 RePr}\nabla_\eta^2 T_0 - \frac{1}{\gamma p_0}\frac{\partial p_0}{\partial \tau'} \tag{5.1}$$

The influence of $\dot{Q}$ and $\dot{Q}'$ (heat release rate fluctuation) on the acoustic pressure field is seen from the dilatation term. Expression (5.1) for dilatation is substituted in Eq. (3.35) to obtain:

$$\frac{\partial \hat{p}_{2a}}{\partial \tau'} + \vec{u}_0.\nabla_\eta \hat{p}_{2a} + \gamma \hat{p}_{2a}[\frac{\gamma-1}{\gamma p_0} HDa(\dot{Q}_0 + \dot{Q}') + \frac{\gamma-1}{\gamma p_0 RePr}\nabla_\eta^2 T_0 - \frac{1}{\gamma p_0}\frac{\partial p_0}{\partial \tau'}] = \frac{\gamma}{RePr}\nabla_\eta^2 \hat{T}_2 \tag{5.2}$$

Assuming a single step chemical reaction, $\dot{Q}'$ can be expressed as:

$$\dot{Q}' = B\rho_2^2 XY e^{-E_a/RT}, \tag{5.3}$$

where B is the preexponential factor and the density fluctuation ρ_2 is a function of τ and τ'. However, $\dot{Q} = \dot{Q}_0 + \dot{Q}'$ appears in Eq. (3.12) as well as in Eq. (5.2). From the derivation of perturbation equations in Chapter 3, we know that the leading order variables are independent of the acoustic time scale. Such a condition was necessary to ensure the convergence of asymptotic expansion. p_0 is the leading order pressure variables. Therefore, to prevent the linear unbounded growth of p_0, we should avoid the dependence of $\dot{Q}'$ on the acoustic time scale. This is done by expressing $\dot{Q}'$ in terms of

$\hat{\rho}_2(\eta, t)$. Substituting a solution of the form $A_i(\eta, \tau')e^{i\omega\tau}$ in Eq. (3.29), we obtain:

$$\hat{\rho}_2 = \frac{p_{2h}}{T_0}e^{-i\omega\tau} + \frac{\hat{p}_{2a}}{T_0} - \rho_0\frac{\hat{T}_2}{T_0} \tag{5.4}$$

As $\epsilon \to 0$, $\tau \to \infty$, because in the relation $\tau = \tau'/\epsilon$, we have assumed τ' of $O(1)$ and τ of $O(1/\epsilon)$. In the limit $\tau \to \infty$, $(p_{2h}/T_0)e^{-i\omega\tau} \to 0$. The expression for $\hat{\rho}_2$ can be rewritten as:

$$\hat{\rho}_2 = \frac{\hat{p}_{2a}}{T_0} - \rho_0\frac{\hat{T}_2}{T_0} \tag{5.5}$$

Here, we have removed the dependence of density fluctuation on the acoustic time scale. Now, the variation of the magnitude of heat release rate fluctuation is on the convective time scale, reflecting the influence of fluid flow on the acoustic pressure field. The new expression for heat release rate fluctuation can now be written as:

$$\dot{Q}' = B\hat{\rho}_2^2 XY e^{-E_a/RT} \tag{5.6}$$

Eq. (5.6) is substituted in Eq. (5.2) to obtain:

$$\frac{\partial\hat{p}_{2a}}{\partial\tau'} + \vec{u}_0.\nabla_\eta\hat{p}_{2a} = \frac{(\gamma-1)HD_a\omega}{p_0}\left(\frac{-\hat{p}_{2a}^3 + 2\rho_0\hat{p}_{2a}^2\hat{T}_2 p_{2a} - \rho_0^2\hat{T}_2^2}{T_0^2}\right) \tag{5.7}$$

$$+\frac{\gamma}{RePr}\nabla_\eta^2\hat{T}_2 - \frac{(\gamma-1)\hat{p}_{2a}}{p_0 RePr}\nabla_\eta^2 T_0 - \frac{(\gamma-1)HD_a\rho_0^2\omega\hat{p}_{2a}}{p_0} + \frac{p_{2a}}{p_0}\frac{\partial p_0}{\partial\tau'} \tag{5.8}$$

where $\omega = BXYe^{-Ea/RT}$. Matching the terms of same order, Eq. (5.7) can be rewritten as follows:

$$\frac{\partial\hat{p}_{2a}}{\partial\tau'} = -\vec{u}_0.\nabla_\eta\hat{p}_{2a} + \alpha\hat{p}_{2a}^3 + \theta\hat{T}_2\hat{p}_{2a}^2 + \vartheta\hat{T}_2^2\hat{p}_{2a} + \lambda\hat{p}_{2a} + \frac{\gamma}{RePr}\nabla_\eta^2\hat{T}_2 \tag{5.9}$$

Substituting (5.5) in Eq. (3.34), we obtained an equation for T_2.

$$\frac{\partial\hat{T}_2}{\partial\tau'} = -\vec{u}_0.\nabla_\eta\hat{T}_2 + \alpha\hat{T}_2\hat{p}_{2a}^2 + \theta\hat{T}_2^2\hat{p}_{2a} + \vartheta\hat{T}_2^3 + \lambda\hat{T}_2 + \frac{\gamma}{\rho_0 RePr}\nabla_\eta^2\hat{T}_2 \tag{5.10}$$

Equations (5.9-5.10) are nonlinear evolution equations for acoustic pressure and second order thermal fluctuations. The coefficients α, θ and ϑ correspond to the physical processes in the system such as heat release rate, temperature diffusion and the rate of

change of the mean pressure p_0. The nonlinear terms in Eqs. (5.9-5.10) have contribution from the thermal and acoustic pressure fluctuations. Therefore, the nonlinear Eqs. (5.9-5.10) represent a 'pressure - temperature' coupling.

5.1 Coupling mechanisms

5.1.1 Pressure-Temperature coupling

As suggested by Clavin *et al.* (1990), the pressure coupling is established when $\dot{Q}'$ and $\hat{p}_{2a}$ are of the same order. In our derivation, we have achieved the same order of magnitude for acoustic pressure and heat release rate fluctuations with $\dot{Q}'$ appearing as a source to $\hat{p}_{2a}$ (see Eq. (5.2)). Apart from the coupling between the acoustic field and the heat release rate fluctuation, we also have the influence of the hydrodynamic field represented as $\vec{u}_0.\nabla_\eta$ (the convective term) in the nonlinear equations. Therefore, using the nonlinear equations we can explain the acoustic-flame-flow interaction.

5.1.2 Convection reaction diffusion equations

Equations (5.9-5.10) can be written as follows:

$$\frac{\partial \hat{p}_{2a}}{\partial \tau'} + \vec{u}_0.\nabla_\eta \hat{p}_{2a} = f(\hat{p}_{2a}, \hat{T}_2) + \frac{\gamma}{RePr}\nabla^2_\eta \hat{T}_2 \tag{5.11}$$

$$\frac{\partial \hat{T}_2}{\partial \tau'} + \vec{u}_0.\nabla_\eta \hat{T}_2 = g(\hat{p}_{2a}, \hat{T}_2) + \frac{\gamma}{\rho_0 RePr}\nabla^2_\eta \hat{T}_2 \tag{5.12}$$

where $f(\hat{p}_{2a}, \hat{T}_2) = \alpha\hat{p}^3_{2a} + \theta\hat{T}_2\hat{p}^2_{2a} + \vartheta\hat{T}^2_2\hat{p}_{2a} + \lambda\hat{p}_{2a}$ and $g(\hat{p}_{2a}, \hat{T}_2) = \alpha\hat{T}_2\hat{p}^2_{2a} + \theta\hat{T}^2_2\hat{p}_{2a} + \vartheta\hat{T}^3_2 + \lambda\hat{T}_2$ are nonlinear functions in the convective reaction diffusion equations. The coefficients α, θ, ϑ and λ are:

$$\alpha = -\frac{(\gamma - 1)HD_a\omega}{p_0 T_0^2} \tag{5.13}$$

$$\theta = 2\frac{(\gamma-1)HD_a\omega}{p_0T_0^2}\rho_0 \tag{5.14}$$

$$\vartheta = -\frac{(\gamma-1)HD_a\omega}{p_0T_0^2}\rho_0^2 \tag{5.15}$$

$$\lambda = -\frac{(\gamma-1)}{p_0RePr}\nabla_\eta^2 T_0 - \frac{(\gamma-1)HD_a\rho_0^2\omega}{p_0} + \frac{1}{p_0}\frac{\partial p_0}{\partial \tau'} \tag{5.16}$$

The linear term $\lambda\hat{p}_{2a}$ can be rewritten as $-(\gamma-1)\hat{p}_{2a}/(p_0RePr) \times \nabla_\eta^2 T_0 - (\gamma-1)\dot{Q}\hat{p}_{2a}/p_0 + (\gamma-1)\dot{Q}'\hat{p}_{2a}/p_0 + (\hat{p}_{2a}/p_0) \times \partial p_0/\partial\tau'$. The factor $\hat{p}_{2a}\dot{Q}'$ represents the product of the heat release rate magnitude and the acoustic pressure amplitude. This factor is similar to Rayleigh index $G(x)$, which is:

$$G(x) = \frac{1}{T}\int q'(x,t)p'(x,t)dt \tag{5.17}$$

which represents the product of the heat release rate fluctuation and the acoustic pressure averaged over one oscillation cycle. The oscillation occurs on the fast acoustic time scale. $G(x) > 0$ implies the growth of acoustic pressure and $G(x) < 0$ implies the damping. The term $\hat{p}_{2a}\dot{Q}'$, which is obtained by the elimination of fast acoustic time scale evolution, represents the Rayleigh index. This term is contained in the linear term. The linear term, therefore determines the linear growth rate. Representing the acoustic-hydrodynamic interaction as a CRD system has an advantage. Now we can say that the stability characteristics of a thermo-acoustic system resemble that of any reaction diffusion system. We can explore the stability of our system using the methods employed in exploring the stability of a wide variety of other dynamical systems. These dynamical systems include the popular Rayleigh-Benard convection model (Newell and Whitehead, 1969), FitzHugh-Nagumo model (for neural oscillators) (FitzHugh, 1955) and Turing model (for morphogenesis) (Turing, 1952). Therefore, our representation of thermo-acoustic system as a convective reaction diffusion system has many advantages. For example, the RD equations represent the propagation of a front. The front can represent the location of inhomogeneity in a system, connecting the homogenous states on either sides of the inhomogeneity. For example, the flame in a thermo-acoustic system represents a front in an otherwise homogenous hydrodynamic field. The temperature

rise at the interface of burnt and unburnt mixtures, caused by a reaction zone is another example of front in combustion. Schvab-Zel'dovich equation is an RD equations to compute the propagation of such fronts. In the present context, we will describe the propagation of localized small pressure perturbation introduced by the heat source.

The CRD equations, with the coefficients representing the physical parameters, gives insight to the role of each parameter on the stability of the system. The coefficient of the linear term (λ) in Eq. (5.9) shows that acoustic pressure amplitude evolves linearly due to the rate of change of the mean pressure and the mean heat release rate. As shown by Eq. (3.12), the rate of change of mean pressure, also known as 'DC shift', has contribution from the heat release rate fluctuation due to the acoustic field. The origin of DC shift and its relation to the acoustic pressure oscillation was theoretically explained earlier (Flandro *et al.*, 2007). Previous investigations reveal that these process, DC shift and growth of acoustic pressure amplitude, share a common mechanism. We have revealed a new mechanism - coupling of acoustic pressure oscillation with heat release rate fluctuation - relating the growth in acoustic pressure amplitude with the DC shift.

Nonlinear terms are derived from the heat release rate fluctuation term. Therefore, 'weights' of the nonlinear terms α, θ and ϑ decide the intensity of heat release rate fluctuation. These weights are functions of Damkohler numeber Da and heat release rate ω. The weights are therefore functions of physical variables. Their magnitudes depend on the type of fuel, mass fractions of fuel and air and the temperature in the system. Another factor that is incorporated in θ and ϑ is density ρ_0. Influence of these weights on the stability characteristic of a thermo-acoustic system is demonstrated in the next section using some examples.

5.1.3 Transition from non-oscillatory state to oscillatory state

In this section we construct an example using which we demonstrate the transitions exhibited by a thermo-acoustic system. In Fig. (5.1), we illustrate the physical meaning of our example problem. The perturbation (shown by a tiny lump) on the long length scale acoustic wave represent the short length scale acoustic perturbation. Equations (3.31-

3.32) describe the spatial evolution of long length scale acoustic field. This evolution encounters the short length scale dissipative effects in the form of thermal diffusion and viscous dissipation. On the long length scale, the evolution equations do not have a source term that drives the acoustic field. On the other hand, the driving terms - the convection term and the nonlinear term representing the heat release rate fluctuation - are written with respect to the short length scale variable η. We have also expressed the dissipative effects on the short length scale in the CRD system. Therefore, the CRD system, describing the spatial evolution of perturbations on the short length scale, is more suitable to study the evolution of any acoustic perturbations. In physical systems, such a small length scale perturbation is introduced by localized heat sources such as premixed flame located in a long tube (Wu *et al.*, 2003; Wu, 2005) or electrically heated mesh in a Rijke tube (Mariappan and Sujith, 2011). The local perturbation grows in amplitude in time. The perturbation also spread spatially. The spatiotemporal evolution eventually modifies the acoustic field in the duct. In real combustors, the local fluctuations in the heat release rate can occur from the localized burning of gases entrapped in vortices (Poinsot *et al.*, 1987). Our model problem serves the purpose of investigating the influence of such a local heat source on the acoustic-hydrodynamic coupling.

As far as the type of heat source is considered, which is localized in space, the model problem represents the heat release rate-acoustic interaction in a horizontal Rijke tube. However, in the previous studies the entire heat source in localized. In our model problem, the heat release rate fluctuation is localized. Uniform heat release rate is specified everywhere else. The localized heat release rate, which is higher than the rest of the computational domain is specified with the help of the coefficients or 'weights' of the nonlinear terms. The weights are function of heat release rate. Therefore, the localized fluctuations are specified by providing the values of α, θ and ϑ to be 1.2 times their values in the rest of the domain. The localized heat release rate can also occur when there is a localized perturbation in species mass fractions. However, the species mass fractions decide the heat release rate. Therefore, we do not specify the values of species mass fractions separately. We use these assumptions to reduce the complexity of the model problem. A simple model problem such as the one formulated will help us to investigate the nonlinear nature of acoustic-hydrodynamic interaction.

We study the short scale acoustic-hydrodynamic interaction using CRD system. We have achieved the isolation of long length scale phenomena from the short length scale phenomena through the derivation (see Eqs. (3.30-3.32)). CRD system, thus obtained, is the mathematical description of flame-acoustic interaction. Therefore, the present investigation emphasize the role of short length scale flame-acoustic interaction in establishing the acoustic-hydrodynamic interaction. The space scale separation that we achieved is an advantage of applying the techniques of MMS.

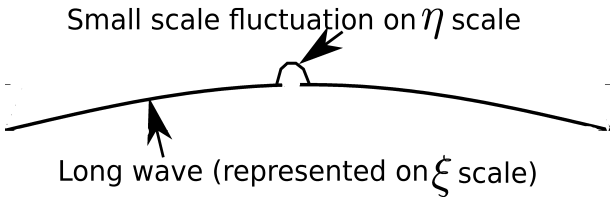

Figure 5.1: Illustration of small but finite amplitude local perturbation on the acoustic field.

A one dimensional domain with N = 56 grid points is created. The CRD system is solved on the one dimensional domain (see Fig. (5.2)). The number of grid points is selected based on a convergence study. The coordinate x defines the spatial location. A small but finite amplitude perturbation (shown in Fig. (5.3)), that represents the small scale perturbation in Fig. (5.1), is applied at the center of the solution domain. The solution of the acoustic field variables on the long length scale acoustic field is separated from solution of the short scale acoustic perturbations. Therefore, assuming an open-open duct, we impose the same boundary conditions (BC) at both endpoints. We impose the values at the endpoints to be same as their adjacent points. This is a simple BC, which we believe will prevent any spurious numerical oscillations and help in the convergence of numerical solution. Also, this BC is sufficient to study the nonlinear dynamics of acoustic-hydrodynamic interaction.

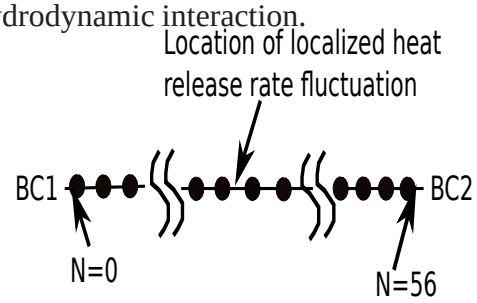

Figure 5.2: 1D representation of an open-open tube with flame located in the centre.

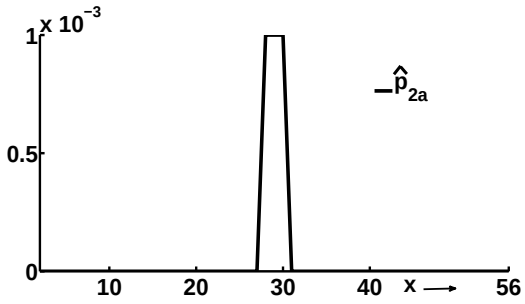

Figure 5.3: The initial condition for acoustic pressure perturbation amplitude. X-axis shows the number of grid points representing the discretized 1D geometry.

Next, we need to choose a bifurcation parameter. We have chosen the coefficient λ of the linear term for this purpose. Our choice is due to the study by Flandro *et al.* (2007), where investigates the significance of DC shift in the transition of acoustic field from non-oscillatory to oscillatory state. We also have contribution from thermal diffusion and mean heat release rate in deciding the magnitude of λ. In our bifurcation study, we use numerical methods available in XPPAUT (Ermentrout, 2002) for the time marching solution and the continuation methods available in AUTO (Doedel *et al.*, 1997) for constructing bifurcation diagrams. We obtained two types of bifurcations: one, a bifurcation that exhibits hysteresis effects and another a supercritical bifurcation that further bifurcates to create a bistable zone. The later is called a secondary bifurcation (Ananthkrishnan *et al.*, 1998).

A model Ginzburg Landau equation (GLE), which is another CRD system, was proposed by Chomaz (1992) as a bistable dynamical system model for studying hydrodynamic stability. Using our derived CRD system, in addition to the study of bistability, we investigate the variation in saturation amplitude and the variation in the threshold point as a response to the variation in the weights of nonlinear terms. Figures (5.4-5.6) show these variations as a result of variation in θ and ϑ.

We have a bifurcation that shows the existence of hysteresis zone where there are two stable states: one is an oscillatory state shown by the higher amplitude state in Fig. (5.4) and other one is a non-oscillatory state shown by the zero amplitude branch. Here, since the bifurcation diagram is computed from the evolution equation for acoustic pressure amplitude, the zero amplitude branch implies non-oscillatory state (i.e. $p_{2a} = \hat{p}_{2a}e^{i\omega\tau}$, when $\hat{p}_{2a} = 0$, $p_{2a} = 0$). This reduction in order, by the separation

of fast oscillation, is an advantage of our approach. As a consequence, the origin of limit cycle oscillations from Hopf bifurcation (Burnley and Culick, 1996; Subramanian *et al.*, 2013) could be interpreted as the transition from zero amplitude to non-zero amplitude branch through pitchfork bifurcation. Computation time can be saved by this separation. In Fig (5.6), we have another type of bifurcation where two oscillatory states that bifurcate from a primary supercritical bifurcation. This type of bifurcation is relevant in mechanical systems (Ananthkrishnan *et al.*, 1998) and in thermo-acoustic systems (Juniper, 2011).

A unique feature of the CRD system is the type of hysteresis shown in Fig. (5.4). This type of hysteresis arise as a result of an 'imperfect' or 'perturbed' pitchfork bifurcation (Hoyle, 2006). Previous investigations (Burnley and Culick, 1996; Subramanian *et al.*, 2013) show that the hysteresis region is created in the vicinity of a subcritical Hopf bifurcation. However, we show that a perturbed pitchfork bifurcation can also create a hysteresis region. In this section, we will show that this perturbation is due to the quadratic nonlinear term ($\hat{p}_{2a}^2$) present in the nonlinear equations. Such type of bifurcation was not discovered earlier in the study of combustion instability. Hysteresis creates a bistable zone.

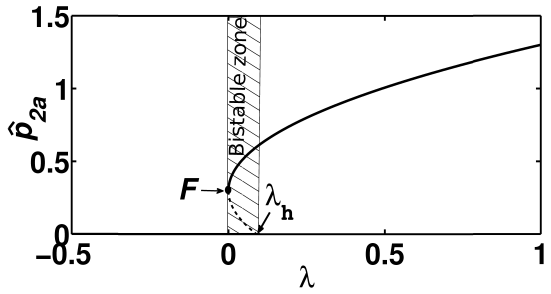

Figure 5.4: Bifurcation diagram, computed using AUTO, for acoustic pressure amplitude p_{2a}. Unstable solutions are indicated by dotted lines and stable solutions are indicated by solid lines. A hysteresis zone exist between the fold point F and $\lambda = \lambda_h$. We have chosen α = -1, θ = 0.6, ϑ = -0.09 and u_0 = 1 for the computation of this diagram.

A bifurcation creating a bistable zone has a bifurcation point λ_h which marks the upper limit of the parameter space in which stable non-oscillatory and oscillatory solutions coexist. When $\lambda > \lambda_h$ zero amplitude or non-oscillatory solution is unstable. Any small perturbation will attain a finite high amplitude branch. We have shown in this thesis, the influence of weights θ and ϑ on the location of λ_h (shown in Fig. (5.5)).

These weights are functions of ρ_0 and are related to each other. As the value of ϑ and θ decreases, λ_h moves towards the point $\lambda = 0$, thereby decreasing the hysteresis width. Also, the amplitude of the non-zero branch reduces as ϑ is reduced in magnitude. The magnitude of burned gas density, therefore, has a significant effect on the hysteresis width. Therefore, the magnitude of weights serves two purposes: the determination of saturation amplitude and the value of bifurcation parameter at which transition occurs.

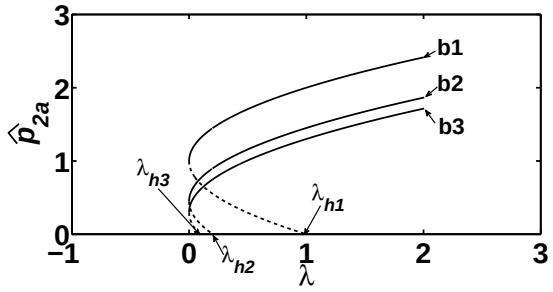

Figure 5.5: We show the influence of the magnitude of θ andϑ on the location of λ_h. We use the values θ = 2 and ϑ = -1 for the computation of b1, θ = 0.9 and ϑ = -0.2025 for b2 and θ = 0.6 and ϑ = -0.09 for curve b3. λ_{h1}, λ_{h2} and λ_{h3} are the bifurcation points for curves b1, b2 and b3 respectively. The curves are obtained by numerical continuation, using AUTO.

The variation in the location of λ, causing the change in the hysteresis width, may interest the researchers in thermo-acoustics. One of the recent investigation by Gopalakrishnan and Sujith (2014) experimentally investigated the cause of change in hysteresis width. The influence of mass flow rate on the reduction of hysteresis width was investigated by Matveev (2003). The weights are decided by factors such as Damkohler number Da, which in turn is the ratio of flow time scale to the chemical time scale. Therefore, Da depends on the mass flow rate. Further, a relation between chemical time scale and acoustic time scale could be made based on the study by McIntosh (1991). Such an investigation is within the scope of our theory. The secondary bifurcation shown in Fig. (5.6) is another promising finding of our investigation. The secondary fold point F_1 creates a another oscillatory branch. The secondary bifurcation is exhibited for weights 2 times their values in the rest of the domain. There are two stable oscillatory branches for the same λ. This implies that the perturbations of magnitude greater than the threshold curve U_2 reaches the higher amplitude branch C_2. Lower magnitude perturbations (magnitude less than U_2) attains the lower amplitude branch C_1. Therefore, secondary bifurcation also create a bistable zone.

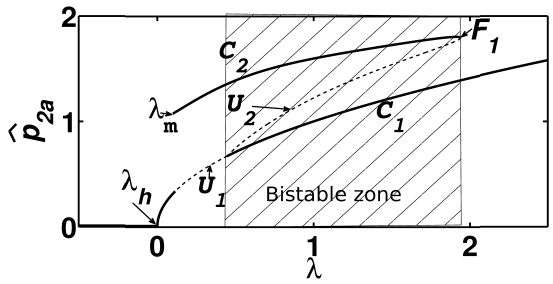

Figure 5.6: Bifurcation diagram, computed using AUTO, showing supercrtitical bifurcation with dotted line showing unstable solutions and solid lines showing stable solutions. A bistable zone is created because of the fold bifurcation at F_1. We have used the values α = -1, θ = 1, ϑ = -0.01 and u_0 = 1. For $\lambda > \lambda_h$, system is unstable.

This type of secondary bifurcation was studied by Ananthkrishnan *et al.* (1998) to show the existence of multiple limit cycles in vibrating mechanical systems. Multiple limit cycles are a consequence of secondary bifurcation. However, he used a Van der Pol oscillator to explain the secondary bifurcation. Later such models were used by Ananthkrishnan *et al.* (2005) to explain multiple limit cycles in a thermo-acoustic systems. Juniper (2011) used a nonlinear heat release rate term ($\propto (u_0/3)^{1/2}$) to show multiple limit cycle in thermo-acoustic system. Our theory also shows that the existence of secondary bifurcation is a result on nonlinear source term. A distinction between two types of bifurcations that we observed is that one type of bifurcation exhibits hysteresis in the vicinity of λ_h and another type does not exhibit hysteresis in the vicinity of λ_h. We will now investigate the transition from one type to another type of bifurcation.

5.1.4 Supercritical bifurcation as a limiting case

Thermo-acoustic systems are known to exhibit both supercritical and subcritical bifurcations (Waugh, 2013). He described these bifurcations as a consequence of the nonlinear processes in the system. A dynamical system that undergoes subcritical bifurcation exhibits hysteresis zone. In a supercritical bifurcation, hysteresis effect is absent. However, a mechanism that causes the transition from a bifurcation with hysteresis to a supercritical bifurcation is unknown. Our nonlinear theory formulated as nonlinear CRD system also can exhibit the bifurcation with hysteresis and the supercritical bifurcation. We show a possible reason for the transition from one type to another type of bifurcation

using CRD system. We use mean density ρ_0 as a parameter for showing the transition. Mean density changes as a response to the rise in temperature during combustion. ρ_0 can also be related to the mass flow rate of air-fuel mixture supplied to the combustion chamber. Mean density is also dependent on the preheat temperature. Fuel-air mixture is preheated to thrice the ambient temperature in many combustion applications (Menon, 2005*a*). Therefore, mean density is a parameter which represents the combustion process. The change in mean density causes variation in θ and ϑ. The manner in which this variation occur is described by Eqs. (5.14-5.15). We can see from Fig. (5.8) that the hysteresis width is reduced while ρ_0 is reduced. The problem description is the same as the one described for the computation of Fig. (5.4). There is a localized heat release rate fluctuation. Therefore, the short length scale acoustic-hydrodynamic interaction is investigated for explaining the phenomenon of variation in the hysteresis width. The reduction in the hysteresis width is linear with respect to the variation in

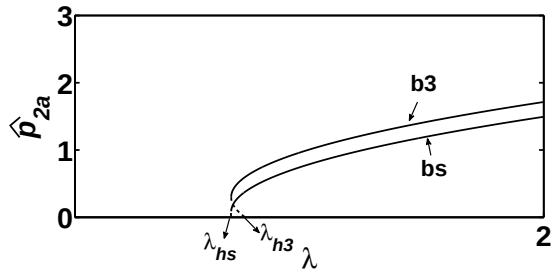

Figure 5.7: Transition from the bifurcation exhibiting hysteresis to a supercritical bifurcation as ϑ, θ are reduced. The change in ϑ and θ is in response to the change in ρ. The relations between the mean density and the weights are described by Eqs. (5.14-5.15).

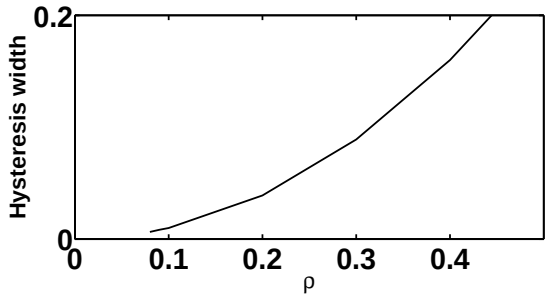

Figure 5.8: Hysteresis width is reduced as $\rho \to 0$. The reduction in ρ reduces the weight θ linearly and the weight ϑ quadratically.

ρ_0. However, as ρ_0 becomes close to zero, the hysteresis width approaches to zero only

asymptotically. The lower values of ρ_0 result in very low values of ϑ ($O(10^{-3})$) in the CRD system. Thereafter, convergence in solution is difficult to achieve. Therefore, we have computed hysteresis width only till $\rho_0 = 0.08$. In the next section, we will show that the change in the type of bifurcation from one that exhibit hysteresis to supercritical is a result of quadratic nonlinearity.

5.1.4.1 Cause of change in the type of bifurcation

The quadratic nonlinearity ($\hat{p}_{2a}^2$) in the nonlinear evolution equations for acoustic pressure amplitude has a significant effect on determining the type of bifurcation. In this section, we will demonstrate this effect by arbitrarily choosing θ, the coefficient of the quadratic nonlinear term, to be 0. In Fig. (5.9b), we show that in the absence of quadratic nonlinear term the bifurcation is supercritical. In Fig. (5.9a), we introduce the quadratic term by imposing a non-zero value for θ and retrieve the hysteresis behavior.

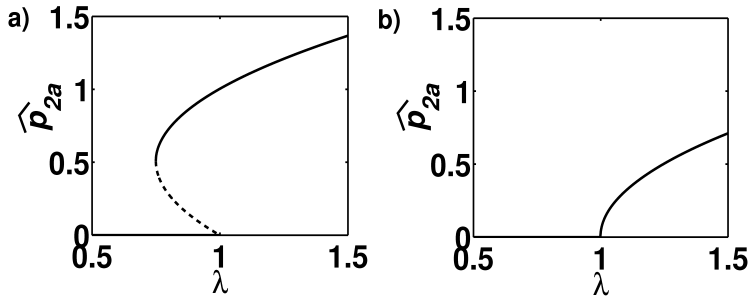

Figure 5.9: a) Bifurcation diagram of $\hat{p}_{2a}$ computed using AUTO with the coefficients α=-1, θ=0 and ϑ=-1, b) Bifurcation diagram of $\hat{p}_{2a}$ with the coefficients α=-1, θ=1 and ϑ=-1.

The hysteresis behavior, in the bifurcation described above, arise from a 'perturbation' of 'imperfection' in the normal form (Eq. (1.16)) of supercritical bifurcation (Hoyle, 2006). The normal form has only a linear term and a cubic term. Therefore, the quadratic term in the CRD system is a perturbation. Perturbed bifurcation problems are discussed widely in the field of beam buckling (Jackson, 1992; Golubitsky and Schaeffer, 1978). For example, in the context of Euler beam buckling problem, Golubitsky and Schaeffer (1978) has explained the effect of a perturbation in the potential energy in causing sudden buckling. They have shown the perturbations in both supercritical and transcritical bifurcations, associated with the bucking of beams, when the critical

compressive force is exceeded. Now we know the influence of quadratic nonlinearity on the hysteresis exhibited by our CRD system. Next, we will discuss the trend in the variation of hysteresis width.

5.1.4.2 Power law variation of hysteresis width

For the parameter range shown in Fig. (5.8), the variation of the hysteresis width in response to the variation in the mean density obeys the power law. The hysteresis width varies as ρ_0^2. A log-log plot is shown in Fig. (5.10). Recently, the power law relation

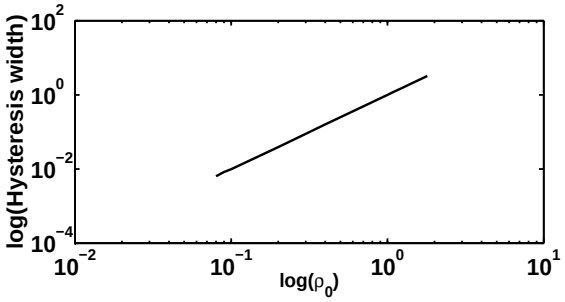

Figure 5.10: Log-log plot showing the variation in the hysteresis width in response to the variation in density. A linear variation in the log-log plot is obtained because the hysteresis width is proportional to ρ_0^2.

between the variation in the hysteresis width and the Strouhal number was shown in experiments by Gopalakrishnan and Sujith (2014). They defined the Strouhal number to be the ratio of the convective to acoustic time scales. ρ_0 can have an influence on the mass flow rate. Mass flow rate determines the convective speed. Also the Damkohler number that appear in the weights is the ratio of the convective time scale to the chemical time scale. Therefore, the weights are also functions of time scales. A conjecture could be made relating the ratio of time scales to the hysteresis width. An investigation in this direction comes under the scope of present work. We show in Fig. (5.7), the transition from a bifurcation resulting in finite width hysteresis region (shown by curve b_3) to a supercritical bifurcation (shown by curve b_s). Such a transition is the consequence of reduction in the magnitude of the coefficients of nonlinear terms due to the reduction in the mean density. Now we need to know the influence of convection on the transition to instability.

5.1.5 Propagating flame inside a duct

Thermo-acoustic instability has also been investigated for an experimental configuration where a premix flame propagates in a tube (Searby, 1992). In such cases, the convective effects are negligible. Therefore, the convective term can be neglected. For studying the influence of propagation of the premix flame on the acoustic field inside a tube, we need to introduce a coordinate transformation. The frame of reference is fitted onto the flame front by introducing the transformation $X = \eta - w\tau'$ for the CRD system. w is the speed of propagation of the flame front. Experiments by Searby (1992) and Clanet *et al.* (1999) confirms 'primary instability' where the heat release rate fluctuation due to the flame front fluctuation leads to the growth in the acoustic pressure amplitude. The growth is exponential followed by a nonlinear saturation. To reproduce this trend, we have applied the coordinate transformation to reduce the CRD system into a set of ordinary differential equations; i.e. $d\hat{p}_{2a}/dX = -1/w(f + (1/RePr)d^2\hat{T}_2/dX^2)$ and $d\hat{T}_2/dX = -1/(\rho_0 w)(g + (\gamma/RePr)d^2\hat{T}_2/dX^2)$, where f represents the nonlinear terms in Eq. (5.9) and g represents the nonlinear terms in Eq. (5.10). To represent the heat release rate fluctuation, we impose values for α, θ and ϑ (As we have discussed before, these coefficients represent the intensity of heat release rate fluctuation). In Fig. (5.11), we show the evolution of acoustic pressure amplitude with respect to the spatio-temporal coordinate X. The exponential growth and the saturation of acoustic pressure amplitude is evident from Fig. (5.11a). In Fig. (5.11b), we plot the evolution with respect to various λ. As the coefficient λ is increased, the growth rate increases (growth rates for the curves $c2 > c3 > c1$). However, we also see that the saturation amplitude is not determined by the growth rate (amplitude for $c3 > c2 > c1$). Saturation amplitude is determined by the coefficients of nonlinear terms. Therefore, we know that λ represents the linear growth rate.

5.1.6 Effect of convection term

In Section 5.1.3, we discussed the transition to instability when a localized perturbation is present in the domain. The localized perturbation spreads over the entire domain and induce global instability. However, the manner in which this spread occurs in not

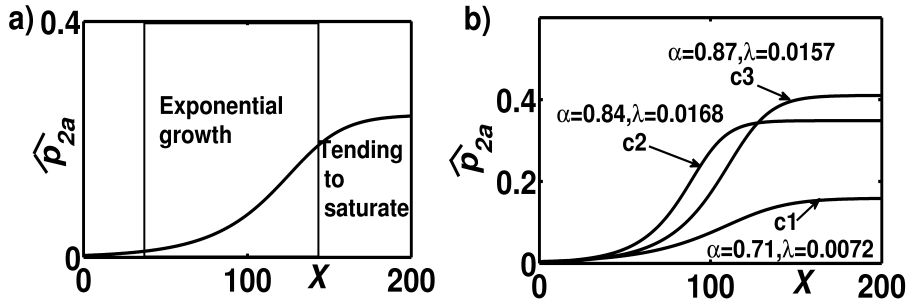

Figure 5.11: The exponential growth of the acoustic pressure amplitude $\hat{p}_{2a}$ which is followed by the nonlinear saturation. a) Regimes of the exponential growth and the saturation. This curve is computed from the coordinate transformed CRD system with $\lambda = 0.0072$, $\alpha = 0.71$, $\theta = 1.42$, $\vartheta = 0.5041$ and $w = 0.23$ (also the curve $c1$ in b). The comparison of growth rates for various values of coefficients is shown in b: curve $c2$ is obtained by using $\lambda = 0.0168$, $\alpha = 0.84$, $\theta = 1.68$, $\vartheta = 0.7046$ and $w = 0.33$ and curve $c3$ is obtained by using $\lambda = 0.0157$, $\alpha = 0.87$, $\theta = 1.74$, $\vartheta = 0.7569$ and $w = 0.35$.

yet clear. In a reaction-diffusion system the local spatial perturbation is communicated to the neighboring spatial location through the diffusion process. Diffusion process is slower than the convective process. In CRD system, we have a convective term in addition to the diffusion term. Therefore, we investigate the influence of this convection term in the spread of local perturbation.

We have provided a non-zero value for u_0 in the computation of bifurcation diagrams 5.4 and 5.6. In Fig. (5.12), we show that without convection the localized perturbation will only grow temporally. Therefore, we suppose that the role of diffusion in the spread of localized disturbances in a reaction-diffusion system is played by the convection term in our CRD system. Each of the grid points represent a node which interact with the neighboring nodes. The information or the disturbances in each node should be communicated with the neighboring nodes for the local perturbation to grow spatially. However, in the absence of convection this communication is absent. In Fig. (5.13), we impose an arbitrary value for u_0 and show that the local disturbances spread all over the solution domain. Therefore, we now know that the localized perturbation spread spatially as a result of convection. In the next chapter, we emphasize the effect of convection in the spatial growth of localized disturbances.

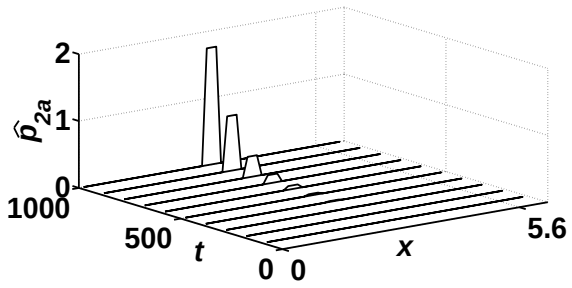

Figure 5.12: The spatiotemporal evolution of $\hat{p}_{2a}$ without the influence of convection

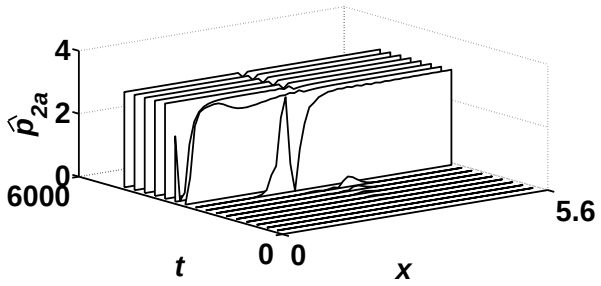

Figure 5.13: In the presence of convection the local perturbations grow both in space and in time when u_0 = 0.1

5.2 Conclusion

In this chapter, we have developed a set of convection reaction diffusion (CRD) equations. The thermal-acoustic interaction that represents the pressure-temperature coupling is explained using the new nonlinear CRD equations. Using the CRD system, the mechanism of acoustic-hydrodynamic interaction that leads to thermo-acoustic instability is examined. The convective term $\nabla_\eta.\vec{u}_0$ represents the influence of hydrodynamic field. The nonlinear reaction term in the CRD equations represent the influence of heat release rate fluctuations. The heat release rate fluctuation is shown to be a consequence of chemical reaction-acoustic interaction. We prove that the chemical reaction-acoustic interaction is responsible for the coupling of the acoustic field variables; i.e. the second order thermal, second order density and the acoustic pressure fluctuations, with the hydrodynamic field.

Solving for the CRD system, we observed two types of bifurcations: 1) a bifurcation that introduces bistable zone consisting of oscillatory and non-oscillatory solutions and 2) a bifurcation that introduces bistable zone with two oscillatory solutions. The theory is formulated through a rigorous mathematical derivation from the governing equations

for compressible fluid flow. The control parameters that determines the bifurcation characteristics are the parameters governing combustion process. These parameters can be related to the ratio of time scales, the mass flow rate and the preheat temperature. Therefore, the weights that determine the strength of nonlinearity have physical meaning. This is an improvement over the present theoretical models.

In this chapter we have explained the origin of hysteresis using the physical parameters such as heat release rate, Damkohler number and mean density in the combustion chamber. In the next chapter, we investigate the influence of convection on the spatiotemporal growth of local pressure disturbances.

CHAPTER 6

Influence of convection on the stability characteristics of thermo-acoustic system

In the previous chapter, we saw that the representation of thermo-acoustic system as a convection reaction diffusion system (CRD). We saw that the fluid flow velocity has a significant role in transporting the local acoustic pressure disturbances, leading to the spread of disturbances in space. As an outcome of our analysis of thermo-acoustic system, we have shown the existence of a hysteresis zone accompanying the bifurcations. In the control parameter space where hysteresis effects are found, oscillatory and non-oscillatory solutions coexist. Such a phenomenon is called bistability. Bistability is a significant stability characteristic of a thermo-acoustic system (Zinn and Lieuwen, 2006; Subramanian *et al.*, 2013; Burnley and Culick, 1996).

As discussed in Chapter 1, the existence of a bistable zone is due to the existence of two types of physical mechanisms - a mechanism that damps the acoustic pressure amplitude and another mechanism that acts to amplify the acoustic pressure amplitude. These physical mechanisms arise from various acoustic sources in a reacting flow field. We use the term 'sources', as they resemble the aeroacoustic sources found using the source filtering approach of aeroacoustic perturbation equations (Ewert and Schröder, 2003). One such mechanism is due to the convection due to the fluid flow. Convection of acoustic energy is one such factor that influences the stability of the system. In chapter 4, from the demonstration of the transition to instability, we also find that the heat release rate and DC shift also contribute to the growth of acoustic pressure amplitude. The heat release rate fluctuation arising from the chemical - acoustic interaction, also appear as a source on the right hand side of the convection reaction diffusion (CRD) equations. Our discussion leads to the fact that the sources that we deal with, in the study of thermo-acoustic system, are convective - acoustic type. In this context, the theoretical framework developed in Chapter 3 reinforces the findings of earlier investigators (Chapter 1, Zinn and Lieuwen, 2006; Shanbhogue *et al.*, 2009). The role of these

sources in the growth and saturation of acoustic pressure amplitude that determines the bistability in a thermo-acoustic system will be discussed in the following section.

6.1 Stability as a consequence of linear vs nonlinear processes

The growth of any infinitesimal disturbances are initially governed by the linear processes (see Fig. (1.2)). The nonlinear saturation processes act when the disturbances grow to a finite amplitude. Therefore, earlier studies emphasize the need for understanding the nonlinear stability characteristics in addition to the stability characteristics revealed from the linear stability analysis (Zinn and Lieuwen, 2006; Noiray *et al.*, 2008). Noiray *et al.* (2008) emphasizes the role of nonlinear processes using a describing function approach. In their analysis, they observed that for some parameters, very small amplitude disturbances grow linearly until the amplitude is reduced to zero by the nonlinear processes. Also, initial negative growth rate was observed to become positive for sufficiently high amplitude. Again, for higher amplitude, the growth rate is reduced to zero. Therefore, we believe that the linear and nonlinear processes are related to the driving and damping that causes bistability in a thermo-acoustic system.

6.1.1 Identification of linear and nonlinear processes

The theoretical studies on flame - acoustic coupling by Wu (2005) and Wu *et al.* (2003) prove the existence of nonlinear sources. These nonlinear sources appear as coupling functions that establish acoustic - hydrodynamic interaction. The origin of these nonlinear functions is due to the jump relations that connect acoustic velocity across the compact flame. Wu *et al.* (2003) expressed these jump relations as

$$[u_a] = q(\overline{(1 + (\nabla F_0)^2)^{1/2}} - 1) \tag{6.1}$$

to represent the acoustic velocity jump across the flame, and

$$[U_0] = q((1 + (\nabla F_0)^2)^{-1/2} - \overline{(1 + (\nabla F_0)^2)^{1/2}}) \tag{6.2}$$

to represent the base flow modification across the flame. In Eqs. (6.1-6.2), F_0 describe the flame front. Therefore, ∇F_0 describes the curvature of the flame. Equation (6.1) suggests that whenever there is a curvature in the flame, an acoustic field is generated. The right hand side of Eqs. (6.1-6.2) represent the unsteady heat release rate concentrated along the flame. Both coupling functions show the influence of heat release rate q on the hydrodynamic velocity U_0 and the acoustic velocity u_a. The jump relations, according to Wu *et al.* (2003), causes a strong nonlinear interaction between the acoustic field and the flame. From an experiment, which studies the interaction of vortices with the heat release rate, Durox *et al.* (2005) proves that the response of the heat release rate to the incoming flow disturbances is nonlinear.

In addition to the nonlinear processes, there are linear processes that act in the initial stages of the growth of pressure disturbances (Culick, 2006). These linear processes are represented as the source terms that appear on the right hand side of equations for the linear harmonic oscillator. The assumption is that the magnitude of disturbances is small in the initial stages of their evolution. These linear equations are obtained as the first order equations after the application of perturbation method. We have obtained such evolution equations (Eqs. 3.24 and 3.25) governing the evolution of acoustic field variables. However, in our equations the source terms are absent at first order. At higher orders we can obtain amplitude evolution equations. In those equations, the linear and the nonlinear growth rates are expressed as the coefficients of linear and nonlinear terms respectively. Wu *et al.* (2003), investigating the interaction of Darrieus-Landau (D-L) instability with the sound field, expressed the influence of linear and nonlinear processes on the growth of amplitude A of the D-L mode as

$$A' = \kappa A + \gamma_s A^3 - \gamma_b |B|^2 A \tag{6.3}$$

$$B' = \chi_s A^2 B + m_p B \tag{6.4}$$

where B is the amplitude of the acoustic pressure and velocity fields. The coefficients κ, γ_s, γ_b, χ_s and m_p depends on the physical system under consideration. They represent the growth rates of D-L instability mode and acoustic field variables. The interaction between the D-L instability mode and the acoustic mode is nonlinear even when their respective magnitudes are small. Such a nonlinear interaction is called weakly nonlinear interaction. Similar splitting of linear and nonlinear processes is achieved by Subramanian *et al.* (2013). The governing equations that describe the contribution from linear and nonlinear processes are also known as slow flow equations (Subramanian *et al.*, 2013). The slow flow equations are obtained as higher order equations after the application of perturbation methods (Culick, 2006; Wu *et al.*, 2003; Subramanian *et al.*, 2013). CRD equations are higher order equations ($O(\epsilon^2)$). Also the CRD equations show the evolution on the slow time scale or the acoustic time scale. Next, we will discuss the linear and nonlinear mechanisms in the context of our CRD system.

6.1.2 The linear and nonlinear processes as represented by the convection reaction diffusion equation

The convection reaction diffusion equations, derived in Chapter 3, show a new nonlinear mechanism. This nonlinear mechanism, which arises from the chemical - acoustic interaction, is also a function of heat release rate (see the expressions for coefficients in Eqs. (5.9, 5.10)). The chemical - acoustic interaction is an inherent mechanism present in low Mach number reacting flows (Oran and Gardner, 1985). Together with the influence of fluid flow disturbances, and the proposed nonlinear mechanism, a better description of driving and damping forces in a thermo-acoustic system is provided in this chapter. In Chapter 1, we have seen that the driving mechanism is generally subjected to the nonlinear effects. The models describing the driving mechanisms tend to adhere to this general rule. In Fig. (1.2) we can see that the driving undergoes nonlinear evolution, whereas the damping undergoes linear evolution. From the discussion of coupled nonlinear CRD equations, we now know that the nonlinear influence appears naturally in reacting flows. Therefore, CRD equations seem to present a better picture of nonlinear stability characteristics of a thermo-acoustic system. Nonlinear terms also prove the amplitude dependency of the driving mechanism (see Fig. (1.2)).

6.2 Nonlinear instabilities

The influence of nonlinear sources on the stability of fluid dynamic system has been well explored (Chomaz, 1992). Chomaz used a Ginzburg - Landau equation (GLE) to model the nonlinear processes in a fluid dynamic system. Earlier, GLE was used to study the stability features of Navier - Stokes equations (Godrèche and Manneville, 2005). The real GLE equation is written as:

$$\frac{\partial A}{\partial t} + U_0 \frac{\partial A}{\partial x} = R(A) + \frac{\partial^2 A}{\partial x^2} \tag{6.5}$$

where, $R(A) = -\partial V(A)/\partial A$ and $V(A) = -\mu A^2/2 - A^4/4 + A^5/5$. The presence of convective term, the linear and nonlinear terms in GLE resemble that of CRD equations. These terms give rise to two nonlinear instabilities - nonlinear convective instability and nonlinear absolute instability.

6.2.1 Nonlinear convective instability

As the name suggests, the convective instability arises from the interaction between convection term and the local instability mechanism. A disturbance on the parallel base flow can be expressed as $A\phi(y,k,\omega)exp[i(kx-\omega t)]$, where k, ω and A are the complex wave number, the frequency and the amplitude respectively. For a control parameter R, the instability occurs when the growth rate $\omega_{imax}(R) > 0$. If a disturbance, local in nature, dies down, then we call the system to be linearly stable. However, if the convection aids in the transportation of the local disturbance to other parts of system, then the system is convectively unstable. The disturbance dies down at a fixed location and grows in a moving frame of reference (see Fig. (6.1)). The stability thus defined is applicable only to linear regime of disturbances. When the sources are nonlinear, the definition is extended to include the disturbance of finite amplitude. Under the action of a constant forcing, for a nonlinearly convective stable system, a disturbance of finite amplitude decays in the laboratory frame of reference (Huerre and Monkewitz, 1990; Chomaz, 2005).

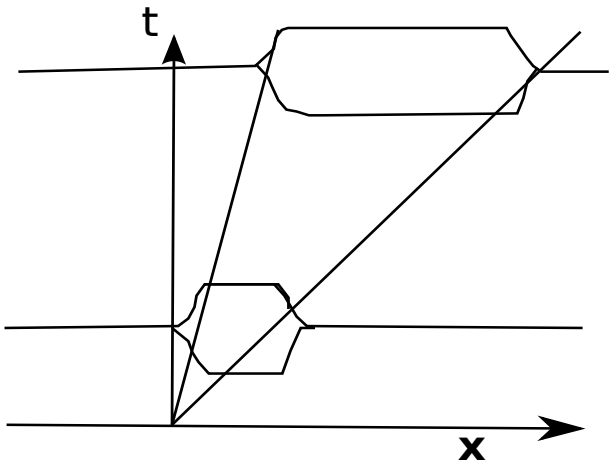

Figure 6.1: The illustration of nonlinear convective instability. The local disturbance at a fixed location decays at that point as time advances. The disturbance is also communicated to other locations.

6.2.2 Nonlinear absolute instability

For an absolute instability, the amplitude A of an infinitesimal disturbance grows to infinity at any fixed point in the laboratory frame of reference. Nonlinear absolute instability is defined for a disturbance of finite extent and amplitude. The amplitude of disturbance grows and achieves a saturation amplitude at any fixed point in the laboratory frame (see Fig. (6.2)) (Huerre and Monkewitz, 1990; Chomaz, 2005).

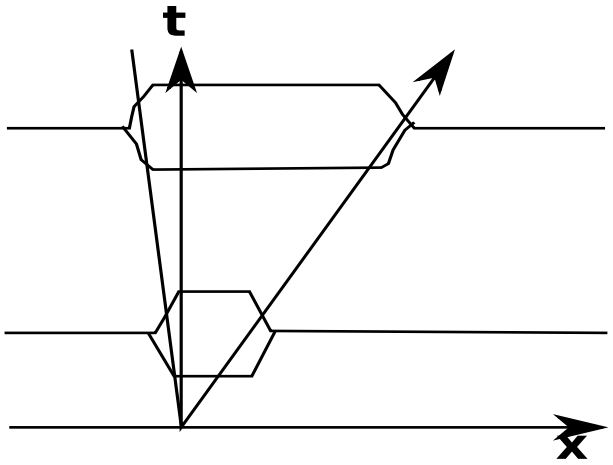

Figure 6.2: The illustration of nonlinear absolute instbility. The local disturbances grow at any location in the laboratory reference frame

Thermo-acoustic system involves acoustic - flame - hydrodynamic interaction. The stability is then defined in terms of the growth or decay of acoustic disturbance amplitude due to the sources from the underlying hydrodynamic field (the unsteady reacting

flow). Therefore in this chapter, we chose to study the stability of flow - acoustic - heat release rate system. To describe the thermo-acoustic system, We have obtained coupled nonlinear CRD equations, obtained from Navier - Stokes equations through rigorous derivation. Therefore unlike GLE equations, the coupled equations are not simple model equations for fluid flow instabilities. The type of nonlinearities inherent to the flow - acoustic - heat release rate will be investigated. Nonlinear instabilities, of absolute and convective nature, will be discussed in the context of thermo-acoustic system using CRD equations.

Finally, with the investigation of the nonlinear instabilities we show that the bistability is a consequence of two mechanisms: 1) the transfer of energy with the flow field when the control parameter exceeds a critical value and 2) the saturation mechanism introduced by the chemical-acoustic interaction. The transfer of energy with the flow field is again two fold. In the region of NLC, the flow carries away the acoustic disturbances from the system. In the NLA regime, the flow aids in the growth of acoustic disturbances to a finite amplitude so that nonlinear mechanisms causes the saturation to self sustained oscillations. In this manner, convection of acoustic disturbances due to flow acts to damp and drive the disturbances depending on the region in the control parameter space.

6.3 Nonlinear instability

6.3.1 Problem description

In a thermo-acoustic system, a localized heat source such as flame can generate a pressure wave. According to Dunlap (1950), the pressure wave leads to thermal fluctuations and eventually causes heat release rate modulation. The heat release rate modulation, in turn, modifies the flow field or introduces local flow disturbances through gas expansion. A theoretical description of these phenomena is provided by the system of Eqs. (3.12, 5.9, 5.10). Equation (5.9) represents the influence of flow field dynamics and heat release rate fluctuations on the generation of acoustic pressure wave. Equation (5.10) represents the coupling of acoustic pressure wave with thermal fluctuations.

Equation (3.12) represents the influence of heat release rate on the flow field.

From the earlier research conducted to understand the interaction between heat release rate and acoustic field, two major coupling mechanisms are revealed. They are pressure coupling and velocity coupling (Clavin *et al.*, 1990, 1994; Pelce and Rochwerger, 1992). In the present study, the nonlinear processes which couple the flow field and acoustic field are found to be due to pressure coupling (a mechanism through which the acoustic pressure and heat release rate fluctuations influence each other). Therefore, our objective is to study the response of the nonlinear thermo-acoustic system described by Eqs. (5.9, 5.10) to an initial infinitesimal acoustic pressure perturbation.

Here, we consider the geometry of thermo-acoustic system to be a duct with no area variation. The duct is filled with fuel-air mixture with premixed flame, a source of heat release rate, is situated at a fixed location. Across the flame, the acoustic pressure does not vary (Clavin *et al.*, 1990, 1994; Pelce and Rochwerger, 1992). This is true for any localized heat release rate fluctuations. To describe acoustic pressure in such a situation, an additional length scale can be introduced as a function of η; i.e. $\delta\eta$. Here δ is the ratio of length scale which describes the localized heat release rate fluctuation to the length scale for acoustic pressure variation. $\delta\eta$ is the length scale describing the spatial variation of acoustic pressure. Using this length scale, which is longer compared to η, we could describe the acoustic pressure wave to be of the form $\hat{p}_{2a}(\eta,\tau')e^{i(k\delta\eta+\omega\tau)}$. The spatio-temporal solution form $e^{i(k\delta\eta+\omega\tau)}$ is thus separated from the perturbation amplitude which is localized in the long length scale (ξ). This scale separation is schematically represented in Fig. (5.2). Initial perturbations can then be applied locally to $\hat{p}_{2a}(\eta,\tau')$. Coefficients of Eq. (5.9) represent the physical parameters of system such as reaction rates, heat release rate and diffusion coefficients, for which values are specified explicitly.

We solve the nonlinear equations numerically in one dimension for the acoustic pressure and thermal fluctuations. A CVODE solver (Cohen *et al.*, 1996), provided with XPPAUT (Ermentrout, 2002), is used for the integration of stiff equations. The initial velocity field for all the cases discussed below is $u_0 = 0$. As a consequence, any flow disturbance is generated due to the acoustic field alone. The zero gradient boundary condition is chosen for the present computations. A numerical experiment, which

we have set up now, will permit us to investigate the mechanism of growth and decay of the initial acoustic disturbance and its interaction with the flow field and the heat release rate. The growth of the acoustic pressure perturbation and its saturation to a finite

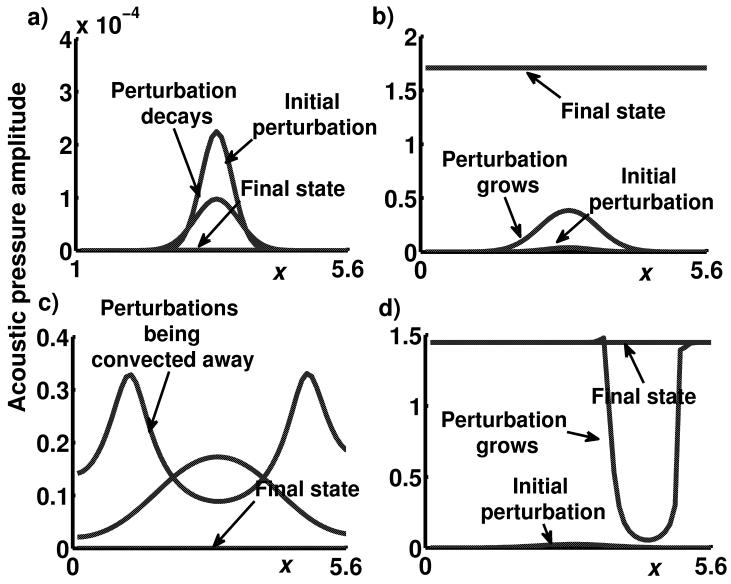

Figure 6.3: Spatio-temporal evolutions computed from Eqs. (5.9, 5.10). These are the solutions obtained by solving nonlinear equations. Initial perturbation to $\hat{p}_{2a}$ is of the order 10^{-3}, a) $\hat{p}_{2a} = 0$ is stable (S), b) $\hat{p}_{2a} = 0$ is unstable (U), c) Nonlinear convective instability (NLC), d) Nonlinear absolute instability (NLA). t_i denotes the time of initial perturbation and t_f is the time when the final state is reached.

amplitude is a characteristic of thermo-acoustic instability. The decay of any infinitesimal perturbation at any specific point in space indicates its stability (S); the growth indicates an unstable system (U). However, apart from these conditions, we show that thermo-acoustic system also exhibits nonlinear convective (NLC) and absolute instability (NLA). The control parameter space for these instabilities, which are governed by the nonlinearities in the system, is explored. The types of instabilities exhibited by the system described by Eqs. (5.9, 5.10) are illustrated in Fig. (6.3). The growth of perturbations in S and U regimes do not depend on the magnitude of perturbation. Perturbations of any magnitude will decay in the S regime and grow in U regime. However, as you can see in Fig. (6.4), the magnitudes of perturbation matter in the NLA and NLC regime which indicates the amplitude dependency in the case of nonlinear instabilities.

In the subsequent sections, we will explain the significance of NLC and NLA and the role of convection in determining the stability of a thermo-acoustic system. Insta-

bility is indicated by a nonzero final amplitude to which the initial acoustic disturbance evolves. To investigate the parameter space of instability, we have computed the bifurcation diagrams (see Fig. (6.4)), from the nonlinear equations, using various values of the physical parameters α, θ, ϑ and D. The bifurcation diagrams are computed using AUTO (Doedel *et al.*, 1997). We have computed the bifurcation diagram for values of $D = 0.1, 0.01, 0.001$ and for $\alpha = -0.6, -0.8, -1$. These diagrams show the same qualitative behavior with respect to the types of nonlinear instabilities. Therefore, in Fig. (6.4) we show a demonstrative case for the types of nonlinear instabilities observed in our thermo-acoustic system. We show the influence of the linear coefficient λ (a function of heat release rate and the mean pressure shift) on the stability of the system. The saturation to the finite amplitude is a consequence of the nonlinear terms; coefficients of which corresponds to the heat release rate fluctuations due to acoustic field.

In a thermo-acoustic system, we observe fluid flow fluctuations that accompany the acoustic oscillations. We believe that the coupling between these two processes is significant in determining the stability characteristics of a thermo-acoustic system. In the following discussion, we attempt to establish this conjecture.

In Fig. (6.4), the significance of two nonlinear instabilities - nonlinearly convective and nonlinearly absolute - is discussed. The parameter space, where there is a possibility of nonlinear instabilities to occur, has two stable branches. One is a zero amplitude branch and other a finite amplitude branch. The points p_1, p_2, p_3 and p_4 indicate the amplitudes of perturbations introduced in the nonlinear instability regimes. These perturbations are introduced uniformly over all grid points ($j = 1$ to N). For perturbations p_2 and p_3, the thermo-acoustic system approaches the zero amplitude state. For the final state to be the zero amplitude state, values of the initial conditions p_2 and p_3 for the time marching are in the range $O(10^{-3}) - O(10^{-1})$. For perturbations of $O(1)$ (p_1 and p_4) the system attains the finite amplitude state. The rest of this chapter studies the spatio - temporal growth of localized acoustic pressure perturbations due to fluid flow.

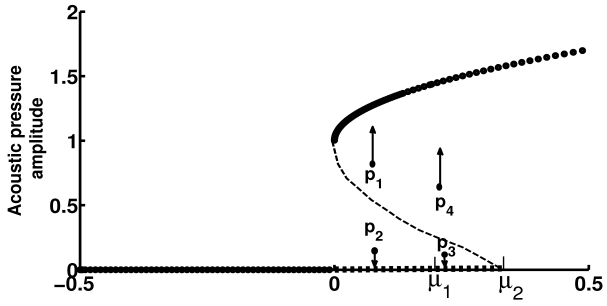

Figure 6.4: Bifurcation diagram (solid circles computed using the method of continuation) with respect to the linear coefficient λ (control parameter). The other system parameters are chosen as $\alpha = -1$, $\theta = 2$, $\vartheta = -1$, $D = 0.01$. The parameter space $0 < \lambda < \mu_1$ shows NLC (convective because the perturbation to the acoustic field in the system eventually leaves the domain, nonlinear because the growth is governed by the nonlinear sources. The initial small perturbation of the order $O(10^{-3})$ reaches a finite amplitude before leaving the domain) and $\mu_1 < \lambda < \mu_2$ shows NLA (absolute because the perturbation to the acoustic field grows in space and time and never decays). $\lambda > \mu_2$ is a region where the system is absolutely unstable. Here, $\mu_1 = 0.179$ and $\mu_2 = 0.231$. The filled circles show the stable states for thermo-acoustic system described by Eqs. (5.9, 5.10). For $\lambda < 0$, stable state is $\hat{p}_{2a} = 0$. The stable states for $\lambda > 0$ are the finite amplitudes obtained due to the nonlinear terms. The time evolutions of perturbation in the parameter space of NLC and NLA are shown in Fig. (6.5) and Fig. (6.6) respectively. The region $0 < \lambda < \mu_2$ is also a bistable region, where zero amplitude state and a finite amplitude state coexist. Point p_2 indicates perturbations of $O(10^{-1})$. As seen in this figure, p_2 in the NLC regime represents a larger perturbation than p_3. Point p_3 corresponds to $O(10^{-3})$ in the NLA regime. Perturbation p_1 is larger than the perturbation p_4. The unstable branch that separates p_2 and p_3 from p_1 and p_4 is not computed from continuation, but drawn to represent the relative magnitudes of perturbations that will result in zero amplitude and finite amplitude branch.

6.3.2 Nonlinear convective instability

For the nonlinearity in Eqs. (5.9, 5.10) to play a significant role in the growth or decay of acoustic pressure amplitude, the initial infinitesimal disturbance should approach a finite amplitude. In this section, we show the influence of the fluid flow velocity in this process. From Eq. (3.12), we can express the dilatation as:

$$\nabla_\eta \cdot \vec{u_0} = \quad \frac{\gamma - 1}{\gamma p_0} HDa(\dot{Q} + \dot{Q}') + \frac{\gamma - 1}{\gamma p_0 RePr} \nabla_\eta^2 T_0 - \frac{1}{\gamma p_0} \partial_{\tau'} p_0 \qquad (6.6)$$

The acoustic field and the flow field interact with each other forming a feedback loop. The solution of (6.6) along with the nonlinear Eqs. (5.9, 5.10) will provide us the evo-

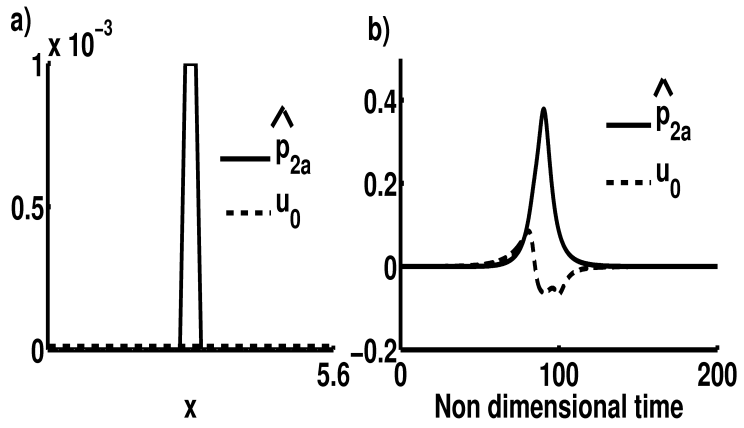

Figure 6.5: The initial perturbation to the acoustic field is shown in Fig. (6.5a). Fig. (6.5b) shows the space - time evolution for $\hat{p}_{2a}$. The parameters correspond to the region of NLC in the bifurcation diagram shown in Fig. (6.4).

lution of the flow velocity and the acoustic pressure and temperature fields. A grid convergence study is conducted with N (number of grid points in x direction) = 28, 56, 112, 224. Converged solution is obtained for N = 56 and above. Therefore we chose N = 56 for the present study. In the region $0 < \lambda < \mu_1$, any infinitesimal perturbation is amplified spatially as it is convected out of the domain. This process is illustrated in Fig. (6.3c). The time evolution of $\hat{p}_{2a}$ at a point in the boundary (where the maximum amplitude is attained) is shown in Fig. (6.5b). Note that the infinitesimal perturbation can be spatially amplified and reach a finite amplitude before before it is convected out of the domain. However, at the point where the perturbation is introduced, it decays to zero amplitude. Note that the time and space evolutions shown in this chapter are of the acoustic pressure disturbance amplitude. This quantity p_{2a} together with the spatial distribution $e^{i(k\delta\eta+\omega\tau)}$ represents the acoustic wave setup inside the duct.

6.3.3 Nonlinear absolute instability

In the region $\mu_1 < \lambda < \mu_2$ in Fig. (6.4), the zero amplitude state $\hat{p}_{2a}$ is a metastable state. The perturbations are not convected out of the domain. The fluid flow disturbances tend to amplify the infinitesimal perturbations to a finite amplitude. Then, the nonlinear processes act on the growth of perturbations resulting in the saturation to a non-zero amplitude. In Fig. (6.6b), there is a rise in the acoustic pressure amplitude whenever there is a flow fluctuation. However, without the aid of flow disturbances (to

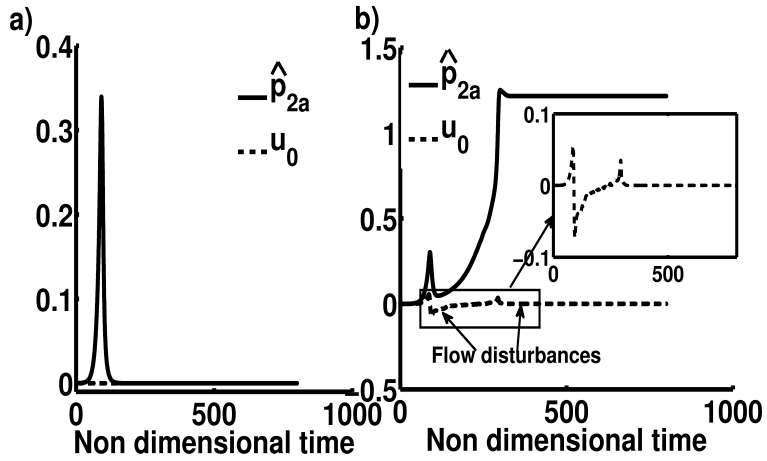

Figure 6.6: The time evolution of the acoustic pressure amplitude in the NLA region ($\mu_1 < \lambda < \mu_2$) of Fig.(6.4). (a) Shows the decay to $\hat{p}_{2a} = 0$ in the absence of flow disturbances (imposing $u_0 = 0$) and (b) shows the saturation to a finite amplitude state in the presence of flow disturbances (letting the flow to evolve according to Eq. (6.6)). Even after the flow disturbances decay, $\hat{p}_{2a}$ remains in the finite amplitude state because of the absolute nature of instability.

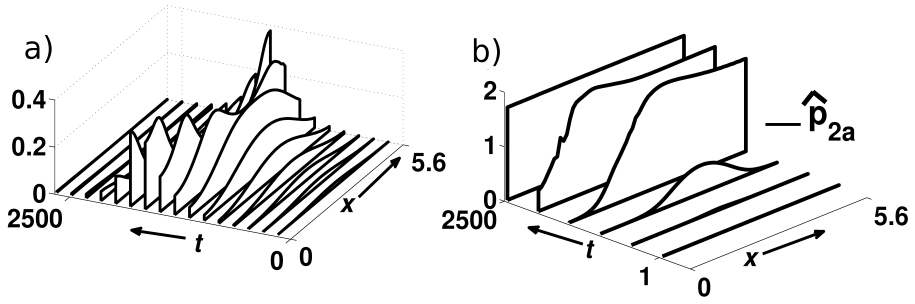

Figure 6.7: The spatial - temporal evolution of the amplitude of acoustic disturbances (p_{2a}) in the a) NLC regime and the b) NLA regime.

demonstrate this we have imposed $u_0 = 0$ in Fig. (6.6a)), the acoustic pressure amplitude cannot reach the magnitude of $O(1)$. As a consequence, the perturbation amplitude decays to the metastable zero amplitude state. An illustration of this type of instability in space and time is shown in Fig. (6.3d). The initial perturbation grows in space and time, till it contaminates the entire domain (see Fig. (6.7b)). For $\lambda > \mu_2$, any infinitesimal perturbation will saturate to a finite amplitude, since $p_{2a} = 0$ is an unstable state. The system is absolutely unstable in this parameter space. The growth of acoustic pressure perturbation in this region is shown in Fig. (6.3b).

6.4 Concluding remarks

As a consequence of the nonlinear saturation mechanism, in the NLA and NLC region, states of zero amplitude and finite amplitude coexist. The coexistence of these states in NLA regime is entirely due to the interaction with the fluid flow. While operating in NLC region, any localized small but finite ($O(10^{-3})$-$O(10^{-1})$) perturbation decays to zero amplitude at that location. Any perturbations of finite amplitude of the order $O(1)$, applied uniformly in space, reaches the finite amplitude state. When parameter region is $\mu_1 < \lambda < \mu_2$ (NLA), without convection only a perturbation of $O(1)$, applied uniformly in space, results in the finite amplitude branch. However, with convection, the flow amplifies the localized small but finite ($O(10^{-3})$) acoustic disturbances to the finite amplitude state. This positive interaction indicates the driving effect of convection. This type of positive interaction is reported here for the first time. Without this driving effect, NLA region is characterized by the decay of infinitesimal disturbances to zero amplitude state. The finite amplitude branch in the bifurcation diagram (6.4) is a state where the localized disturbance has contaminated the entire space. While in this state of finite amplitude, with changing the control parameter below μ_2, the acoustic pressure amplitude do not approach the state $\hat{p}_{2a} = 0$. The zero amplitude state can only be attained when $\lambda < 0$, indicating the hysteresis effect widely studied in thermo-acoustic interaction.

CHAPTER 7

Conclusions and future work

7.1 Conclusions

In this thesis, we have formulated a theoretical framework to study the growth of acoustic amplitude during the acoustic-hydrodynamic interaction. In our derivation, we have revealed a mechanism responsible for the mutual transportation of acoustic and hydrodynamic fields. This mechanism couples the acoustic and hydrodynamic fields. Therefore, any disturbance in the acoustic field is convected by the hydrodynamic velocity field and any disturbance in the hydrodynamic field is convected by the acoustic velocity field. This mechanism was previously known as convective and lift-up mechanism in the study fluid flow instabilities (Marquet *et al.*, 2009). In the nearly incompressible hydrodynamic phenomena, observed in magnetohydrodynamic flows, the mechanism of mutual interaction of the fluctuating and the mean fields is also known as Reynolds stress forces (Dastgeer and Zank, 2004). Our convective and lift-up mechanism, that establishes the acoustic-hydrodynamic interaction, is similar to the wave-mean flow interaction phenomena found in MHD or atmospheric flows. In combustion environment, the mutual interaction of acoustic, heat release rate and hydrodynamic fields give rise to the modification of acoustic field. Therefore, the governing equations derived in Chapter 3, using method of multiple scales (MMS), allow us to perform computations on the combustion generated sound.

We show that the governing equations governing the evolution of acoustic field amplitudes are nonlinear perturbation equations. A positive feedback loop between the acoustic pressure field and the heat release rate may lead to the growth of acoustic pressure amplitude in a thermo-acoustic system. The interaction mechanism of acoustic pressure and heat release rate fluctuations, that can establish a feedback loop, is evident from the nonlinear equations. These nonlinear equations are called convection reaction diffusion (CRD) system. A subsystem of CRD system; i.e. reaction diffusion system,

has been proposed for various phenomena to represent their dynamical nature (Hoyle, 2006). Therefore, proposing thermo-acoustic system as a CRD system is a major advancement of this thesis.

The new theory, formulated as CRD system, provides a mathematical description of combustion instability. Sources responsible for the generation of sound, in a combustion environment, is extracted from the governing equations using a source filtering approach (Ewert and Schröder, 2003). For a low Mach number flow, the convective, vortical, entropy and acoustic sources exist on different time scales. In this context, MMS is advantageous in decomposing the field variables according to the time and space scales. We have described, using the method of multiple scales (MMS), the fast oscillations on the acoustic time scale and the slow time scale evolution of acoustic pressure amplitude on the convective time scale. We have shown that such a description is advantageous for two reasons: 1) we obtain the time scales and space scales of various sources that drive combustion instability and 2) a source filtering approach provides the knowledge of time scales on which acoustic-vortical-entropy modes evolve. The separation of time scales separates the fast acoustic oscillations and the slow modulation of acoustic amplitude. As a consequence, the computation using our nonlinear equations yields a stationary bifurcation. This is in contrast with the previous investigations where Hopf bifurcations are computed (Burnley and Culick, 1996; Culick, 2006; Subramanian *et al.*, 2013). The computation of a stationary bifurcation saves computational resources. On the investigation of low Mach number reacting flows using the evolution equations, we found a nonlinear mechanism that establishes acoustic-hydrodynamic interaction. Mathematically, the interaction is formulated as a class of convection reaction diffusion (CRD) equations. Using the CRD system, we study the stability characteristics of acoustic pressure perturbations introduced in the flow field.

From our investigation, in addition to the time scale separation, we have achieved the space scale separation. We achieved this separation by deriving two sets of evolution equations - one set governing the long length scale modulation and another set governing the small length scale modulation. We believe that such an approach is advantageous, since the hydrodynamic fluctuations that drives the acoustic perturbations are on the small length scale. Furthermore, the nonlinear growth of acoustic pressure

perturbations is captured by following our approach.

We have used the dynamical systems analogy in understanding the transitions observed in thermo-acoustic system. Methods of the theoretical investigation of the stability of thermo-acoustic system has advanced with the application of dynamical systems theory. Previous investigations in this direction proposed that the change in the stability of a thermo-acoustic system can either occur through a supercritical Hopf bifurcation or through a subcritical Hopf bifurcation. The origin of limit cycle oscillations associated with the instability is one of the reason for such a classification. These investigations focused on reducing the governing equations for thermo-acoustic interaction to the normal form of supercritical or subcritical Hopf bifurcations. Transition from oscillatory to non-oscillatory states in a thermo-acoustic system exhibits hysteresis effect. The cause of this hysteresis is the motivation behind the study of change in the stability as a subcritical bifurcation. However, in this thesis, we show that the transitions can occur through a perturbed bifurcation which also exhibit hysteresis effect.

The perturbed bifurcation can be created by introducing an additional term to the normal form of pitchfork bifurcation. This additional term introduces an asymmetry in the pitchfork bifurcation. For example, following Hoyle (2006), this additional term is a quadratic term in the equation given below.

$$x' = \mu x + \epsilon\nu x^2 - ax^3 \tag{7.1}$$

The normal form has both the linear and nonlinear terms; i.e. $\mu x + ax^3$. The additional term is $\epsilon\nu x^2$. As a result of this quadratic term, in addition to the stationary solution at x = 0, we also obtain stationary solutions at

$$x_{1,2} = \frac{1}{2a}(\epsilon\nu \pm \sqrt{\epsilon^2\nu^2 + 4a\nu}) \tag{7.2}$$

which implies that there are two stationary solutions for $\mu > \mu_c \equiv -\epsilon^2\nu^2/4a$. The bifurcation diagram computed from Eq. (7.1) is shown in Fig. (7.1). We can see that there are three solutions when $\mu > \mu_c$. Two of them are described by the stable branches (solid lines) and one of them is described by the unstable branch (dotted line). There is a hysteresis region in the parameter space $\mu_c < \mu < 0$. As the acoustic perturbation

amplitude A is positive, we need to consider only the positive branch; i.e. the solution branches above the zero amplitude branch.

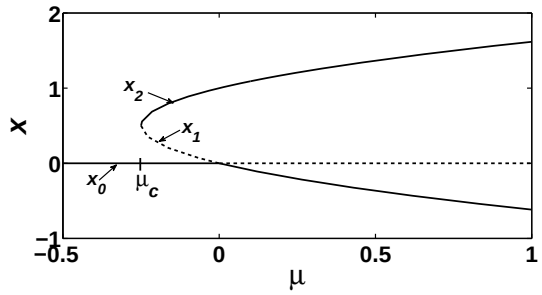

Figure 7.1: Perturbed pitchfork bifurcation that result from including a quadratic nonlinear term in the normal form of supercritical pitchfork bifurcation. Solid lines indicate the stable branch and dotted line indicate the unstable branch. x_1 and x_2 are the solutions given in Eq. (7.2). For an acoustic perturbation amplitude A, x_1 and x_2 are the possible branches that are possible solutions. The negative branch is a solution to example Eq. (7.1) for $\mu < 0$. However, this negative branch cannot be attained by any perturbation to the acoustic pressure amplitude.

The bifurcation shown in Fig. (5.4) exhibits the hysteresis zone near the critical parameter λ_h. There is one more type of bifurcation that is supercritical near the critical parameter. This type of bifurcation, shown in Fig. (5.6), is called a secondary bifurcation. Such a bifurcation creates multiple oscillatory branches. In a thermo-acoustic system, these oscillatory branches correspond to multiple limit cycles. The theory is formulated through a rigorous mathematical derivation from the governing equations for compressible fluid flow. Therefore, the control parameters that determines the bifurcation characteristics have physical meaning. This is an improvement over the present theoretical models. In this thesis, we have explained the origin of hysteresis using the physical parameters such as the heat release rate, the Damkohler number and the mean density in the combustion chamber. The influence of convection is to spread the local pressure disturbances spatially, which will lead to a spatiotemporal growth of initial disturbances.

The mechanism responsible for the transition from non-oscillatory to oscillatory state of acoustic pressure is found to be acoustic-hydrodynamic coupling. The transition can occur in the region of parameter space where system the thermo-acoustic system is not absolutely unstable. Using an example, which provides a mathematical description

of acoustic-hydrodynamic interaction, the influence of convection on introducing the transition is elucidated. Finally, we propose that in addition to stable and unstable regimes, the control parameter space also has a region where pressure perturbations show nonlinear convective instability (NLC) and a region where perturbations show nonlinear absolute instability (NLA). Therefore, we propose that convective effects can be a candidate mechanism for the instability in an otherwise stable operating zone.

7.2 Scope of future work

7.2.1 Application to real combustor configuration

The theory formulated in this thesis can be used to explain the origin of combustion instability in practical combustor configurations. Real combustors exhibit fluid dynamic instabilities. These instabilities can cause heat release rate fluctuations. For example, a combustor configuration with oxidizer inflow at the center and fuel co-flow as shown in Fig. (7.2) can exhibit unsteady base flow field. The unsteady flow field can cause flame instability which in turn cause heat release rate fluctuation. Using an in-house computational fluid dynamics code, we have shown one of such thermo-acoustic instability. In Fig. (7.2), flame surface undergoes flapping in response to the generation and propagation of vortices in the flow field. The vorticity dynamics can cause fluctuations in the base flow velocity. The flapping of flame near to the blowout is known experimentally (Nair, 2006). The generation and propagation of vortices and the resulting non-uniformity in the burning of gases is investigated by Poinsot *et al.* (1987). Therefore, the combustor configuration that we are going to discuss has practical relevance. The combustor has an inflow of oxidizer with velocity U. The co-flow of fuel is at a velocity u which is only 10 percentage of the center flow velocity U. The governing Eqs. (3.10-3.12) for the low Mach number flow are solved to obtain the base flow velocity field. In the numerical study of flow dynamics as the one shown in Fig. (7.2), vortical modes and entropy modes (from the propagation of burned gases in the vortices) interact. Such an interaction will lead to the fluctuations in temperature and vorticity fields (shown in Fig. (7.4)). In such a numerical study, there are more control parameters

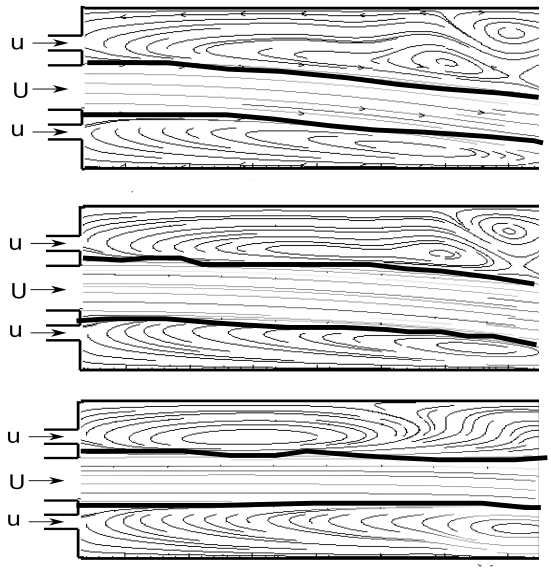

Figure 7.2: The streamlines of the flow for a) generation of vortices in the bottom mixing layer b)the propagation of vortices out of the domain c) generation of vortices in the top mixing layer. The thick solid line indicate the flapping flame surface. This figure is plotted from the data computed using an in-house low Mach number computational fluid dynamics code developed by the author of this thesis. The ratio of fuel to oxidizer velocities, Reynolds number Re and the inlet temperature T_0 are chosen to be $u/U = 0.1$, 2000 and 900K respectively.

than those considered in this thesis. These parameters include the inlet species mass fractions and the length and diameter of the combustor. In Fig. (7.3), we see that there is a fluctuation in u_0 in response to the flapping of the flame. Fluctuations in the base flow is therefore unavoidable when there is thermo-acoustic instability. Solving nonlinear equations 5.9 and 5.10 simultaneously with Eqs. (3.10-3.12) for low Mach number flow will help us to study the evolution of acoustic pressure amplitude in response to the unsteady flow field. However, the boundary conditions for such a two dimensional simulation have to be carefully formulated. Further, such a numerical simulation will be computationally expensive in terms of time and computational power.

7.2.2 Other nonlinear dynamical phenomena

Constructing a computational solver that solves the nonlinear equations coupled with the low Mach number equations will reveal many other nonlinear phenomena. These phenomena may include chaotic oscillations and intermittent oscillations. The theo-

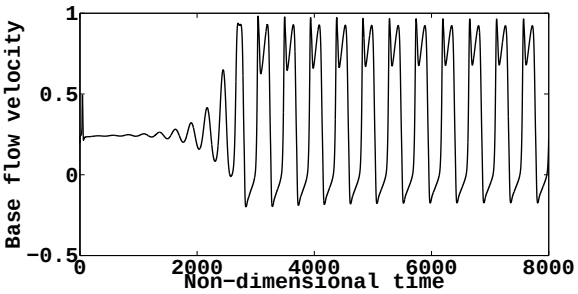

Figure 7.3: The time trace of base flow velocity fluctuations measured near the flame sheet. This measurement correspond to the fluctuation in the base flow velocity that arise from the propagation of vortices that are shown in Fig. (7.2)

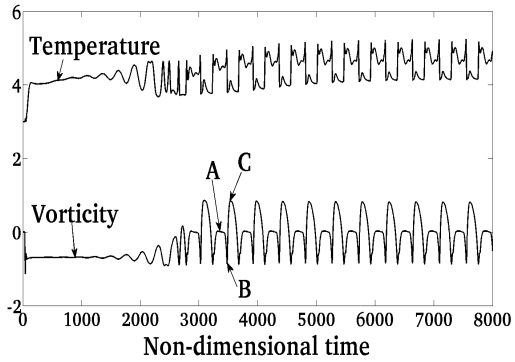

Figure 7.4: The time trace of vorticity and temperature fluctuations. Points A, B and C corresponds to the flow field configuration a, b and c shown in Fig. (7.2). This time trace is computed for the same parameters used for the computation of Fig. (7.2); i.e.the ratio of fuel to oxidizer velocities, Reynolds number Re and the inlet temperature T_0 are chosen to be $u/U = 0.1$, 2000 and 900K respectively.)

retical analysis presented in this thesis is the first attempt to categorize the problem of combustion instability into a mathematical class of equations. The reaction diffusion system is known to exhibit limit cycle oscillations, chaotic oscillations and intermittent oscillations of physical quantities in many fields ranging from chemical oscillators to neural oscillators. Acoustic pressure oscillations driven by unsteady flow phenomena can also exhibit such phenomena. Therefore, the present theory can be extended further to study such phenomena. Using this theory, the fluid dynamic, acoustic and flame instabilities can be investigated for its origin from acoustic-flame-vortex interactions.

REFERENCES

1. **Ananthkrishnan, N.**, **D. Shardul**, and **F. E. C. Culick** (2005). Reduced-order modeling and dynamics of nonlinear acoustic waves in a combustion chamber. *Combustion Science and Technology*, **177**(2), 221–248.

2. **Ananthkrishnan, N.**, **K. Sudhakar**, **S. Sudershan**, and **A. Agarwal** (1998). Application of secondary bifurcations to large amplitude limit cycles in mechanical systems. *Journal of Sound and Vibration*, **215**(1), 183 – 188.

3. **Balaji, C.** and **S. Chakravarthy**, Formulation of combustion acoustic coupling using multiple time and length scales. *In 48th AIAA Aerospace Sciences Meeting including the New Horizons Forum and Aerospace Exposition*. 2010.

4. **Balasubramanian, K.** and **R. Sujith** (2008). Thermoacoustic instability in a rijke tube: Non-normality and nonlinearity. *Physics of Fluids (1994-present)*, **20**(4), 044103.

5. **Beckstead, M. W.**, **R. S. Richards**, and **B. S. Brewsterl** (1984). Distributed combustion effects on particle damping. *AIAA Journal*, **22**(3), 383–387.

6. **Birbaud, A. L.** and **H. Pitsch**, *Combustion noise modeling using compressible simulations*. Center for turbulence research, Annual Research Briefs, 2008, 1–12.

7. **Blomshield, F.**, chapter Historical perspective of combustion instability in motors - Case studies. Joint Propulsion Conferences. American Institute of Aeronautics and Astronautics, 2001.

8. **Boyer, L.** and **J. Quinard** (1990). On the dynamics of anchored flames. *Combustion and Flame*, **82**(1), 51 – 65.

9. **Buckmaster, J. D.**, *The Mathematics of Combustion*. Frontiers in Applied Mathematics. Society for Industrial and Applied Mathematics, 1985.

10. **Bühler, O.**, *Waves and Mean Flows*. Cambridge University Press, 2009.

11. **Burnley, V. S.** and **F. E. C. Culick**, Some dynamics of acoustics oscillations with nonlinear combustion and noise. *In Fourth International Conference on Special Topics in Combustion, Challenges in Propellants and Combustion 100 Years After Nobel*. Stockholm, Sweden, 1996.

12. **Byrne, R.**, chapter Longitudinal pressure oscillations in ramjet combustors. Joint Propulsion Conferences. American Institute of Aeronautics and Astronautics, 1983.

13. **Candel, S.**, **D. Durox**, **S. Ducruix**, **A. L. Birbaud**, **N. Noiray**, and **T. Schuller** (2009). Flame dynamics and combustion noise: progress and challenges. *International Journal of Aeroacoustics*, **8**, 1–56.

14. **Chomaz, J. M.** (1992). Absolute and convective instabilities in nonlinear systems. *Physical Review Letters*, **69**, 1931–1934.

15. **Chomaz, J.-M.** (2005). Global Instabilities in spatially developing flows: non-normality and nonlinearity. *Annual Review of Fluid Mechanics*, **37**, 357–392.

16. **Clanet, C.**, **G. Searby**, and **P. Clavin** (1999). Primary acoustic instability of flames propagating in tubes: cases of spray and premixed gas combustion. *Journal of Fluid Mechanics*, **385**, 157–197.

17. **Clavin, P.**, **J. S. Kim**, and **F. A. Williams** (1994). Turbulence-induced noise effects on high-frequency combustion instabilities. *Combustion Science and Technology*, **96**(1-3), 61–84.

18. **Clavin, P.**, **P. Pelce**, and **L. He** (1990). One-dimensional vibratory instability of planar flames propagating in tubes. *Journal of Fluid Mechanics*, **216**, 299–322.

19. **Cohen, S.**, **Alan**, and **C. Hindmarsh**, Cvode, a stiff/nonstiff ode solver in c. *In in C. Computers in Physics*. 1996.

20. **Crow, S. C.** (1970). Aerodynamic sound emission as a singular perturbation problem. *Stud. Appl. Math.*, **49**, 21–44.

21. **Culick, F. E. C.** (1968). A review of calculations for unsteady burning of a solid propellant. *AIAA Journal*, **6**(12), 2241–2255.

22. **Culick, F. E. C.** (1976*a*). Nonlinear behavior of acoustic waves in combustion chambers I. *Acta Astronautica*, **3**(9–10), 715 – 734.

23. **Culick, F. E. C.** (1976*b*). Nonlinear behavior of acoustic waves in combustion chambers II. *Acta Astronautica*, **3**(9–10), 735 – 757.

24. **Culick, F. E. C.** (1997). A note on ordering perturbations and the insignificance of linear coupling in combustion instabilities. *Combustion Science and Technology*, **126**(1-6), 359–377.

25. **Culick, F. E. C.** (2006). Unsteady motions in combustion chambers for propulsion systems. Technical Report RTO-AG-AVT-039 AC/323(AVT-039)TP/103, RTO AGAR-Dorgraph.

26. **Culick, F. E. C.** and **S. Palm** (2009). Active control of combustors after twenty years' efforts. *EUCASS Proceedings Series*, **1**, 441–468.

27. **Culick, F. E. C.** and **T. Rogers** (1980). Modeling pressure oscillations in ramjets.

28. **Dastgeer, S.** and **G. P. Zank** (2004). Nonlinear flows in nearly incompressible hydrodynamic fluids. *Physical Review E*, **69**, 066309.

29. **Dastgeer, S.** and **G. P. Zank** (2006). The transition to incompressibility from compressible magnetohydroynamic turbulence. *The Astrophysical Journal Letters*, **640**(2), L195. URL `http://stacks.iop.org/1538-4357/640/i=2/a=L195`.

30. **Doedel, E. J.**, **A. R. Champneys**, **T. F. Fairgrieve**, **Y. A. Kuznetsov**, **B. Sandstede**, and **X. Wang** (1997). Auto 97: Continuation and bifurcation software for ordinary differential equations (with homcont).

31. **Dowling, A. P.** (1999). A kinematic model of a ducted flame. *Journal of fluid mechanics*, **394**, 51–72.

32. **Duchaine, P.**, **L. Zimmer**, and **T. Schuller** (2009). Experimental investigation of mechanisms of sound production by partially premixed flames. *Proceedings of the Combustion Institute*, **32**(1), 1027 – 1034.

33. **Ducruix, S.**, **T. Schuller**, **D. Durox**, and **S. Candel** (2005). Combustion instability mechanisms in premixed combustors. *Progress In Astronautics and Aeronautics*, **210**, 179.

34. **Dunlap, R. A.** (1950). Resonance of a flame in a parallel walled combustion chamber. Technical Report Project MX833, Aeronautical research center, University of Michigan.

35. **Durox, D.**, **T. Schuller**, and **S. Candel** (2005). Combustion dynamics of inverted conical flames. *Proceedings of the Combustion Institute*, **30**(2), 1717 – 1724.

36. **Durran, D. R.** (2008). A physically motivated approach for filtering acoustic waves from the equations governing compressible stratified flow. *Journal of Fluid Mechanics*, **601**, 365–379.

37. **Ebeling, W.** and **H. Malchow** (1979). Bifurcations in a bistable reaction-diffusion system. *Annalen der Physik*, **491**(2), 121–134.

38. **Ermentrout, B.**, *Simulating, Analyzing, and Animating Dynamical Systems*. Society for Industrial and Applied Mathematics, 2002.

39. **Ewert, R.** and **W. Schröder** (2003). Acoustic perturbation equations based on flow decomposition via source filtering. *Journal of Computational Physics*, **188**(2), 365–398.

40. **FitzHugh, R.** (1955). Mathematical models of threshold phenomena in the nerve membrane. *The bulletin of mathematical biophysics*, **17**(4), 257–278.

41. **Flandro, G. A.**, **S. R. Fischbach**, and **J. Majdalani** (2007). Nonlinear rocket motor stability prediction: Limit amplitude, triggering, and mean pressure shift. *Physics of Fluids (1994-present)*, **19**(9), –.

42. **Geer, J. F.** and **D. S. Pope**, A multiple scales approach to sound generation by vibrating bodies. *In* **J. C. Hardin** and **M. Hussaini** (eds.), *Computational Aeroacoustics*, ICASE/NASA LaRC Series. Springer New York, 1993, 69–84.

43. **Ghoniem, A. F.**, **S. Park**, **A. Wachsman**, **A. Annaswamy**, **D. Wee**, and **H. M. Altay** (2005). Mechanism of combustion dynamics in a backward-facing step stabilized premixed flame. *Proceedings of the Combustion Institute*, **30**(2), 1783 – 1790.

44. **Giauque, A.** and **H. Pitsch**, *Detailed modeling of combustion noise using a hydrodynamic/acoustic splitting model*. 2009, 1–12.

45. **Gilding, B. H.** and **R. Kersner**, *Travelling Waves in Nonlinear Diffusion-Convection Reaction*. BirkhÃd'user Mathematics, 2004.

46. **Godrèche, C.** and **P. Manneville**, *Hydrodynamics and Nonlinear Instabilities*. 2005.

47. **Golubitsky, M.** and **D. Schaeffer** (1978). A theory for imperfect bifurcation via singularity theory. Technical report, DTIC Document.

48. **Gopalakrishnan, E. A.** and **R. I. Sujith** (2014). Influence of system parameters on the hysteresis characteristics of a horizontal rijke tube. *International Journal of Spray and Combustion Dynamics*, **6**(3), 293–316.

49. **Günther, R.** (1972). Combustion-driven oscillations in industry. *Chemie Ingenieur Technik*, **44**(5), 356–356.

50. **Heckl, M. A.** (1990). Non-linear acoustic effects in the rijke tube. *Acta Acustica united with Acustica*, **72**(1), 63–71.

51. **Howe, M. S.**, *Theory of Vortex Sound*. Cambridge University Press, 2002.

52. **Hoyle, R.**, *Pattern Formation, An Introduction to Methods*. Cambridge, 2006.

53. **Huerre, P.** and **P. A. Monkewitz** (1990). Local and global instabilities in spatially developing flows. *Annual Review of Fluid Mechanics*, **22**(1), 473–537.

54. **Hunana, P.**, **G. P. Zank**, and **S. Dastgeer** (2006). Nearly incompressible fluids: Hydrodynamics and large scale inhomogeneity. *Physical Review E*, **74**, 026302.

55. **Jackson, E. A.**, *Perspectives of nonlinear dynamics*, volume 1. CUP Archive, 1992.

56. **Jones, A. T.** (1945). Singing flames. *The Journal of the Acoustical Society of America*, **16**(4), 254–266.

57. **Juniper, M. P.** (2011). Triggering in the horizontal rijke tube: non-normality, transient growth and bypass transition. *Journal of Fluid Mechanics*, **667**, 272–308.

58. **Kabiraj, L.** and **R. I. Sujith** (2012). Nonlinear self-excited thermoacoustic oscillations: intermittency and flame blowout. *Journal of Fluid Mechanics*, **713**, 376–397.

59. **Kaskan, W. E.** and **A. E. Noreen**, High frequency oscillations of a flame held by a bluff body. *In ASME Transactions*, volume 77. 1955.

60. **Keller, J. .**, **L. Vaneveld**, **D. Korschelt**, **G. L. Hubbard**, **A. F. Ghoniem**, **J. W. Daily**, and **A. K. Oppenheim** (1982). Mechanism of instabilities in turbulent combustion leading to flashback. *AIAA Journal*, **20**, 254–262.

61. **Keller, J.**, **J. Ellzey**, **R. Pitz**, **I. Shepherd**, and **J. Daily** (1988). The structure and dynamics of reacting plane mixing layers. *Experiments in Fluids*, **6**(1), 33–43.

62. **Kerstein, A. R.**, **W. T. Ashurst**, and **F. A. Williams** (1988). Field equation for interface propagation in an unsteady homogeneous flow field. *Physical Review A*, **37**(7), 2728.

63. **Kevorkian, J.** and **D. L. Bosley** (1998). Multiple-scale homogenization for weakly nonlinear conservation laws with rapid spatial fluctuations. *Studies in Applied Mathematics*, **101**(2), 127–183.

64. **Kevorkian, J.** and **J. D. Cole**, *Multiple scale and singular perturbation methods*, volume 114 of *Applied mathematical sciences*. Springer, New York, 1996.

65. **Kim, W.-W.** and **S. Menon** (2000). Numerical modeling of turbulent premixed flames in the thin-reaction-zones regime. *Combustion Science and Technology*, **160**(1), 119–150.

66. **Klainerman, S.** and **A. Majda** (1982). Compressible and incompressible fluids. *Communications on Pure and Applied Mathematics*, **35**(5), 629–651.

67. **Klein, R.**, **N. Botta**, **T. Schneider**, **C. D. Munz**, **S. Roller**, **A. Meister**, **L. Hoffmann**, and **T. Sonar** (2001). Asymptotic adaptive methods for multi-scale problems in fluid mechanics. *Journal of Engineering Mathematics*, **39**(1), 261–343.

68. **Konrad, W.**, **N. Brehm**, **F. Kameier**, **C. Freeman**, and **I. J. Day** (1998). Combustion instability investigations on the br710 jet engine. *Journal of Engineering for Gas Turbines and Power*, **120**(1), 34–40.

69. **Lagerstrom, P. A.** and **R. G. Casten** (1972). Basic concepts underlying singular perturbation techniques. *SIAM Review*, **14**(1), pp. 63–120.

70. **Langhorne, P. J.** (1988). Reheat buzz: an acoustically coupled combustion instability. part 1. experiment. *Journal of Fluid Mechanics*, **193**, 417–443.

71. **Lessen, M.** (1948). On stability of free laminar boundary layer between parallel streams. Technical report, NACA.

72. **Lieuwen, T.** (2003). Modeling premixed combustion-acoustic wave interactions: A review. *Journal of Propulsion and Power*, **19**(5), 765–781.

73. **Lieuwen, T.**, **H. Torres**, **C. Johnson**, and **B. T. Zinn** (2001). A mechanism of combustion instability in lean premixed gas turbine combustors. *Journal of engineering for gas turbines and power*, **123**(1), 182–189.

74. **Lieuwen, T.** and **B. T. Zinn**, The role of equivalence ratio oscillations in driving combustion instabilities in low no x gas turbines. *In Symposium (International) on Combustion*, volume 27. Elsevier, 1998.

75. **Lighthill, M. J.** (1954). On sound generated aerodynamically. ii. turbulence as a source of sound. *Proceedings of the Royal Society of London. Series A. Mathematical and Physical Sciences*, **222**(1148), 1–32.

76. **Mariappan, S.** and **R. I. Sujith** (2011). Modelling nonlinear thermoacoustic instability in an electrically heated Rijke tube. *Journal of Fluid Mechanics*, **680**, 511–533.

77. **Markstein, G. H.**, Flames as amplifiers of fluid mechanical disturbances. *In Proc. Sixth Natl Congr. Appl. Mech.*. 1970.

78. **Marquet, O.**, **M. Lombardi**, **J. M. Chomaz**, **D. Sip**, and **L. Jacquin** (2009). Direct and adjoint global modes of a recirculation bubble: lift-up and convective non-normalities. *Journal of Fluid Mechanics*, **622**, 1 – 21.

79. **Matalon, M.** and **B. J. Matkowsky** (1982). Flames as gasdynamic discontinuities. *Journal of fluid mechanics*, **124**, 239–259.

80. **Matveev, K. I.** (2003). *Thermoacoustic instabilities in the Rijke tube: experiments and modeling*. Ph.D. thesis, California Institute of Technology.

81. **McIntosh, A. C.** (1991). Pressure disturbances of different length scales interacting with conventional flames. *Combustion science and technology*, **75**, 287 – 309.

82. **McIntosh, A. C.** (2007). Pressure disturbances of different length scales interacting with conventional flames. *Combustion science and technology*, **75**, 287 – 309.

83. **Menon, S.**, Acoustic-vortex-flame interactions in gas turbines. *In* **T. C. Lieuwen** and **V. Yang** (eds.), *From Combustion Instabilities in Gas Turbine Engines: Operational Experience, Fundamental Mechanisms, and Modeling*. American Institute of Aeronautics and Astronautics, Inc., 2005*a*.

84. **Menon, S.**, Acoustic-vortex-flame interactions in gas turbines. *In* **T. Lieuwen** and **V. Yang** (eds.), *Combustion Instabilities in Gas Turbine Engines (Progress in Astronautics and Aeronautics)*. American Institute of Aeronautics and Astronautics, 2005*b*.

85. **Michalke, A.** (1984). Survey on jet instability theory. *Progress in Aerospace Sciences*, **21**(0), 159 – 199.

86. **Munz, C.-D.**, **M. Dumbser**, and **S. Roller** (2007). Linearized acoustic perturbation equations for low mach number flow with variable density and temperature. *Journal of Computational Physics*, **224**(1), 352 – 364.

87. **Nair, S.** (2006). *Acoustic characterization of flame blowout phenomenon*. Ph.D. thesis, Georgia Institute of Technology.

88. **Nayfeh, A. H.**, *Perturbation Methods*. Wiley-VCH, 2008.

89. **Newell, A. C.** and **J. Whitehead** (1969). Finite bandwidth, finite amplitude convection. *Journal of Fluid Mechanics*, **38**(02), 279–303.

90. **Noiray, N.**, **D. Durox**, **T. Schuller**, and **S. Candel** (2008). A unified framework for nonlinear combustion instability analysis based on the flame describing function. *Journal of Fluid Mechanics*, **615**, 139 – 167.

91. **Noiray, N.**, **D. Durox**, **T. Schuller**, and **S. Candel** (2009). Mode conversion in acoustically modulated confined jets. *AIAA JOURNAL*, **47**(9), 2053–2062.

92. **Oran, E. S.** and **J. H. Gardner** (1985). Chemical-acoustic interactions in combustion systems. *Progress in Energy and Combustion Science*, **11**(4), 253 – 276.

93. **Paschereit, C. O.**, **E. Gutmark**, and **W. Weisenstein** (2000). Excitation of thermoacoustic instabilities by interaction of acoustics and unstable swirling flow. *AIAA Journal*, **38**(6), 1025–1034.

94. **Pelce, P.** and **D. Rochwerger** (1992). Vibratory instability of cellular flames propagating in tubes. *Journal of Fluid Mechanics*, **239**, 293–307.

95. **Poinsot, T.**, **D. Veynante**, **F. Bourienne**, **S. Candel**, **E. Esposito**, and **J. Surget** (1989). Initiation and suppression of combustion instabilities by active control. *Symposium (International) on Combustion*, **22**(1), 1363 – 1370.

96. **Poinsot, T. J.**, **A. C. Trouve**, **D. P. Veynante**, **S. M. Candel**, and **E. J. Esposito** (1987). Vortex-driven acoustically coupled combustion instabilities. *Journal of Fluid Mechanics*, **177**, 265–292. ISSN 1469-7645.

97. **Rayleigh, L.** (1878). The Explanation of Certain Acoustical Phenomena. *Nature*, **18**, 319–321.

98. **Schadow, K. C.**, **J. E. Crump**, and **F. S. Blomshield**, Combustion instability in a research dump combustor: Inlet shock oscillations. *In APL The 18 th JANNAF Combust. Meeting*, volume 3. 1981.

99. **Schwarz, J. J., A.** (ed.), *Combustion noise*. Springer-Verlag Berlin Heidelberg 2009, 2009.

100. **Searby, G.** (1992). Acoustic instability in premixed flames. *Combustion Science and Technology*, **81**(4-6), 221–231.

101. **Shanbhogue, S. J.**, **S. Husain**, and **T. C. Lieuwen** (2009). Lean blowoff of bluff body stabilized flames: Scaling and dynamics. *Progress in Energy and Combustion Science*, **35**(1), 98 – 120.

102. **Smith, D. A.** and **E. E. Zukoski**, Combustion instability sustained by unsteady vortex combustion. *In AIAA/SAE/ASME/ASEE 21st Joint Propulsion Conference (Monterey, California, July 1985)*. 1985.

103. **Steinberg, A. M.**, **I. Boxx**, **M. Stöhr**, **W. Meier**, and **C. D. Carter** (2012). Effects of flow structure dynamics on thermoacoustic instabilities in swirl-stabilized combustion. *AIAA journal*, **50**(4), 952–967.

104. **Subramanian, P.**, **S. Mariappan**, **R. Sujith**, and **P. Wahi** (2010). Bifurcation analysis of thermoacoustic instability in a horizontal rijke tube. *International journal of spray and combustion dynamics*, **2**(4), 325–355.

105. **Subramanian, P.** and **R. Sujith** (2011). Non-normality and internal flame dynamics in premixed flame–acoustic interaction. *Journal of Fluid Mechanics*, **679**, 315–342.

106. **Subramanian, P.**, **R. I. Sujith**, and **P. Wahi** (2013). Subcritical bifurcation and bistability in thermoacoustic systems. *Journal of Fluid Mechanics*, **715**, 210–238.

107. **Tong, A.** and **W. Sirignano** (1986). Multicomponent droplet vaporization in a high temperature gas. *Combustion and Flame*, **66**(3), 221–235.

108. **Turing, A. M.** (1952). The chemical basis of morphogenesis. *Philosophical Transactions of the Royal Society of London B: Biological Sciences*, **237**(641), 37–72.

109. **Waugh, I.** (2013). *Methods for analysis of nonlinear thermoacoustic systems*. Ph.D. thesis, University of Cambridge.

110. **Waugh, I. C.**, **K. Kashinath**, and **M. P. Juniper** (2014). Matrix-free continuation of limit cycles and their bifurcations for a ducted premixed flame. *Journal of Fluid Mechanics*, **759**, 1–27.

111. **Wicker, J. M.**, **W. D. Greene**, **S.-I. Kim**, and **V. Yang** (1996). Triggering of longitudinal combustion instabilities in rocket motors - nonlinear combustion response. *Journal of Propulsion and Power*, **12**(6), 1148–1158.

112. **Wooten, D. C.** (1967). *The Attenuation and Dispersion of Sound in a Condensing Medium*. Ph.D. thesis, California Institute of Technology.

113. **Wu, X.** (2005). Asymptotic approach to combustion instability. *Philosophical Transactions of the Royal Society A: Mathematical, Physical and Engineering Sciences*, **363**(1830), 1247–1259.

114. **Wu, X.**, **M. Wang**, **P. Moin**, and **N. Peters** (2003). Combustion instability due to the nonlinear interaction between sound and flame. *Journal of Fluid Mechanics*, **497**, 23–53.

115. **Yang, V.** and **F. E. C. Culick** (1986). Analysis of low frequency combustion instabilities in a laboratory ramjet combustor. *Combustion Science and Technology*, **45**(1-2), 1–25.

116. **Yu, K. H.**, **A. TrouvÃl'**, and **J. W. Daily** (1991). Low-frequency pressure oscillations in a model ramjet combustor. *Journal of Fluid Mechanics*, **232**, 47–72.

117. **Zank, G. P.** and **W. H. Matthaeus** (1990). Nearly incompressible hydrodynamics and heat conduction. *Phys. Rev. Lett.*, **64**, 1243–1246.

118. **Zank, G. P.** and **W. H. Matthaeus** (1991). The equations of nearly incompressible fluids. i. hydrodynamics, turbulence, and waves. *Physics of Fluids*, **3**, 69–82.

119. **Zinn, B.** and **Y. Neumeier**, chapter An overview of active control of combustion instabilities. Aerospace Sciences Meetings. American Institute of Aeronautics and Astronautics, 1997.

120. **Zinn, B. T.** (1968). A theoretical study of nonlinear combustion instability in liquid-propellant rocket engines. *AIAA Journal*, **6**(10), 1966–1972.

121. **Zinn, B. T.** and **T. C. Lieuwen**, chapter Combustion Instabilities: Basic Concepts. Progress in Astronautics and Aeronautics. American Institute of Aeronautics and Astronautics, 2006, 3–26.